DEPARTMENT OF COMMERCE
SINCLAIR WEEKS, Secretary

WEATHER BUREAU
F. W. REICHELDERFER, Chief

MONTHLY WEATHER REVIEW

JAMES E. CASKEY, JR., Editor

Volume 85
Number 11

NOVEMBER 1957

Closed January 15, 1958
Issued February 15, 1958

NUMERICAL METHODS IN WEATHER PREDICTION: II. SMOOTHING AND FILTERING*

FREDERICK G. SHUMAN, U. S. Weather Bureau

Joint Numerical Weather Prediction Unit, Suitland, Md.

[Manuscript received June 25, 1957; revised September 26, 1957]

ABSTRACT

A method is developed for the design of finite-difference smoothing and filtering operators which meet predetermined specifications, and which are applicable to automatic computing machinery. The general technique is to build complicated operators from the simplest types. The necessity for smoothing predicted fields of stream functions before inverting the balance equation for heights of isobaric surfaces is brought out.

1. INTRODUCTION

Numerical weather prediction, making use of finite differences and digital computers, has invariably led to amplification of high frequency components in the final product—amplification beyond physical reality. An excess of short-wavelength components detracts from the appearance of the product, is annoying to analysts, and can be downright misleading to the uninitiated. A method of constructing filtering, or "smoothing", operators was devised by the author [1], which have been successfully employed in operational practice to eliminate short-wavelength components from fields of meteorological variables. In one aspect of operational numerical weather prediction, it has proven necessary in the interests of accuracy to filter out the short-wavelength components. Section 6 will deal with this.

2. THE SMOOTHING ELEMENT

First of all, let a smoothing element be defined. The smoothing element will be the building block of more complicated smoothing operators. We shall take as the smoothing element the simplest of one-dimensional symmetrical centered finite difference operators which does not affect the mean value of a field of infinite extent, namely,

$$\bar{z}_i=\mu z_i+\frac{1}{2}(1-\mu)(z_{i-1}+z_{i+1}) \tag{1}$$

where z is the field to be smoothed. The subscripts refer to points equally spaced in the independent variable, x, and consecutively numbered with increasing x. For imminent conceptual convenience, we will rewrite equation (1).

$$\bar{z}_i=z_i+\frac{1}{2}\nu(z_{i-1}-2z_i+z_{i+1}) \tag{2}$$

where

$$\nu=1-\mu.$$

The parameter ν which is twice the weight given the two outer points, will be called the smoothing element index, since it completely defines a given operator of form (1) or (2).

It will be convenient to think of the dependent variable, z, within the region of interest as consisting of the sum of trigonometric (cosine, say) functions of varying amplitudes, phases, and wave numbers. According to this concept, the wavelengths need not be restricted to multiples of the finite-difference increment in x, nor need the number of waves for a given component within the region

*For Part I see *Monthly Weather Review*, October 1957, pp. 329-332. The third, and last, part in this series will appear in a future issue.

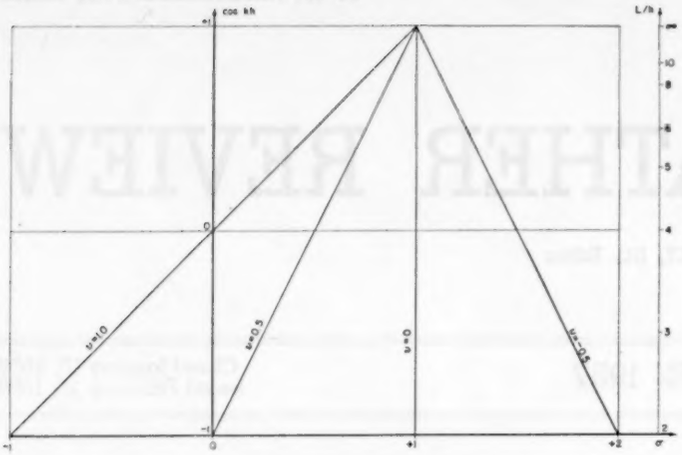

FIGURE 1.—The field of smoothing element index in (σ, cos kh)-space. σ is the ratio of smoothed to unsmoothed amplitude, k is the wave number, h is mesh length, L is wavelength.

of interest be integral. Adopting this concept, we will investigate the effect of a smoothing element on individual cosine components. For example, consider the component

$$z_i=C+A\cos k(x_i-\bar{x})$$

where $\bar{x}$ is an arbitrary constant related to the phase and k is the wave number; i. e., $k=2\pi/L$, where L is the wavelength of the component. Trigonometric identities yield

$$\begin{aligned} z_{i+1}&=C+A\cos k(x_{i+1}-\bar{x})=C+A\cos k(x_i-\bar{x}+h)\\ &=C+A\cos kh\cos k(x_i-\bar{x})-A\sin kh\sin k(x_i-\bar{x})\\ z_{i-1}&=C+A\cos k(x_{i-1}-\bar{x})=C+A\cos k(x_i-\bar{x}-h)\\ &=C+A\cos kh\cos k(x_i-\bar{x})+A\sin kh\sin k(x_i-\bar{x}) \end{aligned}$$

where h is the length of the finite difference increment in x. If these identities are substituted into equation (2), we have, after some rearrangements,

$$\bar{z}_i=C+[1-\nu(1-\cos kh)]A\cos k(x_i-\bar{x})$$

Thus, the smoothing element (2) changes neither the wave number nor the phase, but changes the amplitude of each component by the factor

$$\sigma=\frac{\overline{A}}{A}=1-\nu(1-\cos kh) \tag{3}$$

where A and $\overline{A}$ are the amplitudes of the field before and after smoothing, respectively.

Figure 1 shows the field of ν in (σ, cos kh)-space. It is to be noted that an index of zero does not change the field, and negative indices lead to an increase in amplitude of all components. Positive indices lead to an algebraic decrease in amplitude of all components, although indices greater than unity lead to amplifying oscillations. We thus have a conceptual basis in the sign of the smoothing element index for "zero" smoothing, "negative" smoothing, and "positive" smoothing. It is to be noted further that a smoothing element is not highly selective, so would be a poor filtering operator by itself. For example, if we were to filter out of a field components of wavelength $2h$ (cos $kh=-1$) by means of one smoothing element, components of length $10h$ (cos $kh=0.8$) would be reduced by as much as 10 percent (see the line corresponding to $\nu=0.5$).

3. THE DESIGN OF MULTI-ELEMENT OPERATORS

In order to improve on the selectivity of the 3-point smoothing element, a smoothing operator must be invented which involves more points. The problem in the design of such an operator is to fit it to stated specifications. The approach to this problem set forth in this article is based on the use of more than one smoothing element (2). Successive application of several smoothing elements, with indices $\nu_0, \nu_1, \nu_2, \nu_3, \ldots, \nu_n$ results in the final ratio of smoothed amplitude to unsmoothed amplitude of

$$\Sigma=\sigma_0\sigma_1\sigma_2\sigma_3\ldots\sigma_n=\prod_{m=0}^{m=n}[1-\nu_m(1-\cos kh)] \tag{4}$$

according to equation (3). Equation (4) is a polynomial in (cos kh), with $n+1$ degrees of freedom, represented by the arbitrary constants $\nu_0, \nu_1, \nu_2, \ldots \nu_n$. In principle, one could specify a single-valued curve of Σ against (cos kh) and express it in terms of a product of factors of form (3). One would then know precisely how to accomplish the smoothing desired. In practice, however, this would present a formidable task and furthermore, one is not usually concerned with a precise distribution of Σ in (cos kh). A great deal of improvement, in terms of the desired smoothing end-product, is obtained by combining only two smoothing elements. At the Joint Numerical Weather Prediction (JNWP) Unit, we have not found it necessary as yet to go beyond a combination of three smoothing elements. Our most frequently used multi-element operator will be described in section 5.

4. SMOOTHING IN TWO DIMENSIONS

Extension of the theory to two dimensions may be accomplished in two ways. First, one may smooth in each dimension, independently of the other dimension. It can be shown that the final result is independent of the dimension in which one first smooths, and is also independent of the order in which one applies the smoothing elements. Adopting the view that such an extension of a smoothing element to two dimensions is really the application of two smoothing elements, one in each dimension, the two elements may be combined into a single 9-point operator.

$$\bar{z}_0=z_0+\frac{1}{2}\nu(1-\nu)(z_2+z_4+z_6+z_8-4z_0)+\frac{1}{4}\nu^2(z_1+z_3+z_5+z_7-4z_0) \tag{5}$$

The subscripts refer to mesh points in figure 2, ν being the index of the two smoothing elements, one applied in each dimension.

If, for convenience, we consider the function $z\ (x, y)$ to be composed of the sum of two-dimensional trigonometric components of form

$$z(x,y)=C+A\cos r(x-\bar{x})\cos s(y-\bar{y}), \tag{6}$$

the ratio of smoothed to unsmoothed amplitudes is

$$\sigma=\frac{\overline{A}}{A}=[1-\nu(1-\cos rh)][1-\nu(1-\cos sh)].$$

Since each of the two factors is of the form of the right hand side of equation (3), each factor may be evaluated by means of figure 1.

The second way of extending the theory to two dimensions is through the 5-point operator,

$$\bar{z}_0=z_0+\frac{1}{4}\nu(z_2+z_4+z_6+z_8-4z_0) \tag{7}$$

An analysis of the effect of such an operator on a component (6) reveals that the ratio of the smoothed to unsmoothed amplitudes is

$$\sigma=\frac{\overline{A}}{A}=1-\nu\left[1-\frac{1}{2}(\cos rh+\cos sh)\right]$$

Thus, if we were to replace the ordinate $(\cos kh)$ in figure 1 by $\frac{1}{2}(\cos rh+\cos sh)$, the figure would then apply to the 5-point operator (7).

If the component (6) represented a "wiggle" in one dimension only, (e. g., $r=0, s=2\pi/2h$) the 9-point operator (5) with $\nu=0.5$ would eliminate it, treating it as a one-dimensional element would treat it. The 5-point operator (7), on the other hand, would reduce it by only one-half treating it as a one-dimensional operator would treat a component of wave number $k=2\pi/4h$. Because of this characteristic of the 5-point operator, we have found little use for it. We use almost exclusively combinations of 9-point operators.

The extensions to two dimensions described here have obvious analogues in extensions to spaces of more than two dimensions.

5. COMPLEX SMOOTHING ELEMENT INDICES

There is nothing in the theory which rules out complex indices. A combination of two smoothing elements is equivalent to a single 5-point one-dimensional smoothing operator. If the two smoothing elements have conjugate complex indices, the weights at the five points will be real. Conversely, any 5-point one-dimensional operator is equivalent to a combination of two smoothing elements. Acceptance of complex indices into the theory merely allows this converse to be perfectly general.

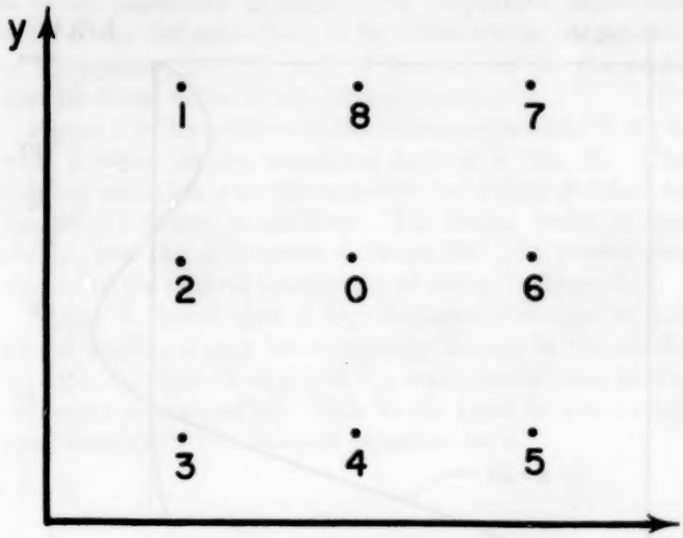

FIGURE 2.—The 9-point mesh.

The multi-element operator in most frequent use at the JNWP Unit consists of an element with a real index, and two elements with conjugate complex indices; i. e.,

$$\begin{aligned}\nu_0&=0.49965\\ \nu_1&=-0.22227+0.64240\mathrm{i}\\ \nu_2&=-0.22227-0.64240\mathrm{i}\end{aligned} \tag{8}$$

A 3-element operator allows the specification of three characteristics of the curve of Σ against $(\cos kh)$. In practice, we have specifications which are not precisely stated, so cannot be handled easily by rigorous mathematical methods.

For example, we want our operational smoothing operator to severely suppress the short waves while retaining essentially unchanged the longer waves. By combining algebraic and graphical techniques, we have arrived at the three elements whose indices (8) are recorded above, and whose effects are displayed graphically in figure 3. Figure 3 shows the result of both one pass and thirty-two passes, the latter to bring out clearly the form for the longer wavelengths.

Complex indices always appear in conjugate pairs, otherwise the multi-element operator would result in imaginary components. Conjugate complex pairs of 9-point operators require smoothing on the boundary for the same reason. We apply the corresponding one-dimensional elements to the boundary, so that in the case of a rectangular grid only the four corner points remain unchanged.

When one comes to programming for automatic computing machinery, the question arises as to whether to perform one scan for each element in a multi-element operator, or to combine the elements into one large smoothing operator. In the case of the operator cited above, if the elements were combined into one large operator, it would be applied to a 7 x 7 mesh of 49 points. More importantly, there would be 10 classes of central

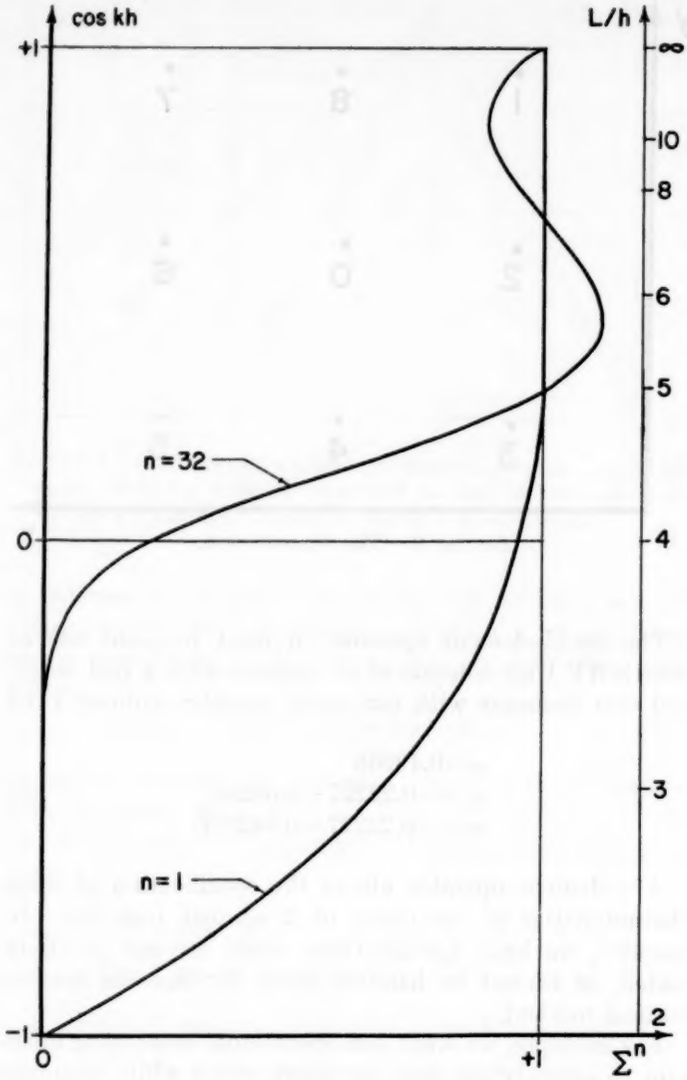

FIGURE 3.—The ratio, Σ, of smoothed to unsmoothed amplitude after N smoothings with the multi-element operator whose smoothing element indices are $\nu_0=0.49965$, $\nu_1=-0.22227+0.64240i$, $\nu_2=-0.22227-0.64240i$.

points, each requiring different treatment. For this reason we believe the advantage lies in performing one scan for each element, the one utility program then handling all multi-element operators for a given grid.

Examples of the application of the smoothing operator represented by the indices (8) will be given in the next section.

6. INVERSION OF THE BALANCE EQUATION FOR THE GEOPOTENTIAL

The one area in which we have found smoothing mandatory in the interest of accuracy is in connection with the inversion of the balance equation (Shuman [2]),

$$\frac{1}{2}(\psi_{xx}+\psi_{yy}+f)^2-\frac{1}{2}(\psi_{xx}-\psi_{yy})^2-2\psi_{xy}^2+\psi_x f_x+\psi_y f_y-\left(gz_{xx}+gz_{yy}+\frac{1}{2}f^2\right)=0 \quad (9)$$

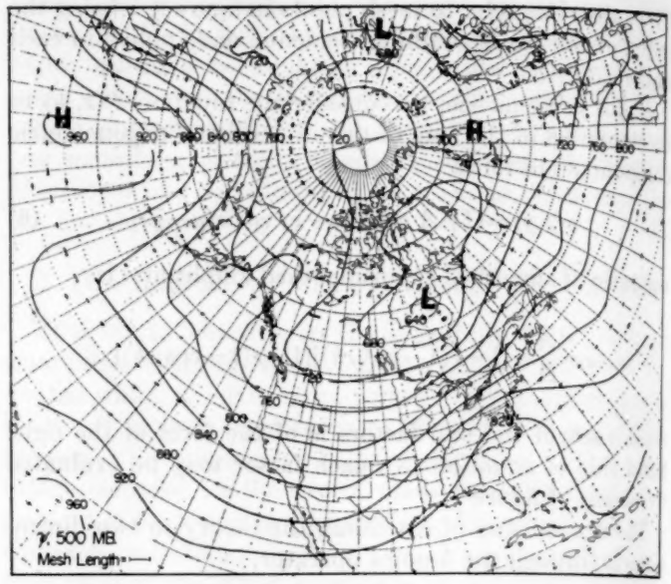

FIGURE 4.—The predicted field of $\bar{f}g^{-1}\psi$ 72 hours after 0300 GMT, April 26, 1956, smoothed 3 times with the multi-element operator (8). Contours are labeled in tens of feet.

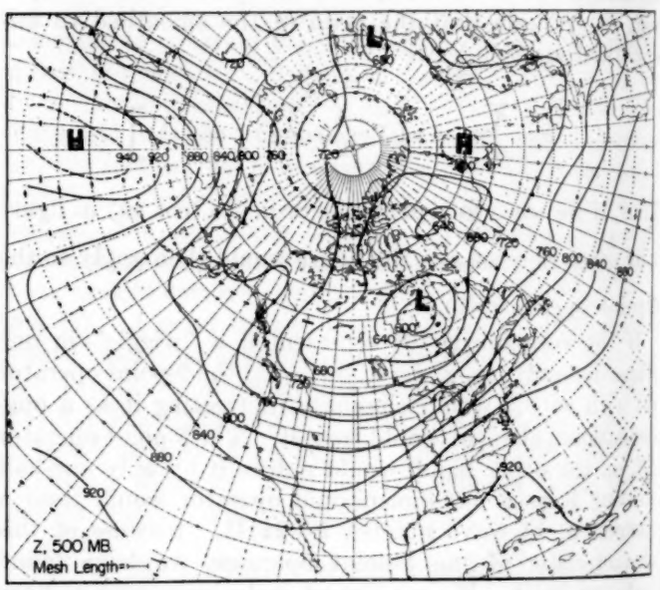

FIGURE 5.—The predicted field of z 72 hours after 0300 GMT, April 26, 1956, inverted from the balance equation and the smoothed field of ψ depicted in figure 4. Contours are labeled in tens of feet.

where z is the height of the 500-mb. contour, ψ is the stream function for the winds at 500 mb., g is gravitational acceleration, f is the Coriolis parameter. Figure 4 shows a 72-hr. barotropic prediction of the ψ-field made with wind fields which satisfy the balance equation. Figure 4 is the predicted ψ-field after being smoothed three times with the operator (8). The ψ-field before smoothing is not shown, but the differences between the smoothed and nonsmoothed fields are portrayed by the lighter curves of figure 6. Only the zero isopleth is shown. The sense (plus or minus) of the differences is not indicated, since it

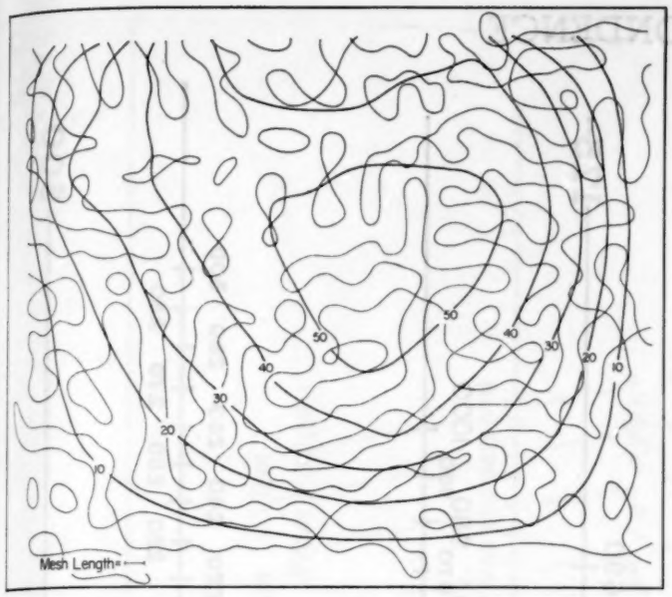

FIGURE 6.—The light curves are the zero isopleth depicting the choppy field of the differences between the ψ-field of figure 4 before and after smoothing. The heavy curves depict the large-scale effect of smoothing the ψ-field, on the z-field implied by the balance equation. The smoothed ψ-field implies a z-field generally higher than the unsmoothed ψ-field. Contours are labeled in tens of feet.

is of no particular interest. The important characteristics of the difference field to be noted are its raggedness, or choppiness, and its lack of consistency in the sense that its mean value is not different from zero.

Figure 5 is the solution of the balance equation (9) for z, with ψ taken as the smoothed field of ψ (fig. 4). The balance equation was also inverted for z with ψ taken as the ψ-field before smoothing. The latter result is not shown, but the differences between the two z-fields are shown by the smooth heavier set of curves in figure 6.

Figure 6 shows that a high-frequency change in the ψ-field implies a very low-frequency change in the z-field through the balance equation (at least through our finite-difference version of it). This result must be due to the non-linearity of the balance equation in ψ.

REFERENCES

1. F. G. Shuman, "A Method of Designing Finite-Difference Smoothing Operators to Meet Specifications," *Technical Memorandum* No. 7, Joint Numerical Weather Prediction Unit, 1955, 14 pp.
2. F. G. Shuman, "Numerical Methods in Weather Prediction: I. The Balance Equation," *Monthly Weather Review*, vol. 85, No. 9, Oct. 1957, pp. 329–332.

CORRESPONDENCE

A Template for Rapid Recomputation of Upper Air Soundings

JAY F. REYNOLDS, JR.

U. S. Weather Bureau, Washington, D. C.

May 8, 1957

In March 1955, the National Weather Analysis Center (NAWAC) increased the area of analysis and prognosis to include the entire Northern Hemisphere. As a result a multitude of upper-air reports must be recomputed as quickly and accurately as possible. The template reprinted here (fig. 1) was designed and adopted for use in NAWAC to expedite the checking of soundings by employing the hydrostatic relationship of layer thicknesses to mean virtual temperatures. Meteorologists at stations or centers receiving many upper-air soundings that require the recomputing of data may find this template useful. It may be reproduced directly from figure 1 as the original size to fit pseudoadiabatic chart (WB Form 770–10) has been preserved.

Reference temperatures (0°, −50°, −40° C.) and pressures (1050, 400, 500, and 175 mb.) have been marked to facilitate the alignment of the template over the pseudo-adiabatic chart. The scales marked off along horizontal lines give the thickness values (tens of ft.) for the layers that are identified by the numbers at the left ends of the lines (1–8 is 1000–850 mb; 8–7, 850–700 mb.; 7–5, 700–500 mb., etc.). The small positive temperature values (°C.) covering the ranges indicated by arrows between selected constant mixing ratio lines (dashed, gm./kg.) are corrections to be applied to the mean temperature of the layers to obtain the mean virtual temperature. It may be noted that these corrections are approximately $w/6$. Thus, $T_v \cong T_m + (w/6)$, where T_v is mean virtual temperature (°C.), T_m is the mean temperature (°C.) of the layer, and w is the mixing ratio (gm./kg.).

The template is used as follows: Superimpose the template on the pseudo-adiabatic chart (WB Form 770–10) on which the temperature and dewpoint soundings have been plotted. The intersection of the plotted temperature curve with a horizontal line on the template gives a close approximation to the mean temperature of the corresponding layer. Similarly the intersection of the plotted dewpoint curve with the horizontal line on the template gives the approximate mean mixing ratio of the layer. The temperature correction corresponding to the interval (dashed lines) in which this mean mixing ratio falls is read from the template and added to the mean temperature to obtain the mean virtual temperature. The latter value determines a point on the horizontal scale of the template from which the thickness value for the layer is read. The height of successive pressure surfaces is obtained in the usual way by accumulating the thickness values, starting with the height of the 1000-mb. surface. The 1,000-mb. height, of course, is readily obtained by any

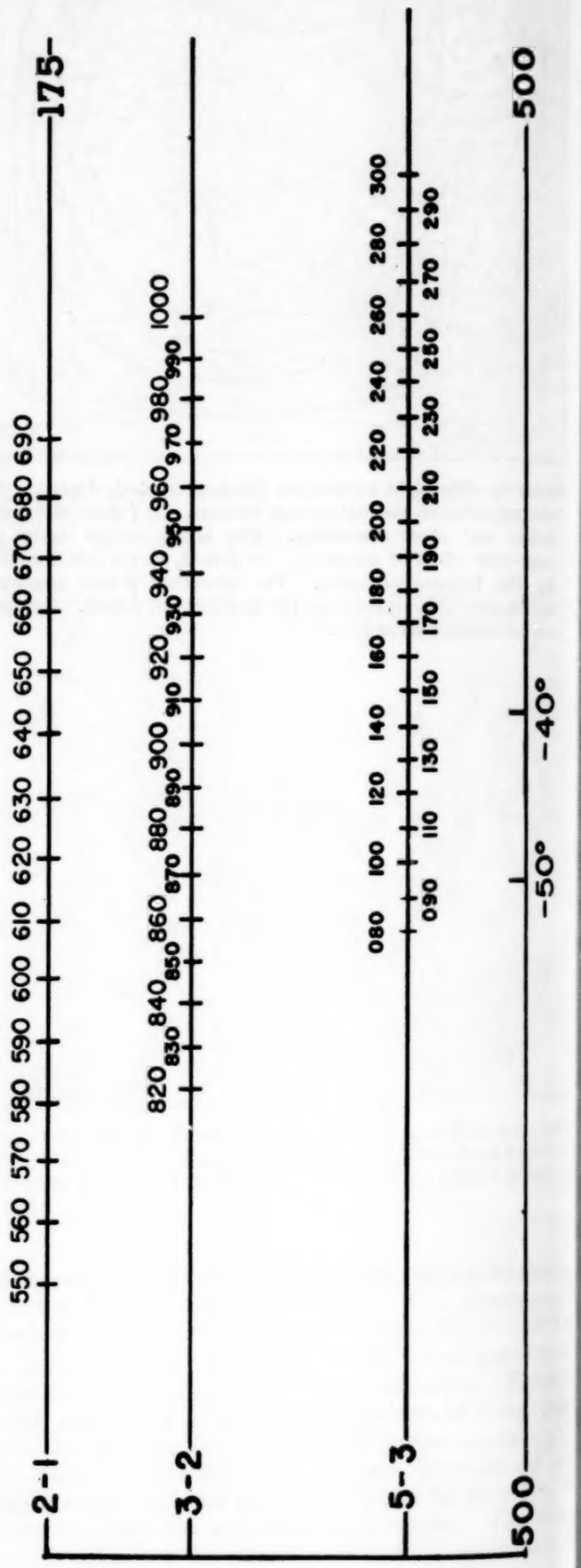

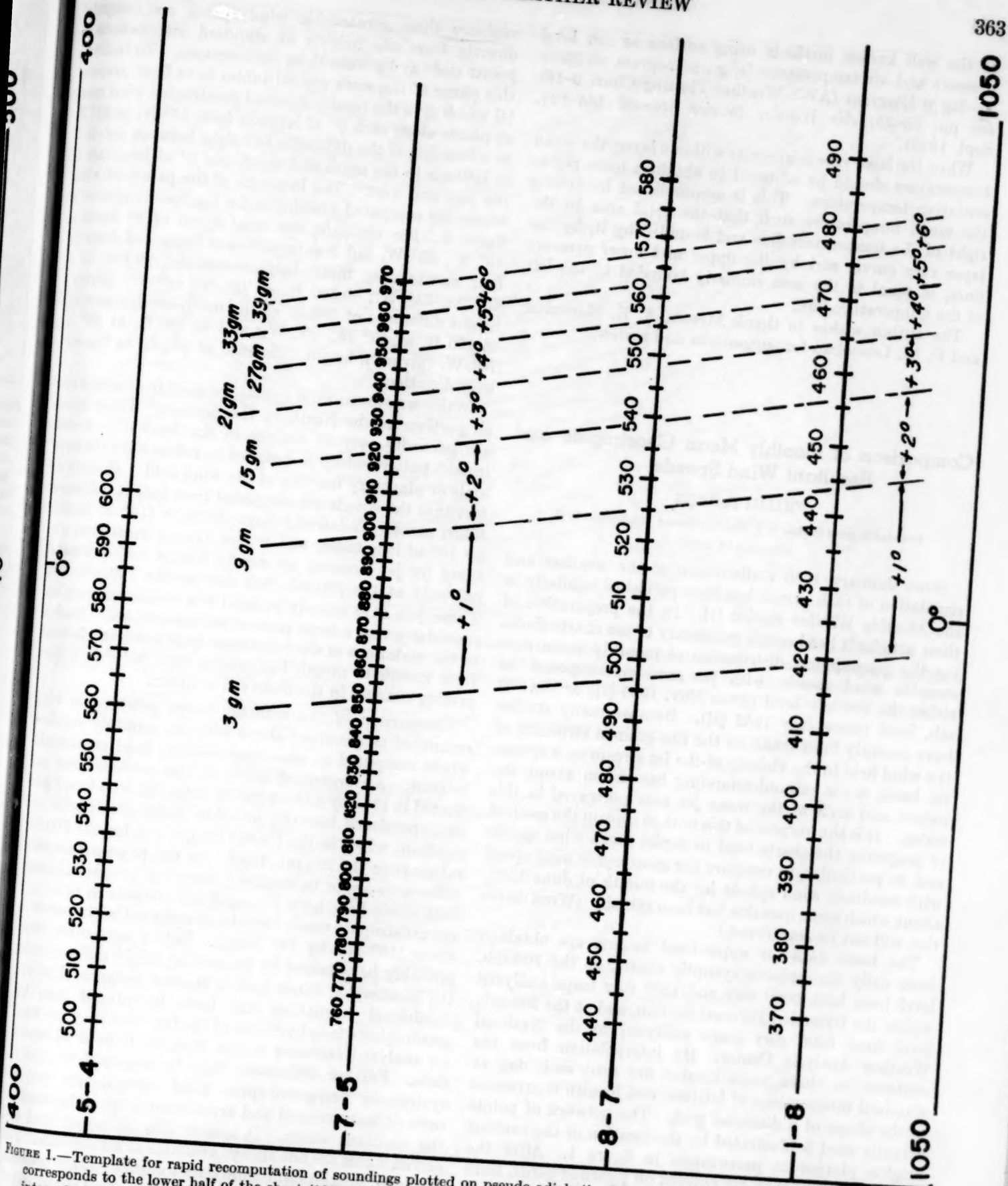

FIGURE 1.—Template for rapid recomputation of soundings plotted on pseudo-adiabatic chart (WB Form 770–10). The portion above corresponds to the lower half of the chart (1050 to 400 mb.); the portion on the preceding page corresponds to the 500 to 175 mb. interval of the upper half of the chart.

of the well known methods using surface or sea level pressure and air temperature (e. g., nomogram on Skew T—log p Diagram (AWS Weather Plotting Chart 9–16) see pp. 23–25, *Air Weather Service Manual* 105–124, Sept. 1952).

When the lapse rate is irregular within a layer, the mean temperature should be adjusted to obtain a more representative temperature. This is accomplished by taking the mean temperature such that the total area to the right of the temperature line and bounded by it, by the lapse rate curve, and by the upper and lower pressure lines, is equal to the area similarly bounded to the left of the temperature line.

The author wishes to thank Messrs. A. K. Showalter and C. M. Lennahan for suggestions and review.

Comparison of Monthly Mean Geostrophic and Resultant Wind Speeds

WILLIAM H. KLEIN

Extended Forecast Section, U. S. Weather Bureau, Washington, D. C.

December 17, 1957

Since January 1950 a discussion of the weather and circulation of each month has been published regularly in the *Monthly Weather Review* [1]. In the preparation of these articles it has become customary to use charts showing the geographical distribution of monthly mean geostrophic wind speeds, with jet axes superimposed, at either the 700-mb. level (since Nov. 1950 [2]) or the 200 mb. level (since July 1952 [3]). Because many studies have recently been made on the fine-grained structure of the wind field in the vicinity of the jet stream on a synoptic basis, some misunderstanding has arisen about the nature and scale of the mean jet axes portrayed in this series. It is the purpose of this note to explain the method of preparing the charts used to depict mean wind speeds and, in particular, to compare the geostrophic wind speed with resultant wind speeds for the month of June 1957, about which some question has been raised. (Wind direction will not be considered.)

The basic data for upper-level heights are obtained from daily hemispheric synoptic charts, at the 700-mb. level from both 0000 GMT and 1200 GMT maps analyzed within the Extended Forecast Section, and at the 200-mb. level from 0000 GMT maps analyzed in the National Weather Analysis Center. By interpolation from the contours on these maps heights are read each day at standard intersections of latitude and longitude arranged in the shape of a diamond grid. The network of points actually used is illustrated by the location of the contour heights plotted in parentheses in figure 1. After the heights are read they are entered on punched cards, from which means of various durations are readily computed.

Wind speeds are obtained indirectly from the mean heights by use of the geostrophic assumption. For convenience these geostrophic wind speeds are computed directly from the heights at standard intersections at points midway between these intersections. To facilitate this phase of the work special tables have been prepared [4] which give the total horizontal geostrophic wind speed at points along each 5° of latitude from 15° N. to 85° N. as a function of the difference in height between points 5° of latitude to the north and south and 5° of longitude to the east and west. The locations of the points at which winds are computed are shown by the speeds plotted in figure 1. For example, the wind speed of 29 knots at 40° N., 65° W. (off Nantucket) was computed from the four surrounding mean heights: namely, 39,800 ft. at 45° N., 65° W.; 40,300 ft. at 35° N., 65° W. (giving a height difference of 500 ft. in the north-south direction); 40,100 ft. at 40° N., 60° W.; and 40,200 ft. at 40° N., 70° W. (giving a height difference of 100 ft. in the east-west direction).

In this way mean wind speeds are quickly obtained over all portions of the Northern Hemisphere. These speeds are generally easy to analyze in the form of a smooth isotach pattern which is designed to reflect only the large-scale or planetary features of the wind field. Despite the fact that the speeds are computed from height differences taken across a relatively large distance (10° of latitude by 10° of longitude), one or two axes of maximum wind speed (or jet streams) are nearly always well delineated, not only at the 200-mb. but also at the 700-mb. level. These jets axes usually parallel the mean contours and meander across a large part of the hemisphere. Analysis of the variations of the jet stream from place to place and from month to month has proven very helpful in interpreting changes in the observed weather.

Comparison of the monthly mean geostrophic winds computed as described above with the monthly resultant winds computed at observing stations is of considerable interest. An organized study of this problem was conducted in 1951 by Aubert and Winston [5], who found good correspondence between monthly mean geostrophic and resultant winds in the United States, but for the 700-mb. rather than the 200-mb. level. In the present case some differences are to be expected, however, because although both winds have been averaged with respect to time, only the geostrophic winds have been averaged with respect to space (10° lat. by 10° long.). Better agreement could probably be obtained by computing height differences for the geostrophic winds over a shorter distance than 10°. Additional smoothing has been introduced into the geostrophic winds by virtue of the fact that they are based on analyzed contours rather than on individual station data. Further differences may be expected because of systematic non-geostrophic wind components and all sorts of instrumental and experimental errors inherent in the resultant winds. It should also be noted that observed winds are not always available at all stations. For instance, the resultant wind data for June 1957 [6] contain from 1 to 3 missing days at no less than 20 stations out of 67 reporting at the 200-mb. level in the United States.

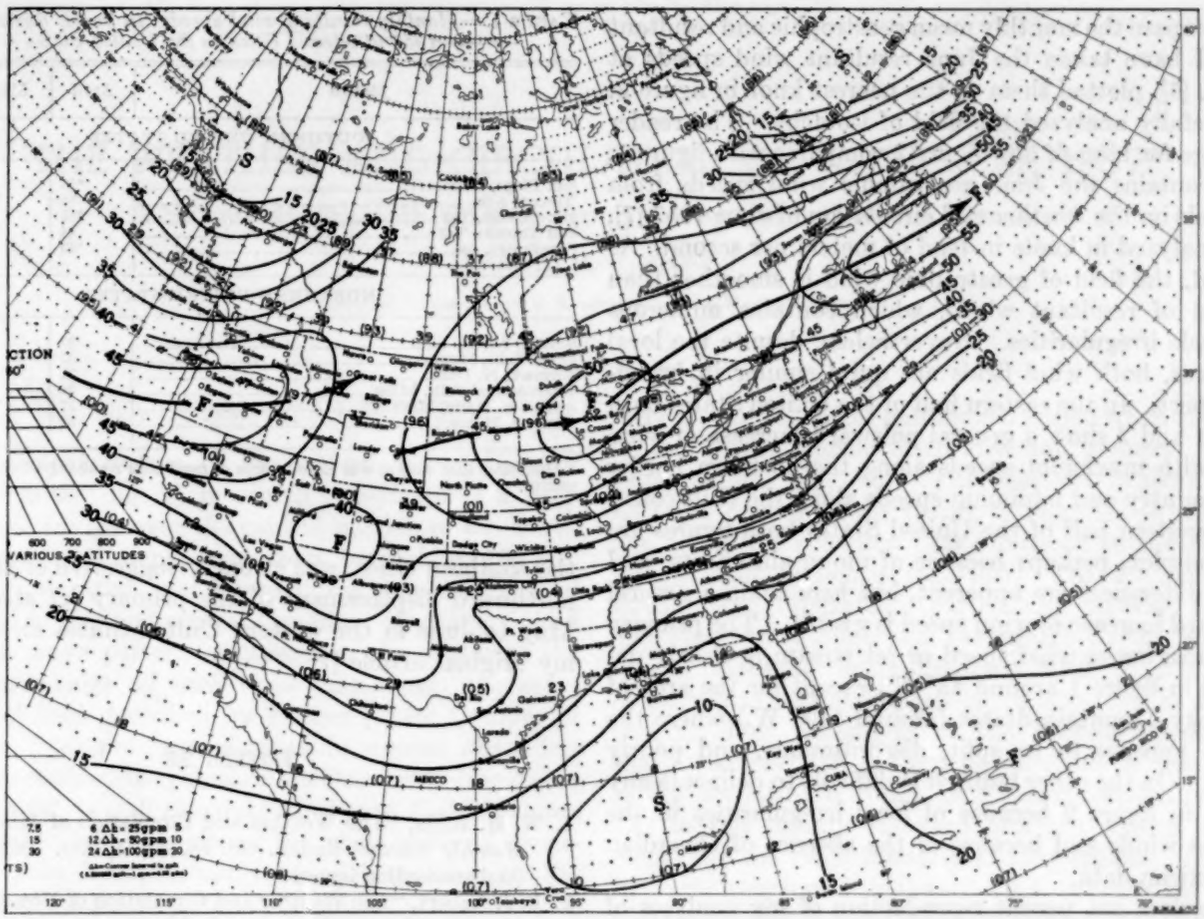

FIGURE 1.—Total (horizontal) geostrophic mean wind speeds (in knots) at the 200-mb. level for June 1957. The numbers in parentheses plotted at standard intersections are the monthly mean 200-mb. heights (in hundreds of feet with first digit omitted) from which the winds were computed. The arrows locate the mean jet streams and are drawn through axes of maximum wind speed. Centers of fast and slow speed are labeled F and S respectively.

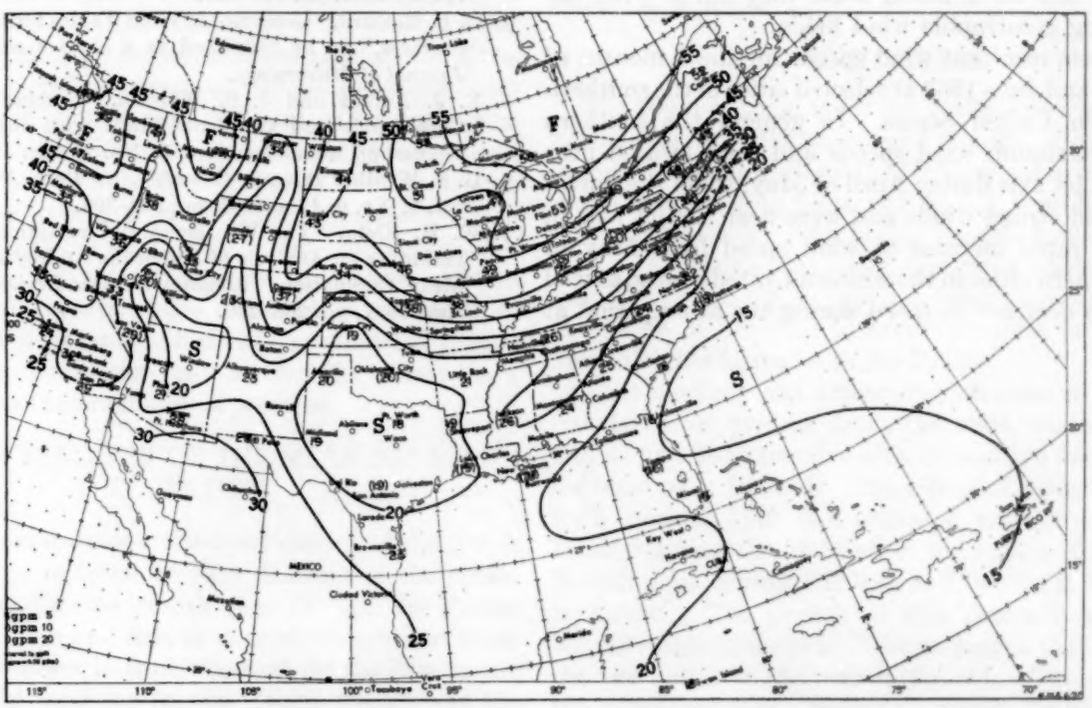

FIGURE 2.—Resultant 200-mb. wind speeds (in knots) for June 1957. Numbers in parentheses are speeds based upon less than 30 days. Centers of fast and slow speed are labeled F and S respectively. All data obtained from *Climatological Data, National Summary*, vol. 8, No. 6, June 1957.

To compare the monthly mean geostrophic and resultant winds, I have taken the June resultant wind speeds at 200 mb. [6], plotted them to the nearest knot in figure 2, and carefully analyzed the field of isotachs. The reader can judge for himself how figure 2 compares with figure 1, which contains the June geostrophic wind speeds from my article on the weather and circulation of June 1957 [7], but is analyzed in knots instead of meters per second. As expected, the field of geostrophic wind is smoother than the field of resultant winds, which contains numerous small-scale irregularities. Nevertheless, despite the local differences, both wind fields are quite similar in broad-scale aspect. In the eastern half of the United States both figures 1 and 2 show a general poleward increase of wind speed, with maximum speeds along the northern border of the country and minimum speeds along the Gulf coast. In the western half of the United States both figures are more complex, perhaps because of mountain effects, and greater differences are apparent, but here again a general northward increase of wind speed is visible. The primary axis of maximum wind speed or jet stream is clearly delineated in figure 1 around 45° N., except for the area of the Rocky Mountain States (around 110° W.) where the jet axis appears to be split, discontinuous, and poorly defined. On the other hand, it is difficult to delineate any jet axis in figure 2 because of local irregularities in the resultant winds and because of the absence of Canadian and Mexican data.

Space does not permit reproduction of my analyses of the resultant wind speeds for April and May 1957, which have been prepared in the same fashion as figure 2. Like figure 2, these analyses exhibit numerous small-scale irregularities, but on a broad scale they agree with the corresponding geostrophic wind fields.

Table 1 lists resultant wind speeds for the 3 months of April, May, and June 1957 at selected cities in the southern and northern United States. In general the southern cities had maximum wind speeds and were located near the primary jet axis during April or May, while the northern cities had strong winds and were near the jet axis in June. The rapid increase in wind speed from May to June at northern cities in the western United States, as well as the sharp decrease in speed during the same period at the southern cities, was strongly suggestive of the abrupt northward displacement of the primary jet stream from May to June in the western United States mentioned in my original article [7].

TABLE 1.—*Monthly resultant wind speeds (in knots) during spring of 1957 at selected cities in the United States*

Station	April	May	June
SOUTHERN UNITED STATES			
San Diego, Calif.	*56	49	29
Tucson, Ariz.	54	*63	28
Brownsville, Tex.	*51	44	23
San Antonio, Tex.	44	*55	19
Shreveport, La.	*53	38	19
NORTHERN UNITED STATES			
Seattle, Wash.	32	10	*49
Great Falls, Mont.	25	11	*49
Bismark, N. Dak.	21	18	*44
International Falls, Minn.	39	39	*53
Sault Ste. Marie, Mich.	57	*64	59
Caribou, Maine	52	58	*62

*Indicates that station was close to area of maximum resultant wind speeds for the month.

REFERENCES

1. W. H. Klein, "The Weather and Circulation of January 1950," *Monthly Weather Review*, vol. 78, No. 1, Jan. 1950, pp. 13-14 (and succeeding issues).
2. E. J. Aubert, "The Weather and Circulation of November 1950," *Monthly Weather Review*, vol. 78, No. 11, Nov. 1950, pp. 201–203.
3. W. H. Klein, "The Weather and Circulation of July 1952—A Month with Drought," *Monthly Weather Review*, vol. 80, No. 7, July 1952, pp. 118–122.
4. O. E. Richard, "Geostrophic Wind Tables for Constant Pressure Surfaces," to be published as a shorter contribution in the *Journal of Meteorology*.
5. E. J. Aubert and J. S. Winston, "Comparison of Monthly Geostrophic and Gradient Winds with Resultant Rawins," *Journal of Meteorology*, vol. 8, No. 2, Apr. 1951, pp. 126–127.
6. U. S. Weather Bureau, *Climatological Data, National Summary*, vol. 8, No. 6, June 1957, pp. 304–309.
7. W. H. Klein, "The Weather and Circulation of June 1957—Including an Analysis of Hurricane Audrey in Relation to the Mean Circulation," *Monthly Weather Review*, vol. 85, No. 6 June 1957, pp. 208–220.

THE WEATHER AND CIRCULATION OF NOVEMBER 1957[1]

A Stormy Month with a Deep Trough over Central North America

CHARLES M. WOFFINDEN

Extended Forecast Section, U. S. Weather Bureau, Washington, D. C.

1. THE NORTH AMERICAN TROUGH

The principal feature of the 700-mb. circulation for November 1957 (fig. 1) in North America was a deep full-latitude trough over the central portion of the continent. Associated departures from normal of 700-mb. height were negative over a broad area including most of the United States and central Canada. Over the United States the wave pattern of trough in the center of the country and ridge off each coast was almost the exact opposite of that described by Frazier [1] for October of this year. This pronounced break in regime, which has often characterized the change from October to November in the past [2], is well illustrated in figure 2 which shows sizeable height falls over almost the whole of North America, with rises limited mainly to offshore areas in the Atlantic and Pacific.

The changeover from October to November was a gradual one, and the first half of November (fig. 3A) exhibited characteristics of each regime. Although the Canadian trough became well established and extended into the United States, the pattern over the southern tier of States was out of phase and more characteristic of the October regime, with a trough off the southeastern coast and another in the Southwest. This latter feature moved inland during this period from its October position along the west coast and eventually joined the Canadian trough to produce the pronounced full-latitude system which dominated the pattern for the latter half-month (fig. 3B). The sharpening of this trough as its central portion deepened and the coastal ridges developed is evident from figure 3C, and it became sufficiently pronounced that it determined the circulation pattern for the month as a whole as well as the anomalies of weather.

2. OTHER FEATURES OF THE MEAN 700-MB. CIRCULATION

It is of interest to review the development of the North American trough in terms of other features of the planetary circulation for the month (fig. 1). In the Pacific the normally dominant Asiatic coastal trough was weak and confined to lower latitudes (except for the Low in the Sea of Okhotsk), and the central Pacific trough was the deeper and more pronounced system. This was particularly true of the latter half-month period when the trough in the central Pacific intensified and assumed a strong negative tilt (fig. 3B). This pattern evolved as the northern portion of the trough retrograded to the Bering Sea, while the southern part advanced to the Hawaiian Islands and deepened (fig. 3C). The reaction downstream was interesting, particularly at low latitudes. The west coast ridge and the trough in the Southwest moved eastward into alignment with their Canadian counterparts and became full-latitude features as described earlier. This phasing-in of the United States trough sharply altered the pattern downstream in the Atlantic as the low-latitude trough off the southeastern coast (fig. 3A) moved rapidly eastward into the central Atlantic, displacing the ridge formerly in that region. This ridge in turn progressed eastward and contributed to the blocking which became established over the British Isles during this period. A complete change of phase also resulted in this area since a pronounced trough previously occupied the region. Figure 3C highlights the extent of these adjustments.

3. BLOCKING

The 700-mb. zonal index for November averaged below normal for the fifth successive month. However it was higher (9.7 m. p. s.) than the October value of 7.3 m. p. s., and it climbed from 8.7 to 10.6 m. p. s. from the first to the latter half-month. This rather sizeable increase of nearly 2 m. p. s. brought the index to slightly above the normal value of 10.5 m. p. s. and was associated with a shift in the locale of blocking to lower latitudes in the Atlantic and to higher latitudes in the Pacific.

That blocking was a prominent feature of the Atlantic circulation is evident from the split westerlies (figs. 1 and 4) and the extensive area of positive height anomaly centered over Iceland. The center of positive departure from normal (340 ft.) migrated from the vicinity of Iceland during the first half of the month (fig. 3A) to the British Isles during the last half, where it became very persistent. The growth of this anomaly produced the largest single increase in 700-mb. height (620 ft.) between the two halves of the month (fig. 3C). The movement of the associated 5-day mean DN center, traced in figure 5, illustrates the tendency first to migrate toward, and then to remain over, the British Isles.

[1] See Charts I-XVII following p. 384 for analyzed climatological data for the month.

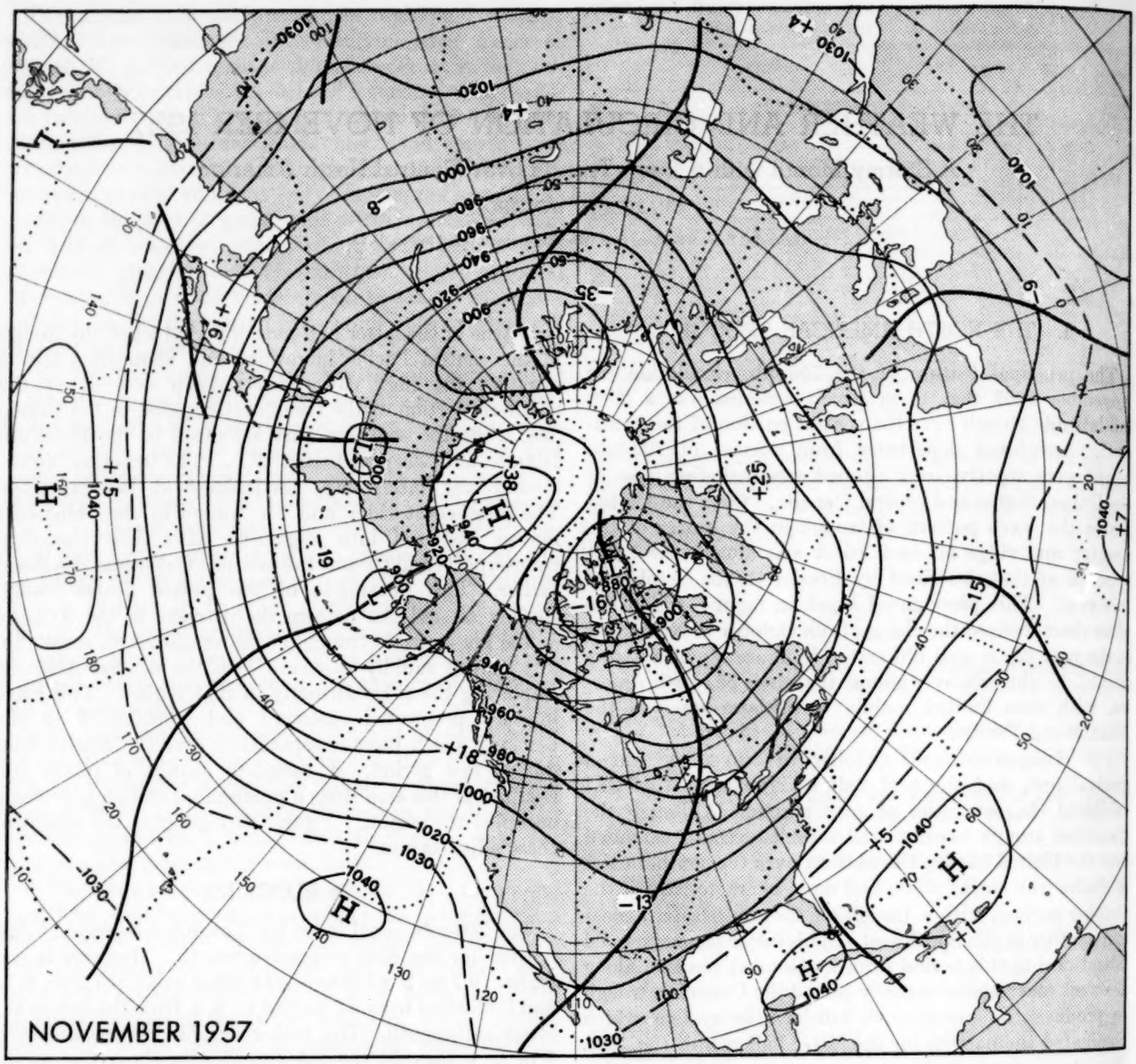

FIGURE 1.—Mean 700-mb. height contours (solid) and departures from normal (dotted) (both in tens of feet) for November 1957. A deep full-latitude trough (heavy vertical line) occupied central North America, with heights below normal over most of the United States and central Canada. Blocking was active over the northern Atlantic and over the polar basin north of the Bering Strait.

The Icelandic area was subject to intense cyclonic activity during October [1], and therefore the advent of blocking in that vicinity in November constituted a sharp reversal in circulation. This is attested by the large change center of +500 ft. observed on the difference chart between the two months (fig. 2).

A rather pronounced "wave of blocking" emanated from the North Atlantic region about mid-month and spread westward to influence North America. The center of positive anomaly split (indicated by the dashed line on fig. 5) during the 5-day mean period, centered on the 14th, with a new center (+470 ft.) appearing in eastern Canada. This in turn intensified and retrograded bodily (solid line fig. 5) to northern Hudson Bay, only to separate into two centers once again as the area of positive anomaly subsequently spread westward. This time the new center (+250 ft.) appeared in the southeastern Gulf of Alaska on the mean chart for the 18th. This center remained stationary and intensified to +450 ft. on the mean chart centered on the 21st. However, the retrogression terminated at this point as the center of positive anomaly subsequently sank south-southeastward to a point off the California-Oregon coast and became affiliated with the subtropical ridge. Thus, this "surge" of

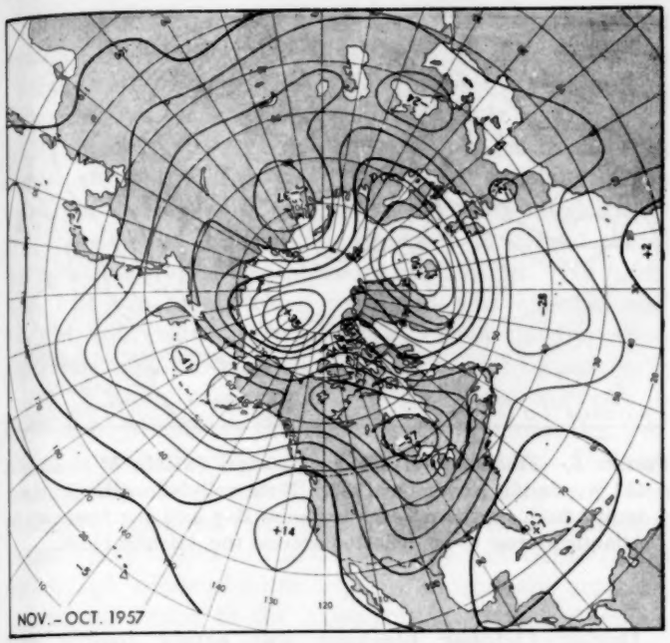

FIGURE 2.—Change in 700-mb. height from October to November 1957. The lines of equal height change are drawn at 50-ft. intervals with the zero line heavier and the centers labeled in tens of feet. The largest changes occured over central North America, illustrating the reversal from the October regime. Note the development of the cyclonic channel over the Aleutians, as blocking retreated to higher latitudes, and increased zonal flow developed to the south. Note also the large changes over Iceland as blocking supplanted the intense cyclonic activity of October.

blocking was accompanied by two periods of discontinuous retrogression of the type often described as typical [3, 4]. Its speed of progress upstream is somewhat difficult to assess. However, assuming a beginning with the first appearance of a positive center near Iceland on the mean chart centered on the 7th and an ending with the development of maximum intensity in the Gulf of Alaska (+450 ft. on the mean chart centered on the 21st), an average speed of approximately 60° longitude per week results, in good agreement with the findings of other studies on blocking [4, 5, 6].

As the center of blocking in the Atlantic shifted from Iceland to the lower latitude of Britian during the month it assumed more of the nature of a middle-latitude block with a stronger connection with the subtropical ridge (fig. 3B). In the Pacific, by contrast, blocking was mainly a high-latitude phenomenon and was located over Arctic waters north of Bering Strait (fig. 1). It developed greater intensity than its Atlantic counterpart since a closed polar High formed with associated departure from normal on the monthly mean chart (fig. 1) of +380 ft., compared to +250 ft. in the Atlantic.

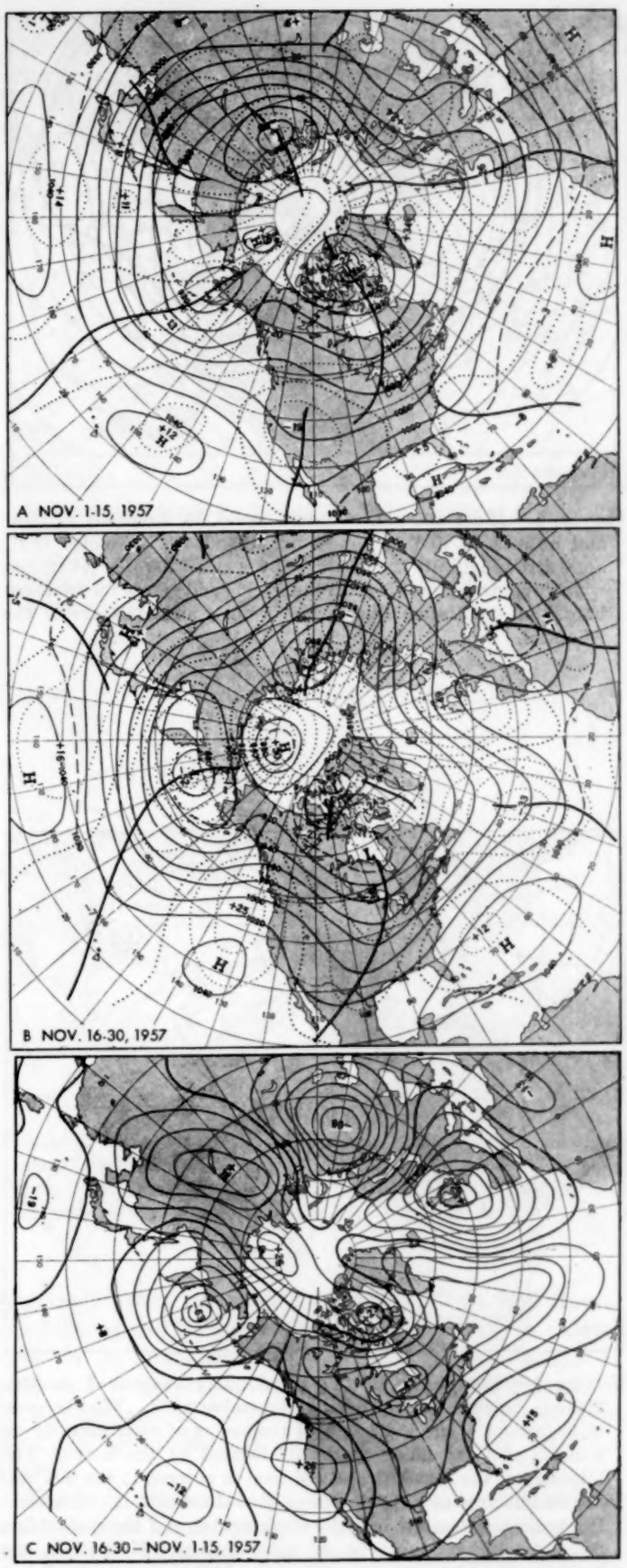

FIGURE 3.—Fifteen-day mean contours (solid) and height departures from normal (dotted) at 700 mb. (both in tens of feet) for (A) November 1–15, and (B) November 16–30, 1957, together with (C) the difference between the two. The North American trough intensified and extended to lower latitudes in accord with the amplification of pattern and increase in westerlies over the Pacific. Note the mid-latitude block over Britain and the large intra-month change which occurred there.

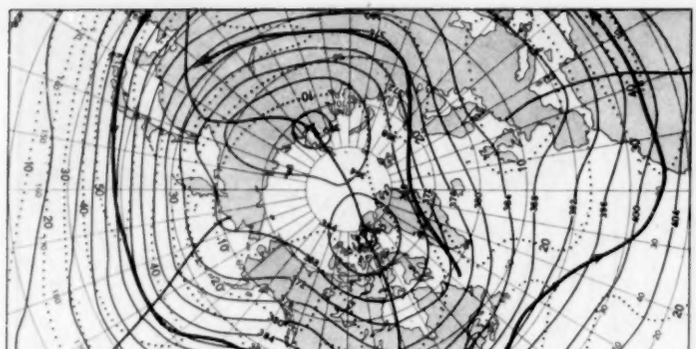

FIGURE 4.—Mean 200-mb. contours (solid, in hundreds of feet) and isotachs (dotted, in meters per second) for November 1957. Solid arrows indicate the position of the mean 200-mb. jet stream which was strong and single in the Pacific and across the southern border of the United States, but weaker and split across the Atlantic.

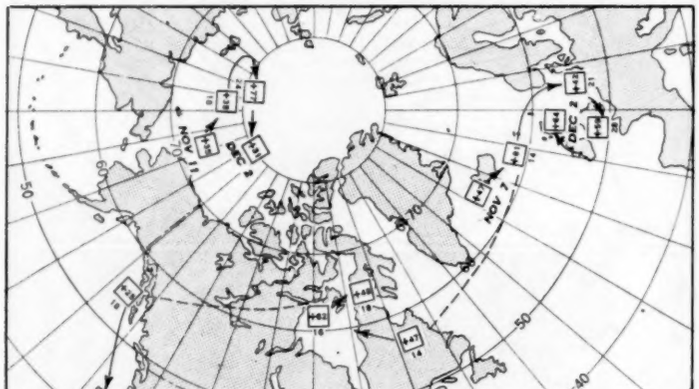

FIGURE 5.—Trajectories of two outstanding centers of positive 700-mb. height anomaly during November 1957. Weekly positions (except where indicated) of the center of each anomaly on a series of 5-day mean charts are located by the boxes. The intensity of the center (in tens of feet) is entered in the box and the middle date of the 5-day mean period beneath it. The solid line indicates translation of the whole center, and the dashed line discontinuous retrogression or split centers. Note that one blocking surge left the Atlantic on the 14th, became established over northeastern Canada, and served as the parent center for another retrograde wave which began to influence the Gulf of Alaska on the 18th.

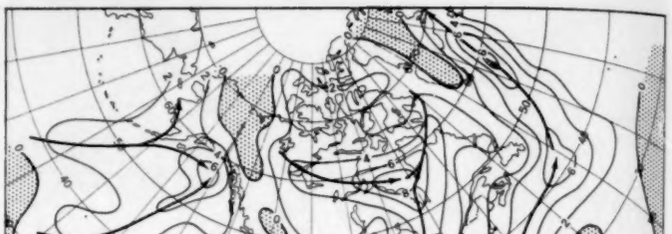

FIGURE 6.—Frequency of cyclone passages (within 5° squares at 45° N.) during November 1957. Note well-defined track (heavy arrow) from northern Texas to James Bay and the tendency for Atlantic storms to be deflected around the Atlantic block.

During October blocking was active mainly over Alaska and western Canada [1], and a vestige thereof appears to have remained during the first half of November in the form of the positive 200-ft. DN center over the Canadian Rockies and the difluent flow along the west coast of North America (fig. 3A). However, the tendency to shift to higher latitudes during the first half-month was clearly indicated by the appearance of a closed High over the polar basin with positive height anomaly of 290 ft. (fig. 3A). It was during the second half-month, however, that this anticyclone became most intense and persistent in that area and dominated the whole polar region. As this happened, the depression to its south in the Bering Sea deepened markedly, with heights diminishing during the half month by 630 ft. (fig. 3C) and during the full month by 410 ft. (fig. 2). It was this tendency for blocking to retreat to very high latitudes, and for cyclogenesis to occur over Alaska and the Bering Sea, which initiated the rise in index in the Pacific during the last half-month. This increase in index is well indicated by the marked change in flow components shown at middle latitudes on figure 2.

4. WEATHER AND CIRCULATION IN THE UNITED STATES

November was a stormy month for most of the country. The deep mean trough in the central United States at 700 mb. (fig. 1) and at 200 mb. (fig. 4) favored a temperature regime of cold in the West versus warm in the East. The baroclinic zone thus established gave rise to frequent intense storminess, and several major systems followed the favored course for the month from Texas northeastward through the Great Lakes and into James Bay. The individual tracks of these cyclones are shown in Chart X, and cyclone frequency per unit box together with principal tracks are summarized in figure 6. One or two centers moved along the southern border and joined the Atlantic storm track extending from South Carolina east-

northeastward and thence north-northeastward toward Iceland. It is noteworthy that this track, like the one in central United States, closely resembled the climatologically preferred track for November [7].

The mean relative vorticity at 700 mb. for the month, charted in figure 7, further illustrates the intensity of the well-organized cyclonic channel in central United States and, in addition, indicates its tendency to extend across the mountains into New Mexico and Arizona. No fewer than five vigorous storms traversed this channel and brought cold waves, record snows, local flooding, and damaging high winds in thunderstorms and tornadoes.

One of these, of particular severity, was spawned in the Gulf of Mexico as the 700-mb. mean trough (fig. 3A) moved into the Southwest early in the month. It deepened rapidly as it moved toward the Lakes and was responsible for flood rains of 6 to 8 in. over northeastern Texas, heavy snows in the Ohio Valley and Great Lakes region, high winds of 40 to 50 m. p. h. from the northern and central Plains to the Appalachians, severe thunderstorm and tornado activity in the South from Texas eastward to North Carolina, and a cold wave in its wake. The Texas floods reached record proportions at Hagansport on the Sulphur River, with a flood crest of 45.6 ft. on November 6. This exceeded the previous record of 45.3 ft. which was recorded, oddly enough, 11 years previously to the day.

Severe storminess continued during the latter half of the month and produced another rash of heavy snows extending from the Rockies to the Great Lakes, with excessive rains and flooding again occurring in the southern States from Texas eastward. Tornadoes were reported in Alabama, Mississippi, Texas, Kentucky, and Tennessee. A particularly damaging one spread destruction in the suburbs of Fort Worth, Tex. on November 17.

Because of this cyclonic activity, precipitation was abundant over most of the country (Chart III–B). The only sizeable areas receiving less than 75 percent of monthly normal were the Northern Rocky Mountain States and the extreme Southwest. Precipitation totals exceeded the normal amount over most of the remainder of the country, were greater than twice the normal over a broad tier of southern States from New Mexico and northern Arizona to the Atlantic coast, and even exceeded 400 percent of normal along the Texas-Oklahoma border and in southeastern Colorado. Comparison of rainfall distribution (Chart III–B) with the 200-mb. flow (fig. 4) reveals that the axis of precipitation corresponded closely with the speed maximum of the mean 200-mb. jet stream over the Southeast. It is also noteworthy that the area under this jet maximum encompassed most of the tornado activity which occurred during the month, in good agreement with the findings of Dunn [8] for May 1957.

Numerous precipitation records were broken. It was the wettest November of record at Cairo, Ill., 13.05 in.; Louisville, Ky., 9.12 in.; Winston-Salem, N. C., 7.15 in.; and Brownsville, Tex., 6.26 in. In addition, new records

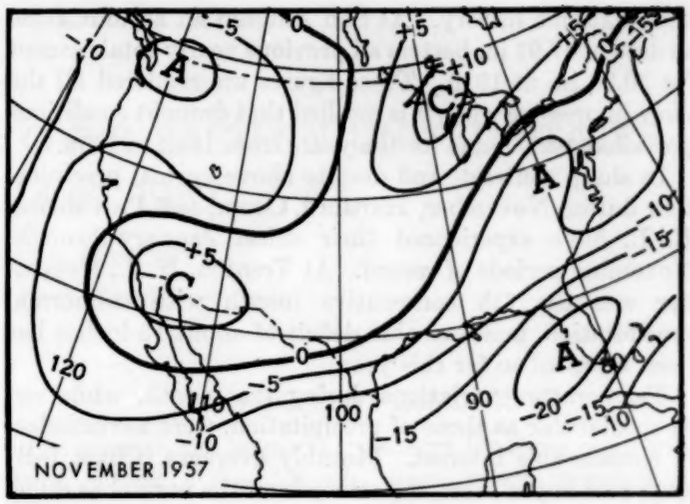

FIGURE 7.—Vertical component of mean geostrophic relative vorticity at 700 mb. for November 1957 (in units of 10^{-6} sec. $^{-1}$). Cyclonic and anticyclonic vorticity are considered positive and negative, respectively, and labeled C and A at centers. Note the marked channel of cyclonic vorticity extending from southern Arizona to the Great Lakes.

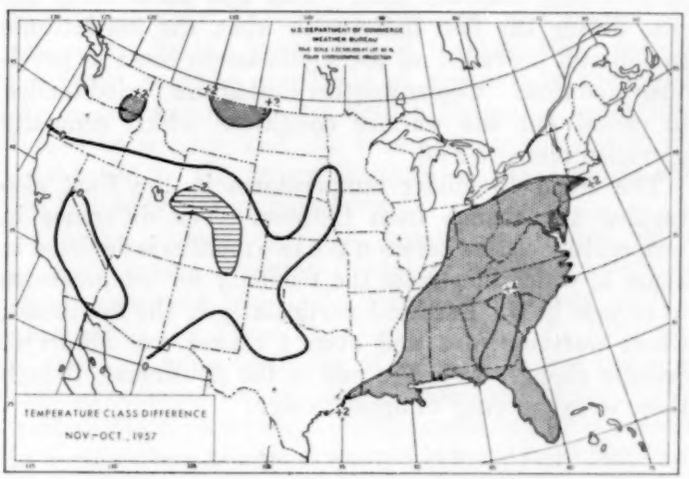

FIGURE 8.—Number of classes the anomaly of temperature changed from October to November 1957, with warming considered positive. Temperatures increased over the eastern half of the country, with the largest changes in the Southeast.

of snowfall were established at Lander, Wyo. and Raton, N. Mex. with 32.5 and 14.5 in. respectively. Also, records of 24-hour snowfall were closely approached or exceeded at several locations in the Central Plains. A 10.2-in. deposit at Concordia, Kans. on the 17–18th, for example, established a new 24-hour record for that station.

Not only were monthly totals excessive, but several stations have accumulated record or near record amounts for the first 11 months of the year and have excellent chances of setting new annual rainfall records. Among these, Dallas, Tex. has a total of 53.00 in. so far this year, which already exceeds any annual total observed in

that station's history. At San Antonio an accumulation to date of 47.91 in. betters all previous yearly totals except for 50.30 in. in 1919. These figures are rendered all the more impressive when it is recalled that drought conditions prevailed over Texas for the years from 1952 to 1956.

In sharp contrast, and despite above normal precipitation during November, Hartford, Conn., and Providence, R. I., have experienced their driest January-through-November periods of record. At Trenton, N. J., November was the 7th consecutive month with subnormal precipitation, and a sizable deficit of about 13 inches has been recorded so far this year.

Temperature variations during the month, while not as spectacular as those of precipitation, were nevertheless of considerable interest. Monthly averages (Chart I–B) were cool in the West, departing from the normal as much as −4° to −6° F. over the Great Basin and West Texas. Temperatures were somewhat warmer in the East and in the Northern Plains, but, with the exception of the extreme Northwest and Northern Plains, positive departures were not large, averaging around 2° F. This was a consequence of the flatness of the ridge in advance of the United States trough which allowed occasional outbreaks of cold air to penetrate into the East. This was particularly the case during the first half-month when the low-latitude trough still prevailed off the southeastern coast as previously described. Cooler weather during this period tended to cancel out the warmer conditions which generally prevailed thereafter [9].

The trend to milder temperatures in the East also typified the change from October. The difference in temperature classes between the two months is depicted in figure 8, which illustrates the tendency for temperatures to reverse in the East and particularly in the Southeast, where warming of 3 and even 4 classes was observed. Smaller changes were the rule in the Southwest, though these were generally of opposite sign.

This temperature pattern, and its change from October, together with the widespread storminess and precipitation, all reflect the pre-eminence of the trough in the central United States during the month, at all levels from sea level up to 100 mb. (Charts XI to XVII).

REFERENCES

1. H. M. Frazier, "The Weather and Circulation of October 1957—A Month with a Record Low Zonal Index for October in the Western Hemisphere," *Monthly Weather Review*, vol. 85, No. 10, Oct. 1957, pp. 341–349.
2. J. Namias, "The Annual Course of Month-to-Month Persistence in Climatic Anomalies," *Bulletin of the American Meteorological Society*, vol. 33, No. 7, Sept. 1952, pp. 279–285.
3. C. M. Woffinden, "The Weather and Circulation of February 1957—Another February with a Pronounced Index Cycle and Temperature Reversal over the United States," *Monthly Weather Review*, vol. 85, No. 2, Feb. 1957, pp. 53–61.
4. J. Namias and P. F. Clapp, "Studies of the Motion and Development of Long Waves in the Westerlies," *Journal of Meteorology*, vol. 1, Nos. 3 and 4, Dec. 1944, pp. 57–77.
5. H. F. Hawkins, "The Weather and Circulation of June 1955—Illustrating a Circumpolar Blocking Wave," *Monthly Weather Review*, vol. 83, No. 6, June 1955, pp. 125–131.
6. Arthur F. Krueger, "The Weather and Circulation of January 1954—A Low Index Month with a Pronounced Blocking Wave," *Monthly Weather Review*, vol. 82, No. 1, Jan. 1954, pp. 29–34.
7. W. H. Klein, "Principal Tracks and Mean Frequencies of Cyclones and Anticyclones in the Northern Hemisphere," U. S. Weather Bureau *Research Paper* No. 40, Washington, D. C. 1957.
8. C. R. Dunn, "The Weather and Circulation of May 1957—A Month with Severe Floods and Devastating Tornadoes in the Southern Plains of the United States," *Monthly Weather Review*, vol. 85, No. 5, May 1957, pp. 175–182.
9. U. S. Weather Bureau, *Weekly Weather and Crop Bulletin, National Summary*, vol. XLIV, Nos. 45–47, Nov. 11, 18, and 25, 1957.

NORTHEASTWARD-MOVING LOWS OVER EASTERN UNITED STATES, NOVEMBER 14–19, 1957

W. T. CHAPMAN AND B. DUBOFSKY

National Weather Analysis Center, U. S. Weather Bureau, Washington, D. C.

1. INTRODUCTION

Three major storms whose history and initial development were very similar dominated the weather in the eastern half of the United States during the period of November 14–19, 1957. Each storm, categorized as Type IV by J. J. George [1] or E_L by California Institute of Technology [2], developed over the South-Central States and moved approximately northeastward accompanied by heavy precipitation.

This paper interprets some of the details revealed by analysis of each storm and the related pattern of instantaneous and maximum 24-hour precipitation. Surface, upper air, and some of the supplemental charts routinely prepared at NAWAC are used. One of the supplemental charts, called the "mean advection chart" (the 1000–500-mb. thickness lines superimposed on the 700-mb. contours), is shown in panels A and B of figures 2, 4, and 6. The relative strength and slope of the warm front and the cold front can readily be appraised qualitatively by noting the gradient of the thickness lines associated with fronts. In addition, for convenience and to save space, the area of maximum 500-mb. relative cyclonic vorticity [1] (prepared by Fjørtoft's [3] technique) and the areas of maximum 24-hour precipitation are shown on the advection charts.

In using the advection chart, NAWAC makes the assumption that the 700-mb. flow may be used to approximate the mean flow in the 1000–500-mb. layer and that the advection of thickness is generally proportional to the mean flow. This assumption saves time in applying Sutcliffe's theory of development and steering. In developing his theory, Sutcliffe [4] used basic equations and a few assumptions to derive mathematically the role of the thermal winds for the 1000–500-mb. layer in the steering and intensification of surface systems.

For convenience in referring to the three storms, they are designated as follows: Storm I,0000 GMT November 14 through 1800 GMT November 15; Storm II, 1200 GMT November 15 through 0600 GMT November 17; Storm III, 0000 GMT November 18 through 1800 GMT November 19. Note that the early stages of Storm II overlap in time the final stages of Storm I.

[1] The value of the vorticity parameter presented on the composite "advection charts" as derived by Fjørtoft's technique is directly proportional to the relative cyclonic vorticity.

451122—58—2

2. ANTECEDENT CONDITIONS

In general, the long-wave patterns for these cases were very similar. The 500-mb. space mean prepared by Fjørtoft's [3] technique for 0000 GMT on November 14 indicated a long-wave trough in the mid-Atlantic and another in the central United States. Zonal westerlies dominated the Pacific as one trough of small amplitude lay off the British Columbia coast and another near Kamchatka. By 1200 GMT on the 15th, the trough in the Atlantic showed little change; but slight retrogression was noted in the trough in the central United States as the trough near Kamchatka deepened and moved 10° eastward. As the wavelength of the long-wave pattern shortened and the amplitude of the pattern increased, the minor trough off the British Columbia coast continued to weaken and the long-wave troughs were reestablished in the central sections of the Atlantic and the United States on November 18.

Storm I crossed the Pacific coast of the United States as a weakening occluded frontal system and continued slowly eastward with little change in intensity until it approached the Texas Panhandle region. At 1200 GMT of the 13th some deepening of this system was noted as another occluded front (Storm II) was crossing the Northwestern States; however, a definite organized wave pattern in northwestern Louisiana was not induced until 0000 GMT of the 14th (fig. 1A). During the same time, Storm II had moved across the Pacific coast as an occluded front with its well-defined Low located over Montana. As Storm I moved northeastward toward the Great Lakes, little change in intensity was found in Storm II as it moved southeastward (figs. 1B, C) until it began slowly deepening in eastern Colorado (fig. 1D). By 1200 GMT of the 15th (fig. 3A), a well-defined center had formed in south-central Kansas as Storm I moved toward the southern portion of James Bay and another weak occlusion approached the Pacific Northwest (Storm III). At the surface, the movement of Storm III through the western States was completely masked although it was still a marked trough at 500 mb. (fig. 3C). A sharpening in this upper trough occurred with the approach of a fairly strong system off the Washington-Oregon coast (fig. 5A). Subsequent surface deepening through Texas resulted in a wave crest in eastern Oklahoma. By 1200 GMT on the

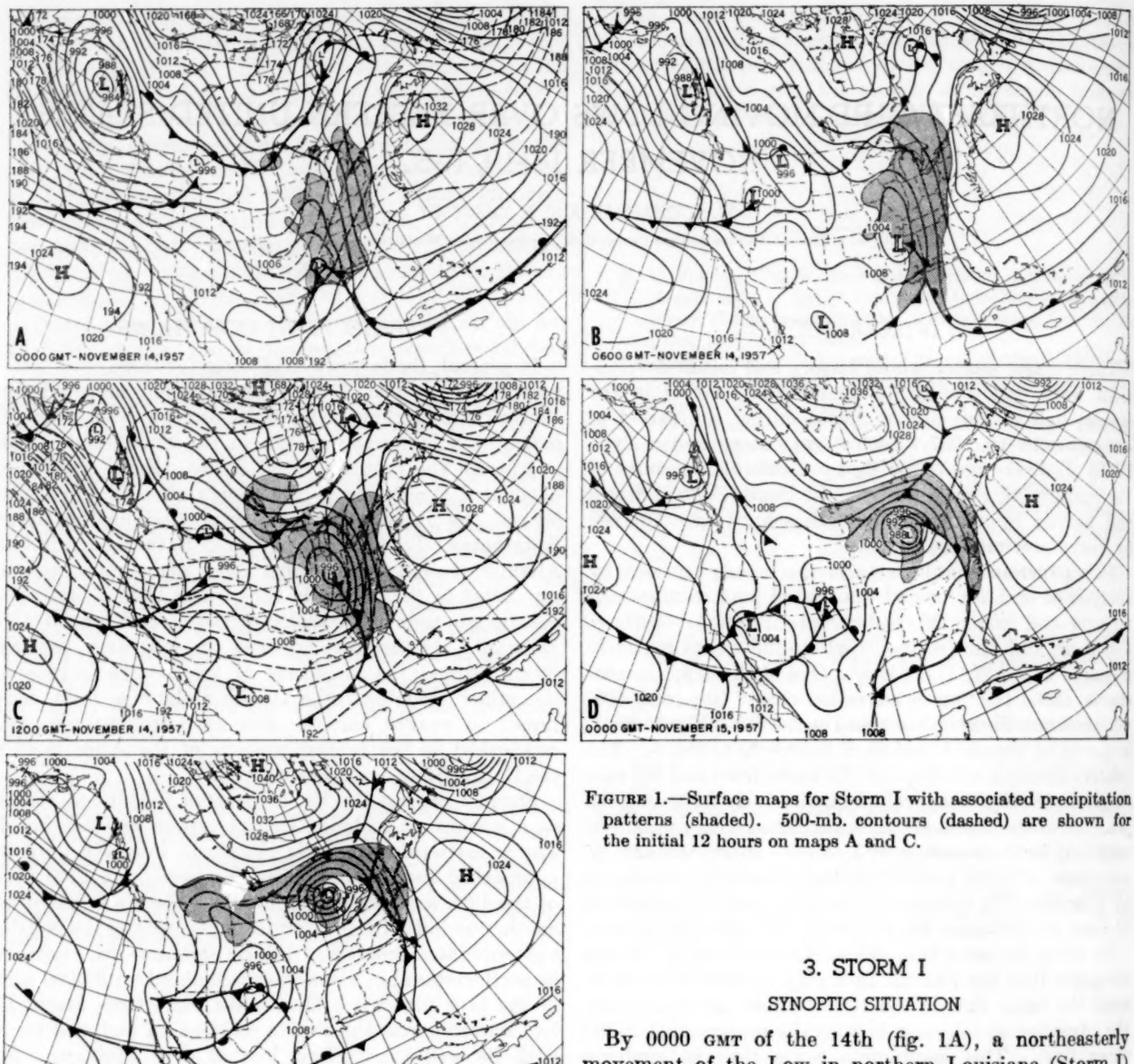

FIGURE 1.—Surface maps for Storm I with associated precipitation patterns (shaded). 500-mb. contours (dashed) are shown for the initial 12 hours on maps A and C.

18th, the strong surface Low (Storm III) had moved into southern Missouri (fig. 5C).

This conspectus of their histories illustrates the similarity of formation of all three cases which follows to some extent the sequence of events in the development of Colorado Type Lows as described by Jacobson et al. [5].

This type of storm (George Type IV or the final phases of CIT Type E_L) definitely poses a threat of excessive precipitation over the entire eastern half of the United States; therefore, some details of the storms and their differences as related to the maximum 24-hour precipitation anomalies are studied in the following sections.

3. STORM I

SYNOPTIC SITUATION

By 0000 GMT of the 14th (fig. 1A), a northeasterly movement of the Low in northern Louisiana (Storm I) was indicated by negative pressure tendencies over northern Mississippi, the positive tendencies over eastern Texas, and southwesterly flow at 500 mb. over the Low center; however, the magnitude of the isallobaric field indicated little deepening. The advection chart for Storm I (fig. 2A) at 0000 GMT on the 14th indicated that the strongest warm advection extended from eastern Louisiana southeastward through Alabama and north-northeastward toward the Great Lakes—generally over the area of current precipitation shown by the shading through the Mississippi and Ohio Valleys in figure 1A. The field of maximum relative cyclonic vorticity outlined in figure 2A by the +100-foot isoline was located upstream over Nebraska, Kansas, western Oklahoma, and western Texas, somewhat northwest of the 700-mb. trough. Apparent warm advection at 500 mb. upstream ahead

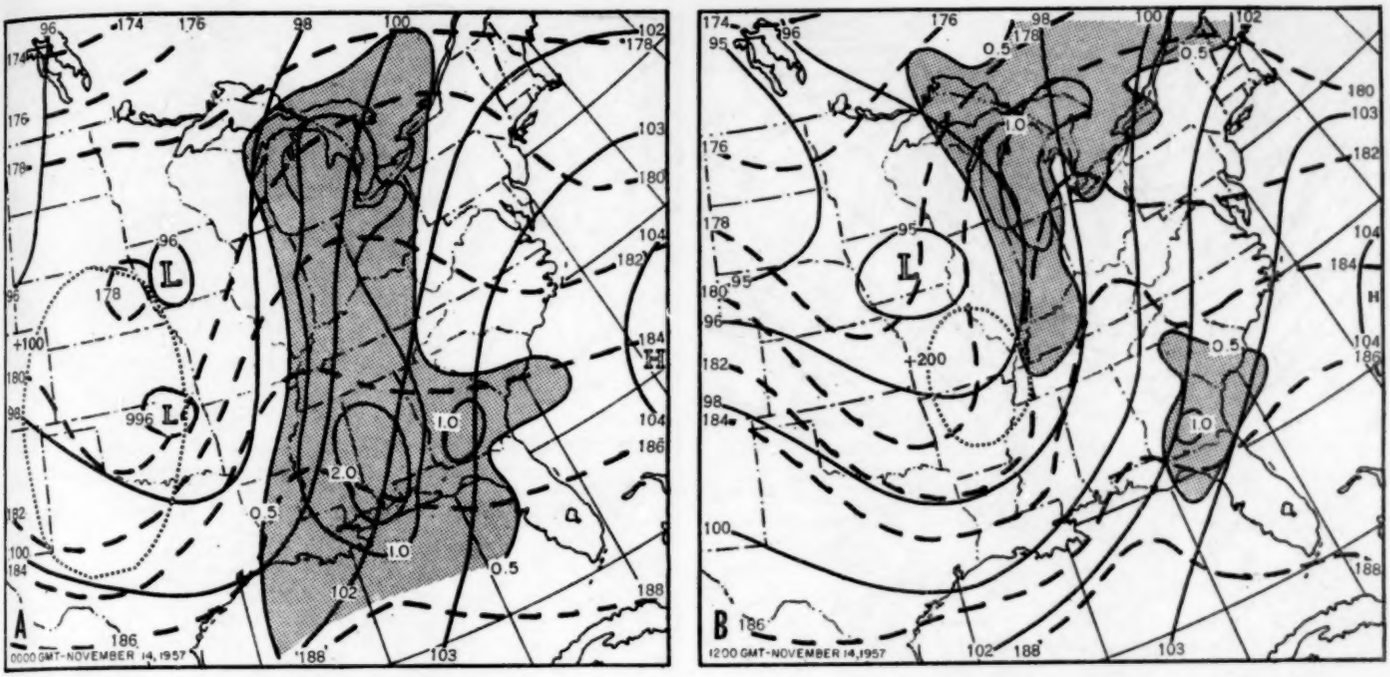

FIGURE 2.—Advection charts for Storm I with 700-mb. contours (solid), 1000–500-mb. thickness lines (dashed), areas of maximum precipitation ending 24 hours after chart (shaded), and areas of maximum relative vorticity according to Fjørtoft's method (dotted lines).

of the occluded system in northwestern United States suggested some sharpening of the upper trough in the central United States (increasing the curvature contribution to vorticity), whereas the wavelength and the strength of the flow upstream suggested some acceleration of the upper trough.

By 0600 GMT on the 14th (fig. 1B), either or both of these developments were indicated by the increasing area of the katallobaric field west of the surface center. By 1200 GMT (fig. 1C) the surface Low had deepened 8 mb. and moved northeastward at approximately 40 knots; the 500-mb. trough had deepened about 100 feet in the vicinity of Missouri and had moved closer to the surface center. The advection chart at this time (fig. 2B) showed still fairly strong warm advection east of the Mississippi River, but the flow through Louisiana and Texas was now parallel to the thickness pattern with a shallow cold zone indicated over northern Arkansas and Missouri. The maximum relative cyclonic vorticity also increased as indicated by the +200-foot isoline and moved more into phase with the 700-mb. trough. Since the cold advection term was decreasing in the southern portion of the trough, little change or flattening of the trough was expected; however, continued rapid movement of the trough was indicated by the strong upstream flow at both the 700- and 500-mb. levels.

The main contribution to further deepening of the Low apparently came from the upper-level advection of vorticity and the indicated warm advection ahead of the system (Petterssen [6]). Large surface tendencies to the east and north of the Low, now in eastern Illinois (fig. 1C), confirmed this. By 0000 GMT of the 15th (fig. 1D) the Low, then south of Sault Ste. Marie, had almost reached its maximum depth. In the next 6 hours it moved northeastward with little deepening (fig. 1E). At this time the intensity of the katallobaric field was equal to that of the anallobaric field. By 1200 GMT November 15 the cyclone became a cold Low as the cold air spread rapidly eastward south of the center in response to the acceleration of the upper trough south of the Low. This rapid motion eastward served to "cut off" the southerly or warm advection flow east of the surface system. Following this development the deepening ended. Figure 3B shows the Low as it filled near the tip of James Bay and as the remaining warm advection became associated with a secondary wave on the rapidly eastward-moving cold front off Nantucket.

MAXIMUM PRECIPITATION

The areas of maximum 24-hour precipitation in the three storms have been indicated on figures 2, 4, and 6. As Storm I was first developing in northern Louisiana (fig. 1A, 0000 GMT of the 14th), it produced a narrow but effective warm, moist, southwesterly influx of air off the western Gulf of Mexico. At 850 mb. (not shown), this narrow current was well delineated by the 10° C. isodrosotherm. The associated area of maximum 24-hour precipitation (from the north central Gulf States to the eastern Great Lakes region), including a sizable 2-inch region (over eastern Mississippi and western Alabama), is delineated in figure 2A. Note the axis of this maximum area and its relationship to the zone of maximum indicated warm advection; note also how this axis became more

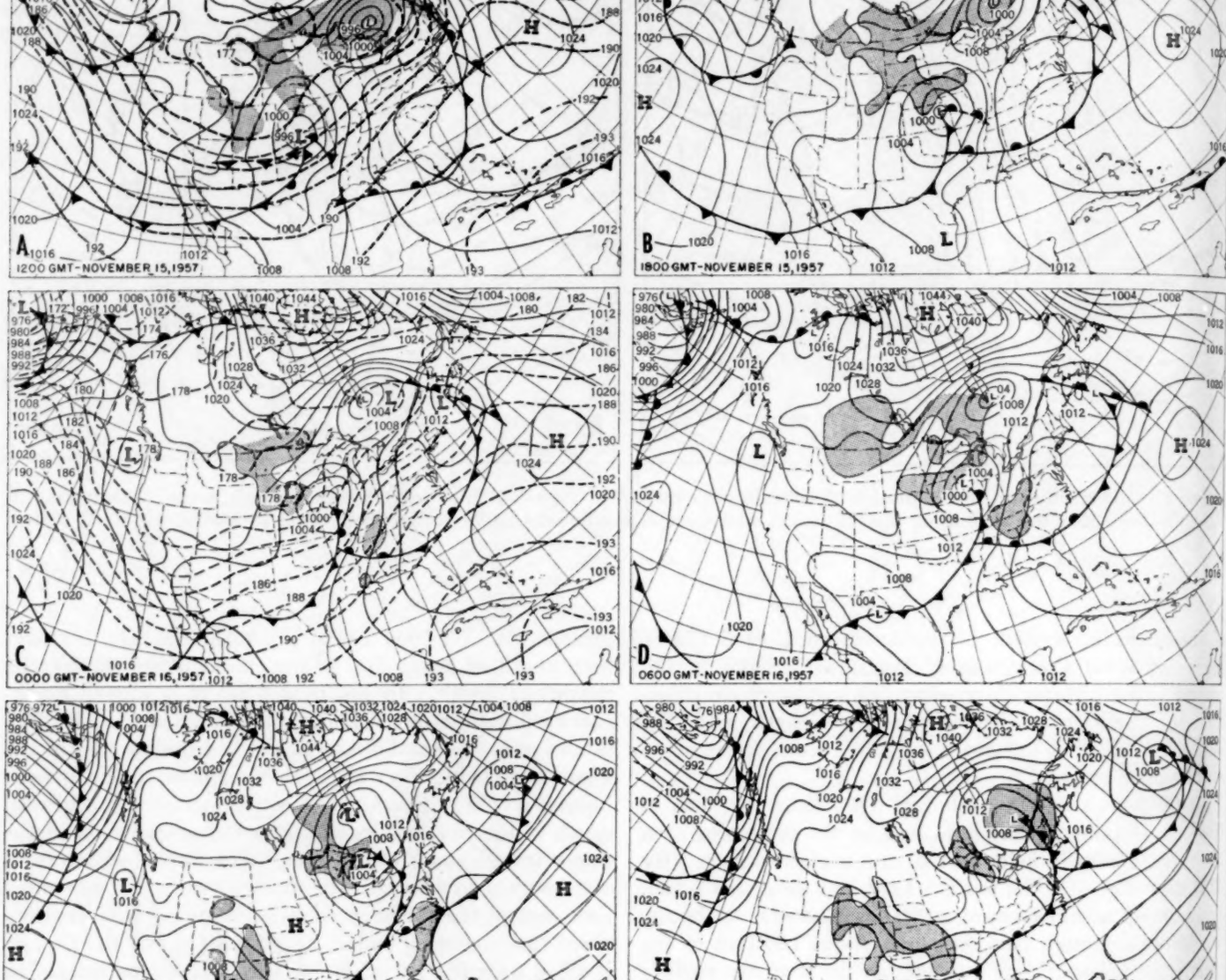

FIGURE 3.—Surface maps for Storm II with associated precipitation patterns (shaded). 500-mb. contours (dashed), are shown for the initial 12 hours on maps A and C.

closely related to the path of the deepening Low with time.

By 1200 GMT of the 14th (fig. 2B), the axis of maximum precipitation had split into two segments as the area of the 10° C. isodrosotherm at 850 mb. decreased to an even narrower zone near Mobile, Ala., with marked veering of the southerly flow at 850 mb. The lower portion of the maximum precipitation area moved generally eastward and lessened as the northern section developed an axis more in phase with the actual path of the rapidly deepening storm in eastern Illinois (fig. 1C). At the point of maximum deepening and intensification (fig. 1D) the axis of maximum precipitation of the northern portion (fig. 2B) coincided with the path of the deep Low. Note the increased gradient north of the 18,200-foot thickness (steeper slope of the warm front) in the vicinity of the eastern Great Lakes. Also note on the advection chart for this time the relationship of the axis of strongest warm advection (along the 10,000-foot contour) to the axis of maximum precipitation in this area. The lower portion

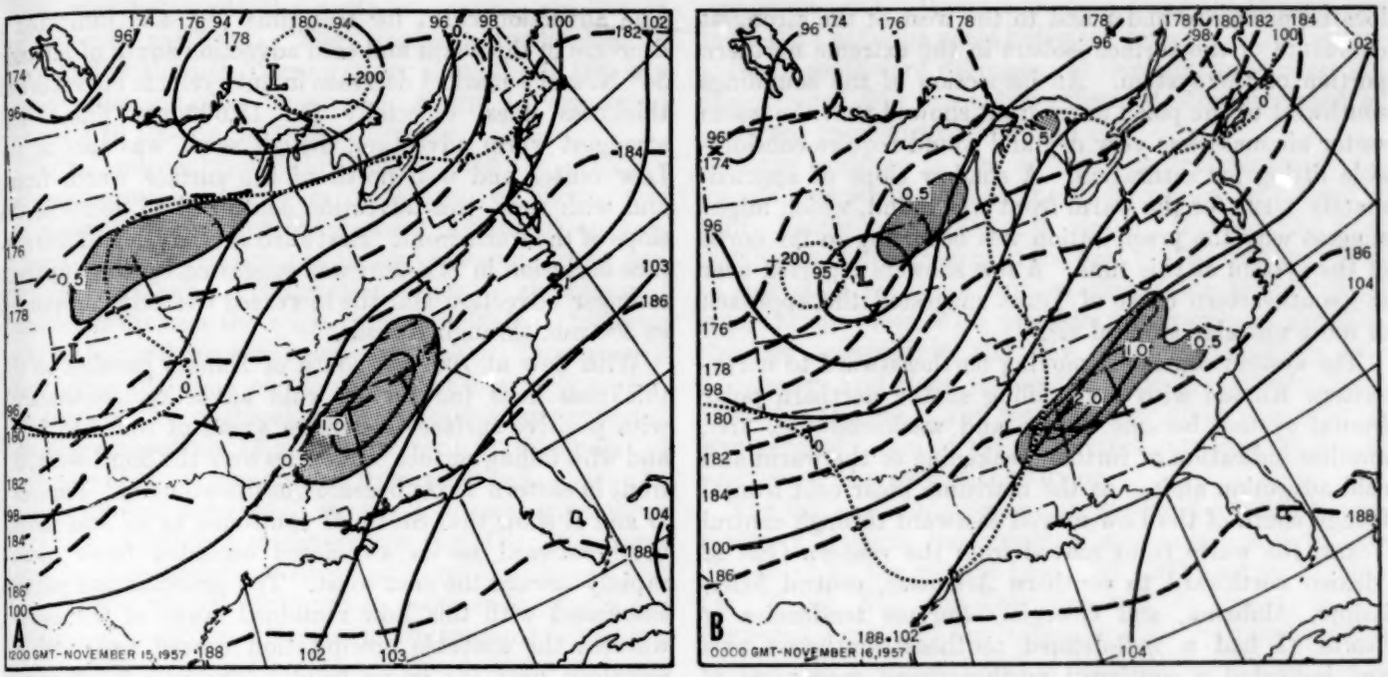

FIGURE 4.—Advection charts for Storm II with 700-mb. contours (solid), 1000–500-mb. thickness lines (dashed), areas of maximum precipitation ending 24 hours after chart (shaded), and area of maximum relative vorticity according to Fjørtoft's method (dotted lines).

or cell of the maximum zone of precipitation contained primarily heavy showers and thundershowers which were "triggered" by lifting along the warm and cold fronts (figs. 1A–D).

On the stability index chart for 0000 GMT of the 14th (not shown), an area of zero values lay over Louisiana, approximately the area of the warm sector. By 1200 GMT, this area was depressed southward along the Gulf coast. (See fig. 1, D and E). Note the relationship to the anticyclonic curvature of the 18,600-foot thickness line (fig. 2B) which encompassed the surface frontal structure. As the thickness gradient became weaker, suggesting a significant decrease in warm advection, the magnitude of surface pressure tendencies ahead of the front diminished along the eastern Gulf States. In time, cold advection decreased with consequent filling or flattening of the upper trough. This brought further weakening of surface negative pressure tendencies and produced a filling of the surface frontal trough over the southeastern United States (fig. 1, D and E), thereby decreasing the influx of southerly moist air and reducing the "trigger action" of the cold front.

4. STORM II

SYNOPTIC SITUATION

At 1200 GMT of the 15th (fig. 3A), a weak occluded system was located off the west coast with indications of further weakening as another strong Low was moving toward the western Aleutian chain. Storm I at this time was centered northeast of Sault Ste. Marie and Storm II was a well-developed Low in south-central Kansas. The axis of the surface pressure tendencies associated with Storm II was oriented northeast-southwest and indicated a northeastward movement with little change in intensity. At 500 mb. a fairly broad trough over the western United States was associated with Storm II while a shallow ridge extended southeastward from Ohio to the Carolinas. The upstream flow had a fairly long fetch but was broken up by two troughs, one over the extreme western States and the other, a weak and shallow trough just east of Ship "Papa" (50° N., 145° W.) associated with the weak surface occluded front just off the west coast.

On the advection chart for this time (fig. 4A), the pattern associated with Storm II showed a relatively steep frontal slope with marked anticyclonic curvature; however, note the shallow weak warm advection along the warm sector side of the 18,600-foot thickness line. The strongest warm advection was located due east of the surface Low in eastern Kansas and northern Missouri. Note the contrast of the north-south amplitude of the warm advection area with the warm advection area for Storm I shown in figure 2A. The cold advection associated with Storm II was in the Texas Panhandle and western Texas and was of approximately the same magnitude as the warm advection. Further investigation of these two cases revealed some contrast in the magnitude of maximum relative cyclonic vorticity: in figure 2A the +100-foot isoline is located upstream over Nebraska, Kansas, western Oklahoma, and western Texas; in figure 4A the zero isoline suggests that the maximum relative cyclonic vorticity of Storm II was very shallow and less than +100 feet.

At this time, the precipitation pattern of Storm II was

located primarily under and to the west of the strongest curvature of the surface isobars in the extreme northern portion of the system. An inspection of the soundings southwest of the polar warm front showed that the warm sector air mass was very dry and would require considerable lifting for saturation. A shallow slope of approximately 1/125 for the warm front was found, which might suggest why the precipitation was occurring so far north of the system at this time. A few showers reported near the southeastern coast of Texas suggested the approach of more unstable tropical air.

The system continued moving northeastward to northeastern Kansas with some filling as the northern polar frontal system became diffuse and weakened (fig. 3B), another indication of further weakening of the warm and cold advection aloft. As the maritime polar cold frontal trough south of the Low moved eastward through central Texas, the warm front moved from the western Gulf of Mexico northward to southern Arkansas, central Mississippi, Alabama, and Georgia. Surface tendencies of Storm II had a well-defined northeast-southwest axis and indicated a continued northeastward movement of 25 knots with further weak filling. The precipitation pattern was still north of the surface Low center but had spread eastward from Nebraska to northern Iowa while widely scattered showers persisted along the western Gulf. By 0000 GMT of the 16th, the Low had moved to extreme northern Missouri with further weak filling (fig. 3C). The cold front moved slowly through Texas and the warm front advanced to central Arkansas. The 500-mb. chart showed that some sharpening of the upper trough had occurred in Nebraska as a closed Low formed in southern South Dakota. This was reflected on the advection chart (fig. 4B) as a small +200-foot area of relative cyclonic vorticity formed just west of the 700-mb. Low and as the region of positive vorticity extended southward through eastern Texas. This increase in amplitude or sharpening of the trough resulted from height rises (ridging) over New Mexico and Colorado following marked deepening over Nevada and southern California. This change over the Southwest—a process known as discontinuous retrogression of the long-wave pattern—was induced by large height rises east of Ship "Papa" as a very strong occluded system moved toward the Gulf of Alaska.

As the experienced forecaster would have expected at this point, the original trough in the central United States continued to move eastward as a minor or short wave while the new trough in the southwestern United States assumed major proportions with the development of a new storm on the polar front. The surface anallobaric field now intensified as rises also occurred ahead of the cold front in the warm Gulf air. The katallobaric field weakened mainly east-northeast of the center. Showers and thundershowers began just north of the warm front in Mississippi, Alabama, and western Tennessee. The advection chart for this time (fig. 4B) indicated a decrease in the warm and cold advection south of latitude 34° N. and a marked decrease in anticyclonic curvature of thickness lines, especially the 18,600-foot line. The strongest warm advection, though weak, was east of the Low center and well north of the surface warm front; and with time, this advection continued to decrease the slope of the warm front. Eastward acceleration of the surface occlusion in Missouri was suggested by the apparent stronger advection and the increased westerly component at 500 mb. through Kansas.

With flow at 700 mb. south of Kansas parallel to the thickness lines (no further cold advection southward), with positive surface tendencies ahead of the cold front, and with falling surface tendencies over the Southwest, the front in eastern Texas became quasi-stationary. Figures 3 D and E show that Storm II continued to fill and moved northeastward as its associated occluded front moved rapidly toward the east coast. The precipitation pattern associated with this Low remained north of the center, whereas the unstable precipitation moved eastward and remained near the warm front. The cold front moved slowly eastward through northern Mississippi and central Tennessee before stalling. By 0600 GMT of the 17th (fig. 3F) the polar front in eastern Texas began moving northward as a moderate warm front, as deepening occurred in southwestern Texas and as the ridge through the Dakotas southeastward to Kentucky strengthened. Overrunning precipitation north of the warm front fell in eastern Oklahoma northwestward through Wyoming.

MAXIMUM PRECIPITATION

The 1-inch isohyet of 24-hour maximum precipitation ending at 1200 GMT of the 16th associated with Storm II (fig. 4A) was well to the east of the maximum anticyclonically curved 18,400- and 18,600-foot thickness lines. One marked difference between the advection charts for Storm II (fig. 4A) and for Storm I (fig. 2A) was that the 700-mb. trough over Texas was somewhat farther east and much sharper in Storm I. Warm and cold advection on the 18,600-foot thickness line was much stronger in Storm I and the thickness ridge was somewhat farther east of the 700-mb. trough line. It has long been known that the influx of warm, moist air from the western Gulf of Mexico depends on the "opening-up" or southward deepening of the polar trough through eastern Texas. Experience has also shown that a definite influx of maritime tropical air occurs whenever the flow aloft in this air backs to a direction south of west (preferably southwest to south) in eastern Texas. This flow is frequently associated with the 10,000-foot contour at 700 mb. or the 18,800-foot contour at 500 mb. The greater the amplitude of the contour and the stronger the geostrophic flow east of the trough line, the greater the moist influx. As previously noted, advection for this case indicated that either little change or filling in the southern portion of the trough in Texas was

to be expected while the northern portion accelerated and moved eastward. The resultant predominantly westerly flow through Texas was dry along the 10,000-foot contour; the influx of moisture in Storm II was found along the 10,100- or 10,200-foot contour.

The 850-mb. chart for this time showed the +10° C. isodrosotherm located over southeastern Texas and Louisiana; the stability index chart delineated an area of zero stability encompassing southeastern Texas and western Louisiana. Precipitation began as showers and thunderstorms near the warm front (18,600-foot thickness contour) in northern Mississippi and western Tennessee 12 hours after the time of the advection chart, figure 4A. The time of this outbreak of precipitation corresponded with a northeasterly 12-hour movement (at 25 knots) of the center of moist unstable air from western Louisiana to the downstream position of strongest thermal wind shear along the 18,600-foot thickness line (fig. 4B). The continued northeastward movement of Storm II and the filling of the frontal trough continued to decrease the warm advection and terminated the maximum amounts of precipitation in the western Carolinas. The decrease of warm advection was borne out by the weakening of the isobaric gradient across the Gulf of Mexico in the surface maps of figures 3 C–F. The difference in intensity of the maximum precipitation area on figure 4B from that in figure 4A occurred because the precipitation began in the mid-period of figure 4A and moved eastward so slowly it overlapped and persisted for a longer period in figure 4B.

5. STORM III

SYNOPTIC SITUATION

As the short-wave trough, associated with the surface occluded front, moved over the ridge in the eastern Pacific, the deepening trough over the southwestern United States (discussed above) continued eastward. As this latter trough in western New Mexico became a major feature of the upper air it provided the energy for the development of Storm III on the polar front in northeastern Texas (fig. 5A).

The advection chart at this time (fig. 6A) indicated a very strong thickness gradient associated with the cold front through Texas, a fairly steep gradient ahead of the warm front, and a secondary packing of the thickness lines through northern Missouri and Illinois. The area of maximum positive relative vorticity was encircled by a small +200-foot isoline in northeastern Colorado; however, the area enclosed by the zero line was quite large with a probable secondary maximum over New Mexico. This secondary maximum of positive relative vorticity appeared to be in phase with the 700-mb. trough. It suggested that any further eastward movement of the southern portion of the 500-mb. trough, or the vorticity maximum over New Mexico, would produce marked instability in the level between 700 and 500 mb. and would probably result in an accelerated movement of the 700-mb. trough through Texas and likewise an increase in the cold advection term. Warm advection along the Oregon and northern California coast indicated some continued sharpening or southward deepening of this trough, whereas the strong zonal flow through northern Mexico suggested an eastward movement.

Some evidence of the unstable characteristics of the system was manifested on the surface chart by a band of fairly heavy precipitation in western Texas. (El Paso reported a thunderstorm to the east.) The southerly flow of definitely maritime tropical air off the western Gulf was heavily laden with moisture; showers and thundershowers occurred in the flow through Louisiana and Mississippi and along the leading edge of the warm front (figs. 5A and B). The main over-running precipitation was generally west of the wave crest, due to some extent to upslope flow east of the Divide.

The fields of strongest warm and cold advection suggested a definite northeasterly movement and further deepening of the surface Low. By 1200 GMT on November 18 (fig. 5C), the Low was well developed; it had deepened 4 mb. and the isallobaric field indicated further deepening. The orientation of the isallobars also suggested a more northerly movement of the Low. The katallobaric field to the north of the Low had falls of 5 to 6 mb. per three hours. The cold front, under the influence of increasing isobaric gradient along it, accelerated eastward as the warm front moved more slowly northward to southern Missouri and western Kentucky. Thunderstorms continued in the area along the warm front and along the entire length of the cold front. In general, the precipitation pattern enveloped the system; however, the pattern spread through northern Illinois and southern Wisconsin and all of Iowa (under and to the west of the strongest surface isobaric curvature and associated with the strong katallobaric field north of the Low).

From figure 6B, the advection chart for 1200 GMT, the thermal wind shear along the 18,600-foot thickness contour still suggested a warm front in southern Missouri and western Kentucky; however, it had definitely weakened as the stronger gradient in northern Illinois became more prominent. The strong warm advection indicated by this stronger gradient coincided with the increasing katallobaric field noted above. Cold advection through Oklahoma and eastern Texas had definitely increased and insured a strong surface cold front passage through the Gulf States, and also tended to further deepen or maintain the amplitude of the 500-mb. trough. The positive relative vorticity maximum shown in figure 6B had increased to a +200-foot value of fair size located south-southwest of the 700-mb. Low which had also deepened some 200 feet. Warm advection was still very strong and thus suggested a more northerly movement of the Low. Sustained strong cold advection across the Gulf, plus the advection of relative cyclonic vorticity at 500 mb., continued to deepen the system until it occluded as the cold advection persisted eastward and cut off the influx of warm air. In figure 5, D and E, the Low continued to deepen approximately 25 mb. as it turned sharply north-

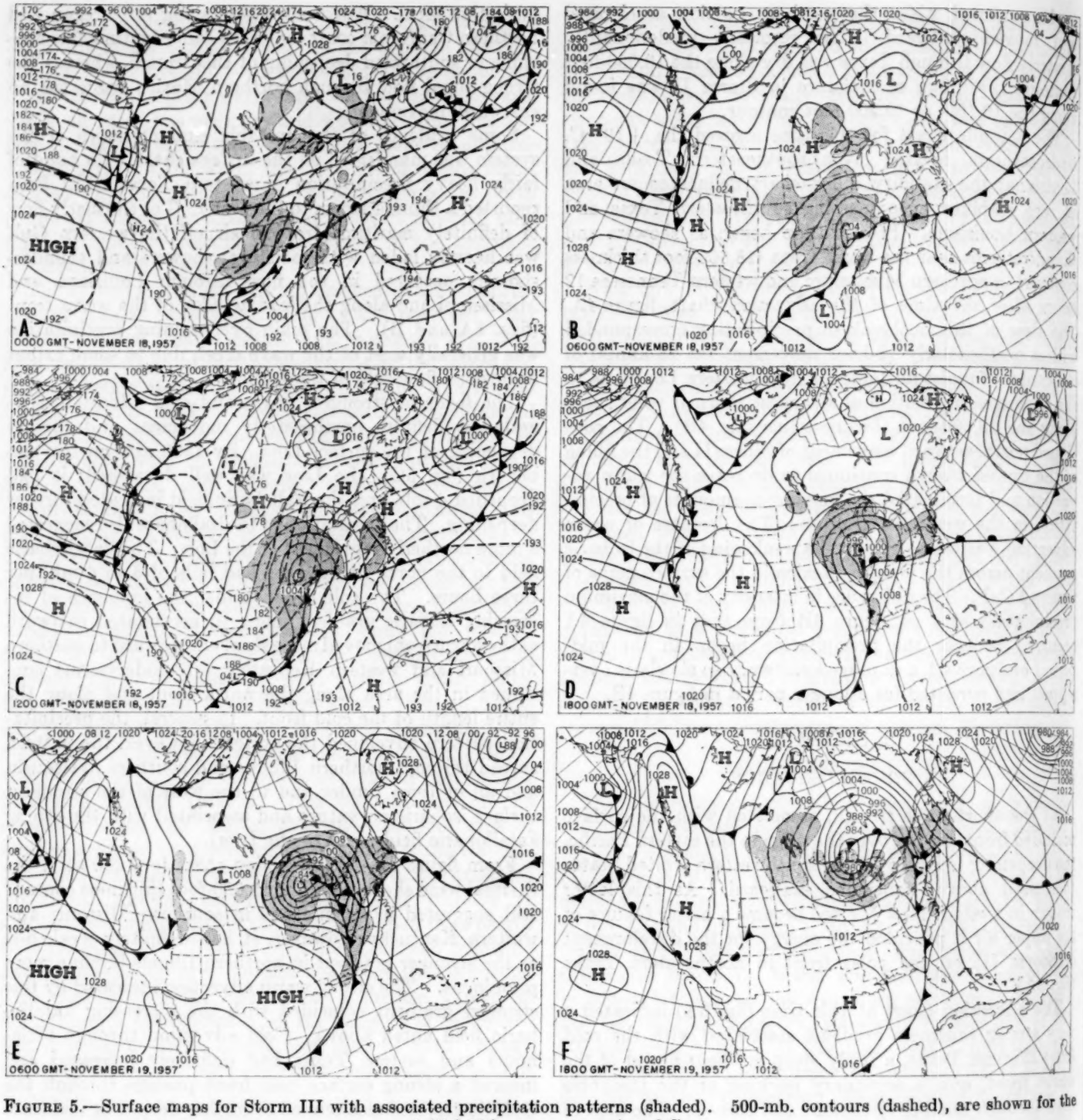

FIGURE 5.—Surface maps for Storm III with associated precipitation patterns (shaded). 500-mb. contours (dashed), are shown for the initial 12 hours on maps A and C.

ward across the western Great Lakes. By 1800 GMT of the 19th (fig. 5F), deepening had begun to level off with positive pressure tendencies spreading east of the Low as the cold front approached the Eastern Seaboard of the United States.

MAXIMUM PRECIPITATION

By 0300 GMT on November 18, thunderstorms began developing near Waco, Tex. along the leading edge of the cold front and also in eastern Oklahoma and northern Arkansas (north and east of the surface wave crest and under the strong warm advection on the 18,600-foot thickness contour.) Three hours later (fig. 5B), as the surface wave developed a closed circulation with a marked increase in shear across the cold front in eastern Texas, thunderstorms and heavy showers had occurred along the entire length of the front. Thunderstorms continued along the leading edge of the warm front in Arkansas and western Tennessee as over-running precipitation gradually appeared north of the band of thunderstorms. By 1200

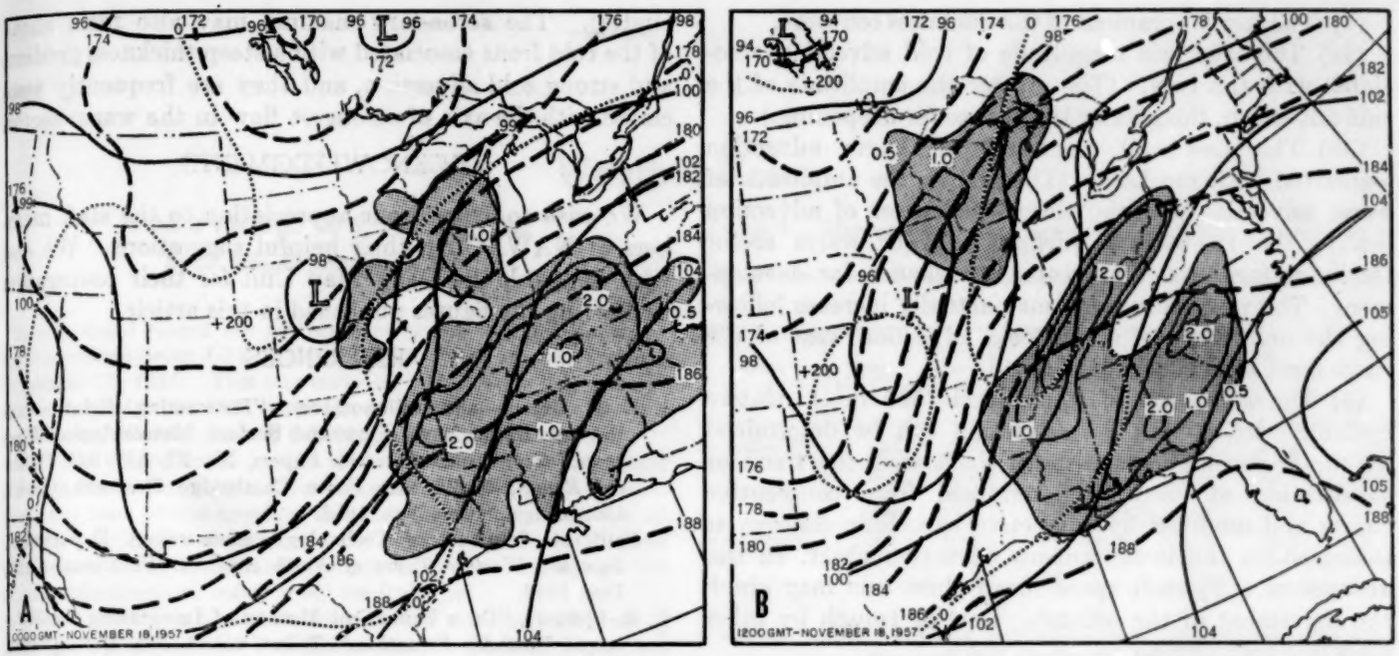

FIGURE 6.—Advection charts for Storm III with 700-mb. contours (solid), 1000–500-mb. thickness lines (dashed), areas of maximum precipitation ending 24 hours after chart (shaded), and area of maximum relative vorticity according to Fjørtoft's method (dotted lines).

GMT (fig. 5C) the over-running precipitation spread northward and westward as the warm front, under the influence of stronger southerly flow along it, moved northward to southern Missouri and western Kentucky. Thunderstorms with very heavy precipitation continued along the front in this area. In general the precipitation pattern enveloped the system; however, a diminishing precipitation was observed through central Missouri and central Illinois and an area of increasing precipitation was found through northern Illinois, southern Wisconsin, and all of Iowa. This region of increasing precipitation was under and to the west of the larger tendency falls.

The advection chart for 1200 GMT (fig. 6B) still gave good evidence for the warm front in southern Missouri and western Kentucky; however, the warm front had definitely weakened as the stronger gradient in northern Illinois and Indiana became more prominent. The strong warm advection associated with this steeper gradient coincided with the increasing rain pattern and large falling tendencies noted above. Some aspects of the diminishing rain pattern through central Missouri and central Illinois can be explained by the advection chart which shows a narrow flow parallel to the thickness pattern (no advective qualities) through Missouri.

At 0000 GMT of the 18th, the total precipitable water[2] associated with the southerly flow was well over 1 inch, and by 1200 GMT the 1-inch contour was carried northward to the latitude of the Low in northern Illinois and a 1.50-inch area was located over western and central Tennessee. The 24-hour maximum precipitation pattern which ended at 0000 GMT of the 18th (fig. 6A) was located over eastern Texas, western Louisiana, northeastward through southeastern Missouri, southern Illinois, southern Indiana, and western Kentucky, with a lobe shown over northern Illinois. The major axis of this maximum (2 inches or more) followed the movement of the peak of the warm sector as it moved north and eastward. The forming lobe was probably due to the main over-running associated with the steeper gradient of thickness values over northern Illinois and Indiana plus the intense isobaric curvature of the deepening surface Low. By 1200 GMT the 24-hour precipitation pattern (fig. 6B) displayed maxima along three axes: (1) The northernmost axis in northern Illinois (fig. 6A) coincided with the path of this deepening Low. (2) Another axis followed the path of the apex of the warm sector and overlapped values of the maximum precipitation indicated in figure 6A. (3) The third axis began as an intense area of thunderstorms along the cold front in eastern Texas and western Louisiana (fig. 5, C, D, and E) and moved eastward with the cold front.

6. CONCLUSIONS

Three major storms whose history and initial development were very similar have been discussed. An attempt has been made to show how further developments of each storm depended on the changes in the 1000–500-mb. thickness patterns, and how the instantaneous flow could be used to indicate how such changes would occur. One characteristic of this type of storm is that the influx of moist, unstable, maritime tropical air is induced into the storm circulation as it develops east of the Divide with the rate of influx varying as the development varies.

Deepening or increased development of this type of storm appears to be related to the following three parameters:

[2] On November 16 a precipitable water chart was started at NAWAC.

(1) The current gradient of the thickness contours.

(2a) The area and magnitude of cold advection associated with the Low. (The greater the amplitude of the cold advection, the greater the chance for deepening.)

(2b) The area and magnitude of warm advection associated with the Low. (The greater the amplitude of warm advection and the closer the center of advection lies to the 18,600-foot thickness line or warm sector thickness contours, the greater the chance for development. The warm advection may actually increase following the occurrence of strong cold advection west of the wave crest as in Storm III.)

(3) The advection of upper-level (500 mb.) relative cyclonic vorticity. (The advection can be determined by the Fjørtoft [3] space mean chart with the trend or acceleration of vorticity determined from consecutive charts and modified by subjective baroclinic changes as indicated on the instantaneous advection chart. In the absence of a Fjørtoft space mean chart one may check the movement of the 500-mb. Low or trough by other objective techniques.)

Areas of maximum 24-hour precipitation are directly related to the rate of influx of moist, unstable, or conditionally unstable, maritime tropical air and with the thickness gradient of the warm front. In time, the maximum precipitation moves along a path prescribed by the movement of the areas of warm advection. With intensification of the surface Low, areas of secondary maxima may form well north of the warm front and become aligned with the path of the Low (diminishing as the Low occludes). The secondary maxima may also form ahead of the cold front associated with a steep thickness gradient and strong cold advection, and they are frequently associated with the axis of strongest flow in the warm sector.

ACKNOWLEDGMENTS

We wish to express our appreciation to the staff members of NAWAC for their helpful suggestions. We also wish to thank the Daily Map Unit for their cooperation in drafting the figures published in this article.

REFERENCES

1. J. J. George and collaborators, "Forecasting Relationships Between Upper Level Flow and Surface Meteorological Processes," *Geophysical Research Papers*, No. 23, AFCRC *Technical Report*, 53–28, Air Force Cambridge Research Center, Cambridge, Mass., Aug. 1953.
2. California Institute of Technology, Meteorology Department, *Synoptic Weather Types of North America*, Pasadena, Calif., Dec. 1943.
3. R. Fjørtoft, "On a Numerical Method of Integrating the Barotropic Vorticity Equation," *Tellus*, vol. 4, No. 3, Aug. 1952, pp. 179–194.
4. R. C. Sutcliffe and A. G. Forsdyke, "The Theory and Use of Upper Air Thickness Patterns in Forecasting," *Quarterly Journal of the Royal Meteorological Society*, Vol. LXXVI, No. 328, Apr. 1950, p. 189.
5. H. L. Jacobson, R. A. Sanders, and D. M. Hanson, "The Central High Plains Storm of November 1–3, 1956," *Monthly Weather Review*, vol. 84, No. 11, Nov. 1956, pp. 401–414.
6. S. Petterssen, "A General Survey of Factors Influencing Development at Sea Level," *Journal of Meteorology*, vol. 12, No. 1, Feb. 1955, pp. 36–42.

Weather Notes

WORLD RECORD LOW TEMPERATURE

South Pole, September 17, 1957*

A new world record low temperature of −102.1° F. was set at the Amundsen-Scott IGY Station (South Pole) at 2137 GMT on September 17, 1957. This was lower by 1.7° F. than the previous world record of −100.4° F. set at the same station on May 11, 1957 (see *Monthly Weather Review*, vol. 85, No. 6, June 1957, p. 207).

The new record came as the climax to the coldest sustained period in the coldest month so far experienced at this frigid outpost. From the time of the previous record-breaking mark on May 11 the daily minimum temperature went below −95° F. on 17 occasions, while during the period in which the new record was set the temperature remained below −90° for 93 hours!

It is interesting to note that this period of extreme cold came at the very close of the South Pole winter season. In fact, throughout this period the sun's image (although greatly distorted) was observed as a flaming mirage of the upper limb. Due to refraction phenomena in the highly stratified air, the sun reappeared "prematurely" about a week before the "official" sunrise on September 23, 1957, when the actual disk was about 3 degrees below the horizon.

Table 1 presents the significant surface and near-surface meteorological data about the time at which the new record was established The 2-m. air temperatures are those observed in the screen and constitute the official air temperatures for the station.

A deck of cirrostratus began advancing at 2200 GMT on September 17 and the sky became overcast by 0800 GMT on the 18th, at which time light snow began to fall. Thus the rapid warming observed between 0245 and 1200 GMT September 18 was undoubtedly the result of increased long-wave radiation to the surface from the cloud cover.

Reference to the note and comparable figures in the *Monthly Weather Review* reporting the May 11 observations brings out noteworthy differences and similarities. On September 17 the wind directions veered significantly from those observed on May 11, giving further substantiation to the hypothesis that the occurrence of extreme low temperatures is probably related to the diminution of vertical mixing rather than advection or cold-air drainage from elsewhere.

However, surface wind directions in the sector 60° E. through 160° E. were accompanied by significantly lower temperatures than surface winds from any other direction. It should be pointed out that greater than 90 percent of the surface winds were from a direction 20° W. clockwise to 180° (through 90° E.). Further, the wind speeds immediately preceding the −102.1° reading were lower than those preceding the −100.4° reading on May 11, and the surface inversion nearly 3 times as great. At the time of the −102.1° reading the inversion from 2 to 10 m. was 22.6 F.°, while for the −100.4° reading on May 11 that inversion was only 8.4 F.° On September 17 there was a rise of over 70 F.° in the lower 30 mb. or so of the atmosphere compared to about 50 F.° rise on May 11.

Table 2 is a continuation of the monthly data presented in the note on p. 207 of the June 1957 *Monthly Weather Review*.

*A previous note in the *Monthly Weather Review* (vol. 85, No. 9, Sept. 1957, p. 326) reported this record low temperature as having been observed at 2137 GMT, Sept. 18, 1957. That note should be corrected to indicate 2137 GMT, Sept. 17, 1957.

TABLE 1.—*Meteorological data, Amundsen-Scott IGY Station (South Pole), September 17–18, 1957*

Date	Time (GMT)	Wind		Temperature (° F.)			
		Direction (Meridian)	Speed (kt.)	Sfc.	Air		
					2m.	5m.	10m.
September 17	1800	70E	5	−99.3	−96.6	−94.7	−77.8
	1930	----------	calm	−100.0	−93.7	−90.8	−75.2
	2003	90E	2	−101.7	−100.0	−97.5	−85.9
	2137	110E	4	−103.3	−102.1	−101.0	−79.5
	2200	90E	5	−99.0	−94.9	−88.0	−75.6
	2340	110E	4	−102.2	−101.7	−101.1	−82.0
September 18	0245	135E	6	−100.5	−100.0	−98.8	−90.6
	1200	70E	7	−69.1	−69.1	−69.1	−68.8

TABLE 2.—*Mean wind data, mean and extreme temperatures. Amundsen-Scott IGY Station (South Pole)*

Month	Mean Wind		Temperature (° F.)		
	Direction (Meridian)	Speed (kt.)	Mean	Max.	Min.
1957					
January*	0°	9	−18.1	−6.0	−29.8
February	20E	10	−36.8	−18.0	−69.2
March	30E	11	−64.7	−35.0	−82.5
April	20E	15	−69.7	−25.6	−89.1
May	30E	15	−68.3	−30.1	−100.4
June	40E	17	−69.6	−42.3	−97.0
July	20E	15	−77.5	−40.7	−98.8
August	20E	16	−72.7	−45.4	−99.7
September	30E	13	−80.1	−57.7	−102.1
October	30E	14	−62.9	−45.4	−86.1
November	20E	10	−34.4	−2.2	−55.1
December	20E	7	−13.4	−2.0	−21.5

*Period Jan. 11–31.

During the whole of the winter night the mean temperature was approximately −73° F., with a maximum of −25.6° on April 6 and the minimum of −102.1°. During 90 percent of the whole time the temperature was below −58° F., with temperatures below −90° F. about 12 percent of the time. The mean wind speed was about 15 kt. with only 25 hours of calm weather observed. The peak gusts were on the order of 47 kt.—*E. C. Flowers and R. A. McCormick, U. S. Weather Bureau, Washington, D. C.* (Mr. Flowers was Chief Meteorologist at Amundsen-Scott IGY Station, January–December 1957.)

POST-FRONTAL OROGRAPHIC MAMMATOCUMULUS,

Sackets Harbor, N. Y., July 5, 1957

On the afternoon of July 5, 1957, a cool post-frontal mass of polar continental air was moving briskly eastward from Lake Ontario toward the Tug Hill Plateau and Adirondack Mountains of northern New York State, producing vivid evidence of strong on-shore winds and of pronounced convective instability in the form of a strange-looking lenticular cloud with a pronounced mammatocumulus formation on the lower surface. At least one thundercloud was also seen in the general area, but the entire area had, otherwise, large areas of very clear blue sky until late in the afternoon. The observer was taking a pleasure ride by automobile, and the spectacular appearance of very large, very widely spaced cumuli

boldly outlined in the very clear atmosphere led him to watch carefully the clouds and weather encountered.

About noon, near Syracuse, N. Y., cumulus and stratocumulus nearly covered the sky, the temperature was 79° F., the dewpoint, 59° F., and the wind was west at about 13 knots and somewhat gusty. About an hour later, at Mexico, N. Y., about 30 miles north of Syracuse near the southeastern corner of Lake Ontario, the sky was almost clear with a very few small cumuli; visibility was excellent, and the sky was a very deep blue, rare in central New York. A few miles farther north, a few minutes later, at Port Ontario close to the southeastern shore, the sky was still beautifully blue and almost cloudless, but far in the northern sky was a towering cumulonimbus with anvil, with its hard, turbulent surface brightly illuminated with a remarkable, distinctive pink glow, unlike the yellowish white of the nearer small clouds. The crackle and crashes of distant lightning were noticed on the auto radio. Farther north along the shore, the west wind, which had been increasing, became strong enough to make steering difficult on this highway. But the sky became perfectly cloudless, except for the very distant thundercloud. A short distance northeast of Sackets Harbor (slightly west of Watertown, near the northeastern corner of the lake), about 70 miles north of Syracuse about 2 p. m. EST, the sun seemed to become weaker, at first by a thin, nearly invisible white web that was first thought to be cirrus, but soon considered to be altostratus because it became a white layer that was obviously lower and thicker. It extended a few miles west, a few miles north, and many miles south, but it did not extend east of the zenith. By now, the distant thundercloud was much nearer, white instead of pink, and displaced eastward.

On Pillar Point, about 12 miles west of Watertown, around 2:30, the cloud layer observed previously farther southeast had become threateningly dark. It extended many miles south, but its western edge was clean and sharp, oriented approximately along the lake shore. To its west the sky was clear over the lake. To its immediate east the sky was clear, and farther east there were many moderate-sized cumuli. The layer did not extend north beyond Pillar Point; northward the overhead sky was clear, and much farther north there were small cumuli. The tallest cumulus clouds were in the northeastern sky, where the thundercloud had been. Fresh puddles were noticed here along the road, as if the thundercloud had passed here earlier.

By now, the dark layer cloud had a remarkable appearance. It seemed almost as low as the cumulus clouds, so all the while it must have been stratocumulus and not altostratus. But it remained quite shallow, with a smooth, flat, white top and smooth, sharp, white edges, as if it were a large, detached sheet of white altostratus, but much lower and somewhat thicker. It had a definite lenticular appearance, similar to the "wave" clouds near Bishop, Calif. It did not seem to progress eastward. But its outstanding peculiarity was its lower surface: hanging down over a large area were numerous black hemispherical mammatocumulus bulges, each bulge immediately adjacent to its neighbors; the dimensions of each bulge were not larger than about one-tenth of the dimensions of medium-sized fair-weather cumulus clouds. No precipitation or lightning were observed in connection with this cloud, but it had a black, stormy appearance.

At about 3:30 p. m. EST, on the isthmus joining Point Peninsula to the mainland, about 20 miles west of Watertown, where the road passes closely to the shore of the main open part of the lake, the waves were large and white, and spray was driven by the wind across the road. The temperature there was 68° F. and the dewpoint 56°. By comparison, the observer's instruments near Syracuse registered a high of 81° that afternoon. The wind at the shore was estimated to be about 42 m. p. h. from the west, sometimes as high as 50 m. p. h. It was difficult to stand still while using a camera, in such a wind. The sun was shining here. The dark elongated lenticular cloud with mammatocumulus was still there, oriented north-south along the shore and extending far southward from a point a short distance to the south. It seemed to be forming on the west edge and dissipating on the east edge. The sky was still cloudless to the west over the lake, and there were hard, sharply-defined cumuli southeast, east, northeast, and north, the largest northeast. It was clear overhead. Very far in the south-southwest very large, boiling cumulus clouds were seen to be increasing in size.

About 5:15, for a stretch of many miles, beginning a few miles northwest of Watertown and continuing many miles south-southwest of Watertown, the elongated lenticular cloud with dark mammatocumulus was still oriented along the shore, west of the route being travelled, with clear sky beyond it to the west over the lake, clear sky overhead, and many medium-sized cumuli along the eastern horizon. No precipitation or lightning was seen yet.

Near Pulaski, near the southeastern corner of the lake and much closer to the lake than Watertown, at around 5:45 p. m., the highway was well within the area covered by the layer cloud, but now the layer cloud looked like an ordinary flat, high stratus layer, very closely resembling lo[illegible]hick altostratus in appearance; it was fibrous, and seemed to be actually in two layers, the lower layer broken. Here there was no lenticular appearance, and there was no mammatocumulus structure. Not far east, there were cumulus clouds instead of the overhead stratus, and there was no clear strip along the east edge of the layer. A few miles southwest there was a conspicuous thunderstorm cell, with cloud-to-ground lightning and a dense shaft of rain. This storm was moving east. Winds were still strong enough to require extra caution in steering the automobile.

Much farther south, in the vicinity of Central Square and Brewerton, about 15 miles north of Syracuse, stratocumulus connecting that thundercloud with another thunderstorm several miles south was passing eastward overhead, with lightning and a sprinkle of large raindrops. The time was now about 6:15 p. m. The north thunderstorm appeared much more intense than the south thunderstorm. Many miles east there was an isolated cumulonimbus with heavy shower. In Syracuse at 7 p. m., the sky was almost covered with bulky stratocumulus masses, and the streets were wet. Shortly afterward the sky had fewer clouds, and the observer's instruments showed 62° F. temperature, 55° dewpoint, west wind at about 5 knots, and 0.02 inch of rain caught in the gage while he was gone. No fronts or squall lines appeared on the published weather maps in connection with these storms.

The weather thus described was evidently influenced by topography. A line running east-west through Syracuse separates the Alleghany Plateau (1,200 to 2,200 feet above mean sea level) to the south, from the Lake Plain (400 feet above m. s. l.) to the north. Lake Ontario is less than 300 feet above sea level, and the Tug Hill Plateau, about 25 miles in diameter, immediately east of Lake Ontario (centered east-northeast of Pulaski which is near the southeastern corner of the lake), is generally about 1,800 to 2,000 feet above sea level; this plateau is about 25 miles south-southeast of Watertown. Ordinarily the weather patterns here under similar synoptic conditions are obscured by widespread overcast and poor visibility, but on this day the patterns were vivid and sharp because of the strong wind, low moisture content, and clear air.—*C. R. Embree, 214 Draper Ave., Syracuse 4, N. Y.*

U. S. GOVERNMENT PRINTING OFFICE: 1958

Chart I. A. Average Temperature (°F.) at Surface, November 1957.

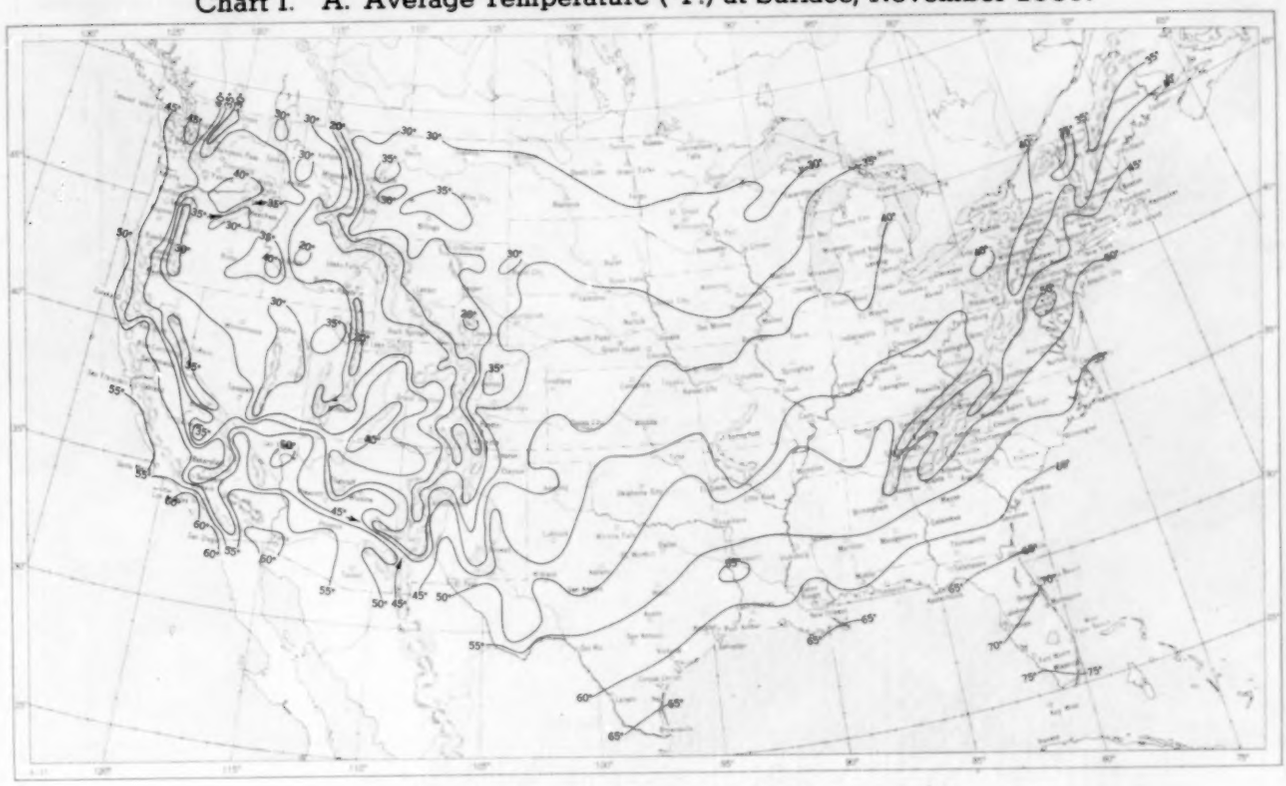

B. Departure of Average Temperature from Normal (°F.), November 1957.

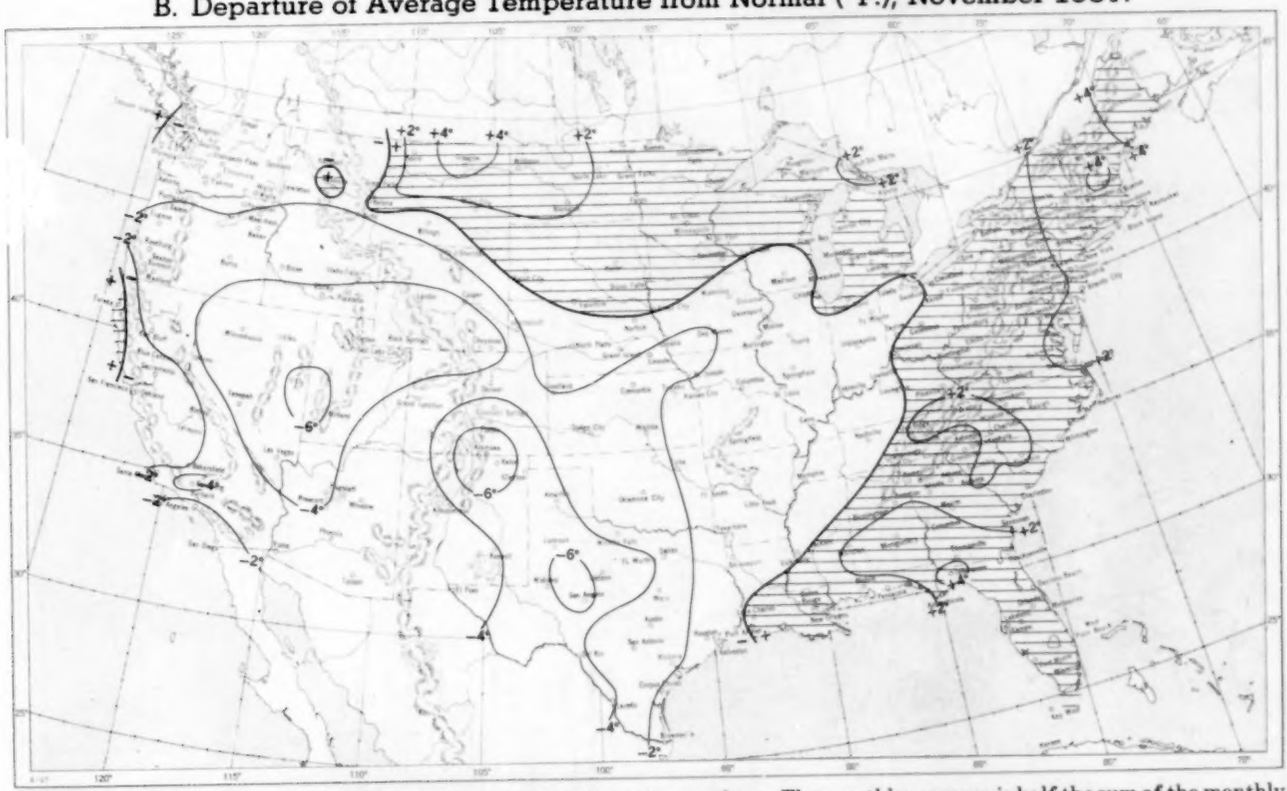

A. Based on reports from over 900 Weather Bureau and cooperative stations. The monthly average is half the sum of the monthly average maximum and monthly average minimum, which are the average of the daily maxima and daily minima, respectively.

B. Departures from normal are based on the 30-yr. normals (1921-50) for Weather Bureau stations and on means of 25 years or more (mostly 1931-55) for cooperative stations.

Chart II. Total Precipitation (Inches), November 1957.

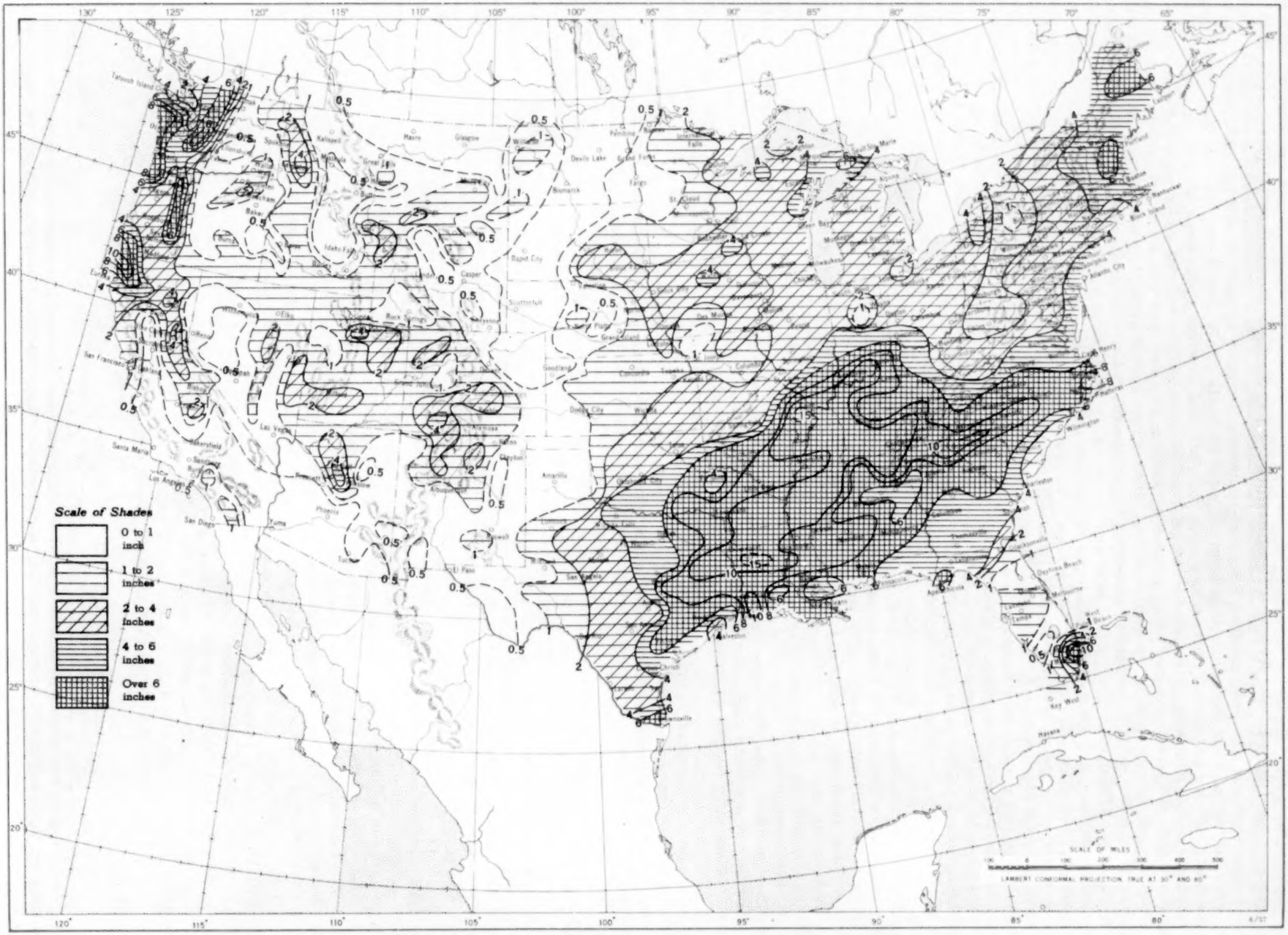

Based on daily precipitation records at about 800 Weather Bureau and cooperative stations.

Chart III. A. Departure of Precipitation from Normal (Inches), November 1957.

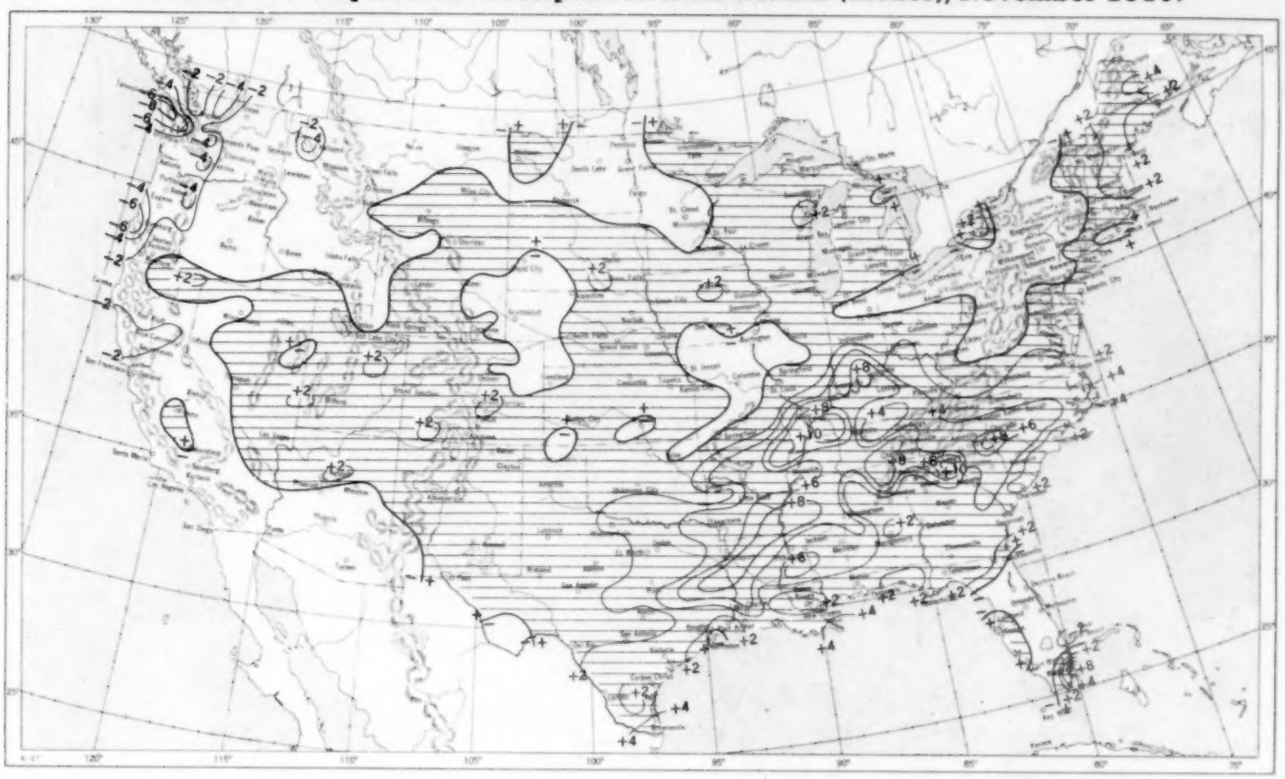

B. Percentage of Normal Precipitation, November 1957.

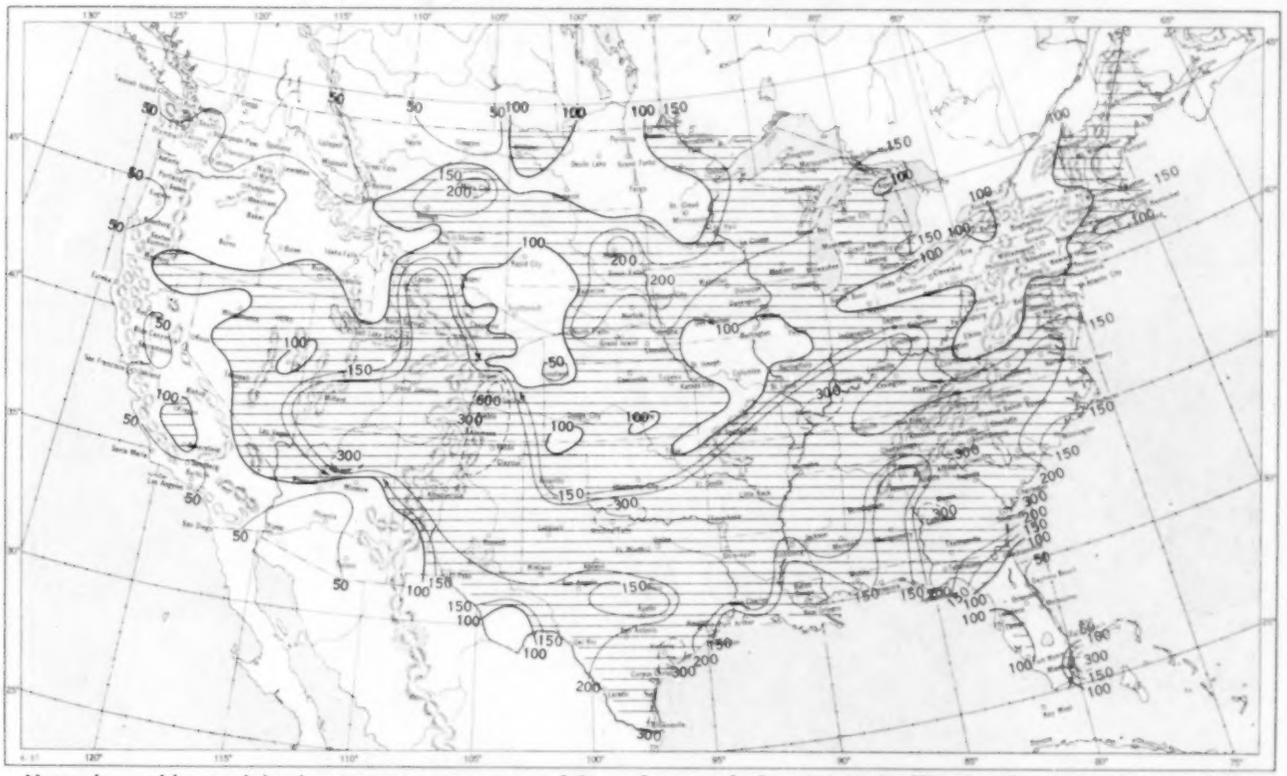

Normal monthly precipitation amounts are computed from the records for 1921-50 for Weather Bureau stations and from records of 25 years or more (mostly 1931-55) for cooperative stations.

Chart IV. Total Snowfall (Inches), November 1957.

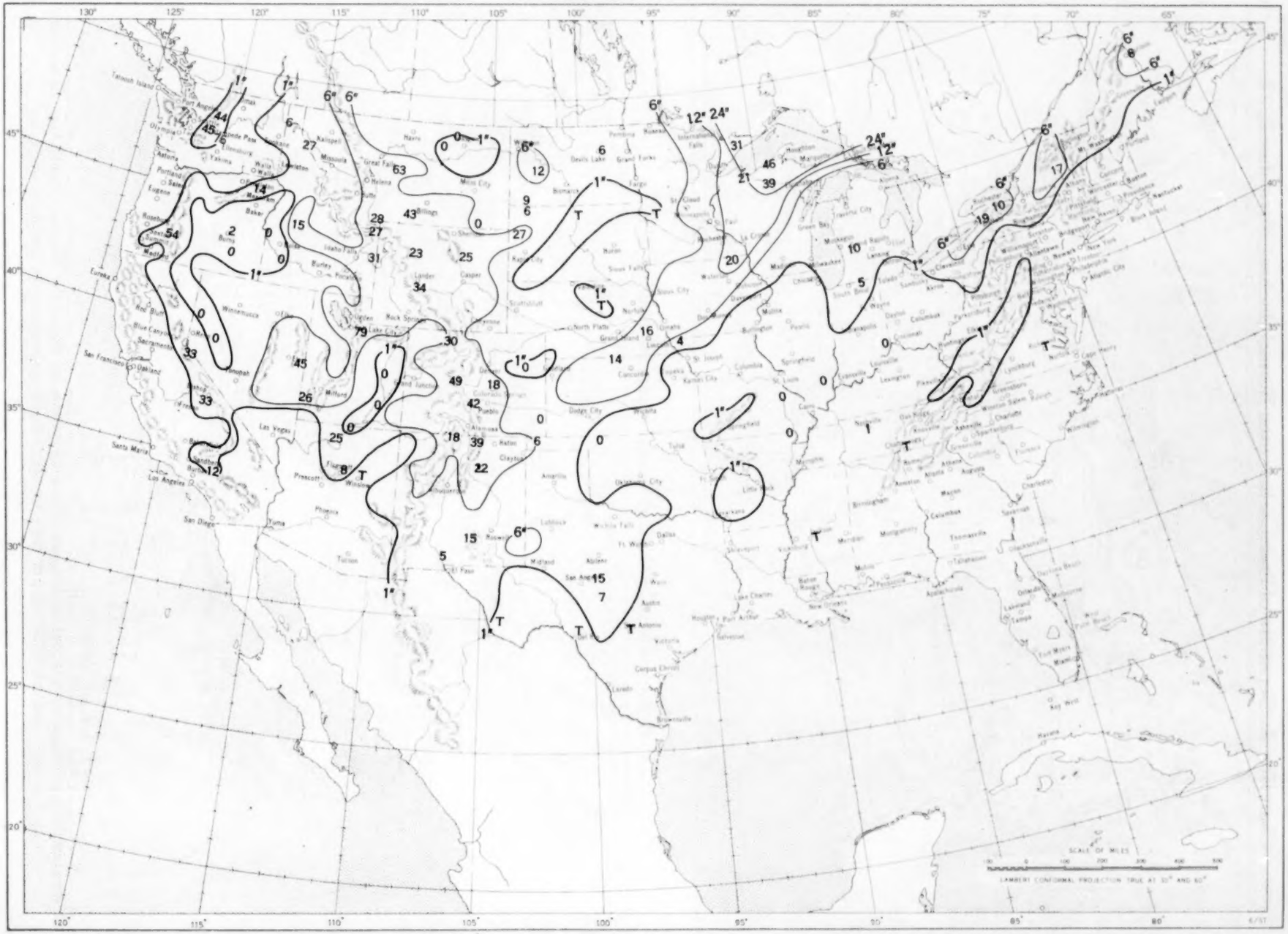

This is the total of unmelted snowfall recorded during the month at Weather Bureau and cooperative stations. This chart and Chart V are published only for the months of November through April although of course there is some snow at higher elevations, particularly in the far West, earlier and later in the year.

Chart V. A. Percentage of Normal Snowfall, November 1957.

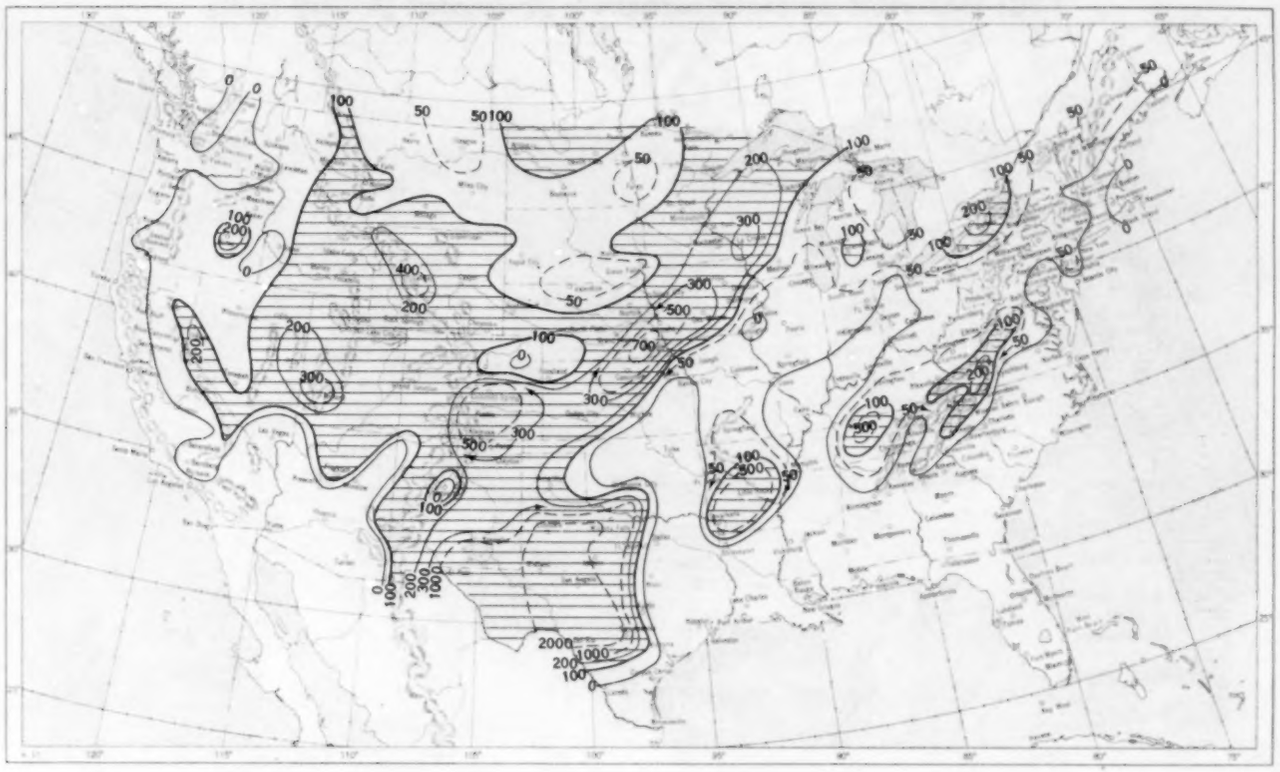

B. Depth of Snow on Ground (Inches), 7:00 a. m. E. S. T.

A. Amount of normal monthly snowfall is computed for Weather Bureau stations having at least 10 years of record.
B. Shows depth currently on ground at 7:00 a. m. E. S. T., of the Monday nearest the end of the month. It is based on reports from Weather Bureau and cooperative stations. Dashed line shows greatest southern extent of snowcover during month.

Chart VI. A. Percentage of Sky Cover Between Sunrise and Sunset, November 1957.

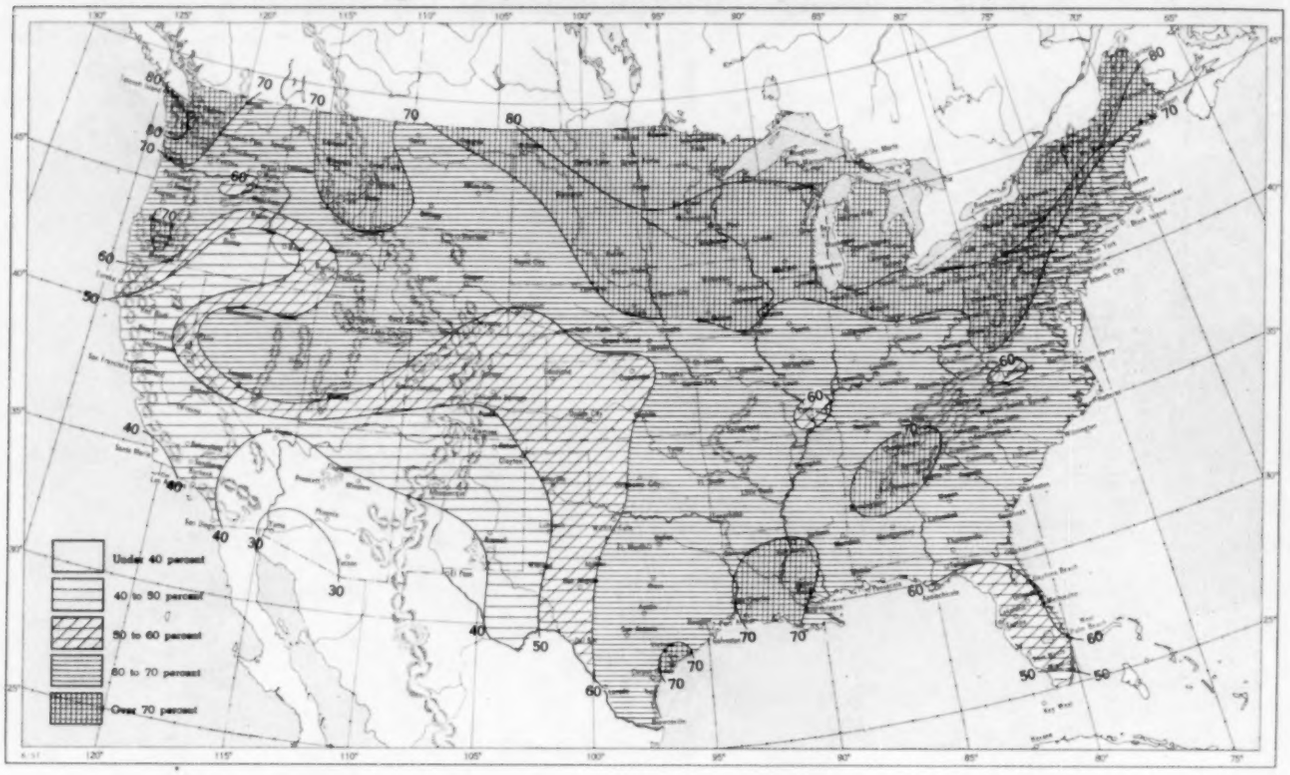

B. Percentage of Normal Sky Cover Between Sunrise and Sunset, November 1957.

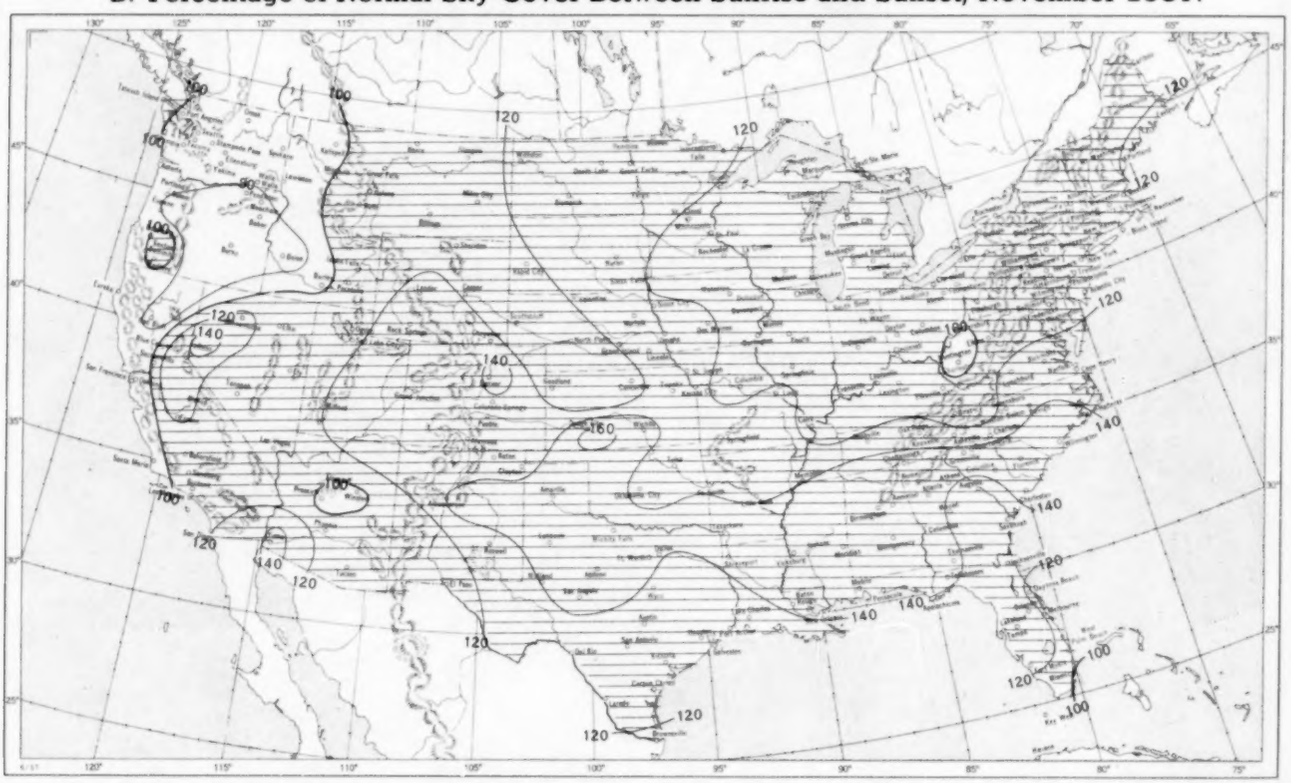

A. In addition to cloudiness, sky cover includes obscuration of the sky by fog, smoke, snow, etc. Chart based on visual observations made hourly at Weather Bureau stations and averaged over the month. B. Computations of normal amount of sky cover are made for stations having at least 10 years of record.

Chart VII. A. Percentage of Possible Sunshine, November 1957.

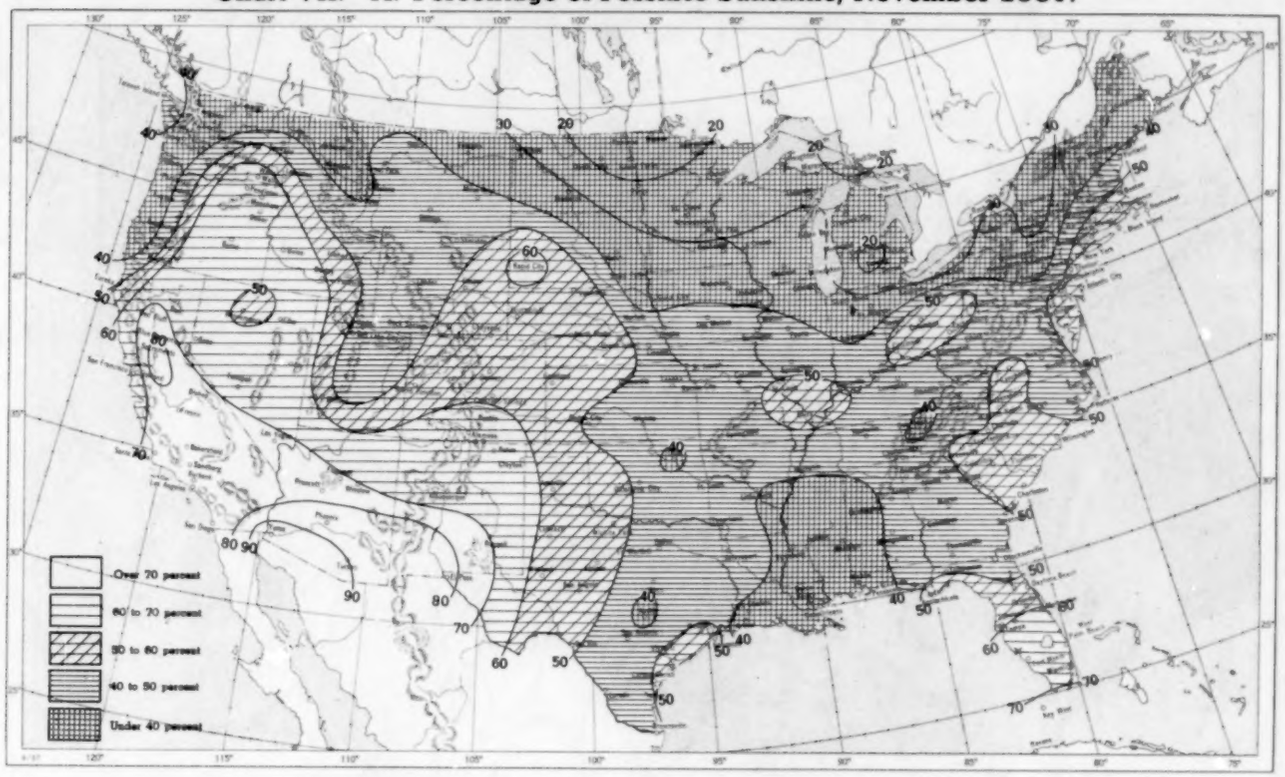

B. Percentage of Normal Sunshine, November 1957.

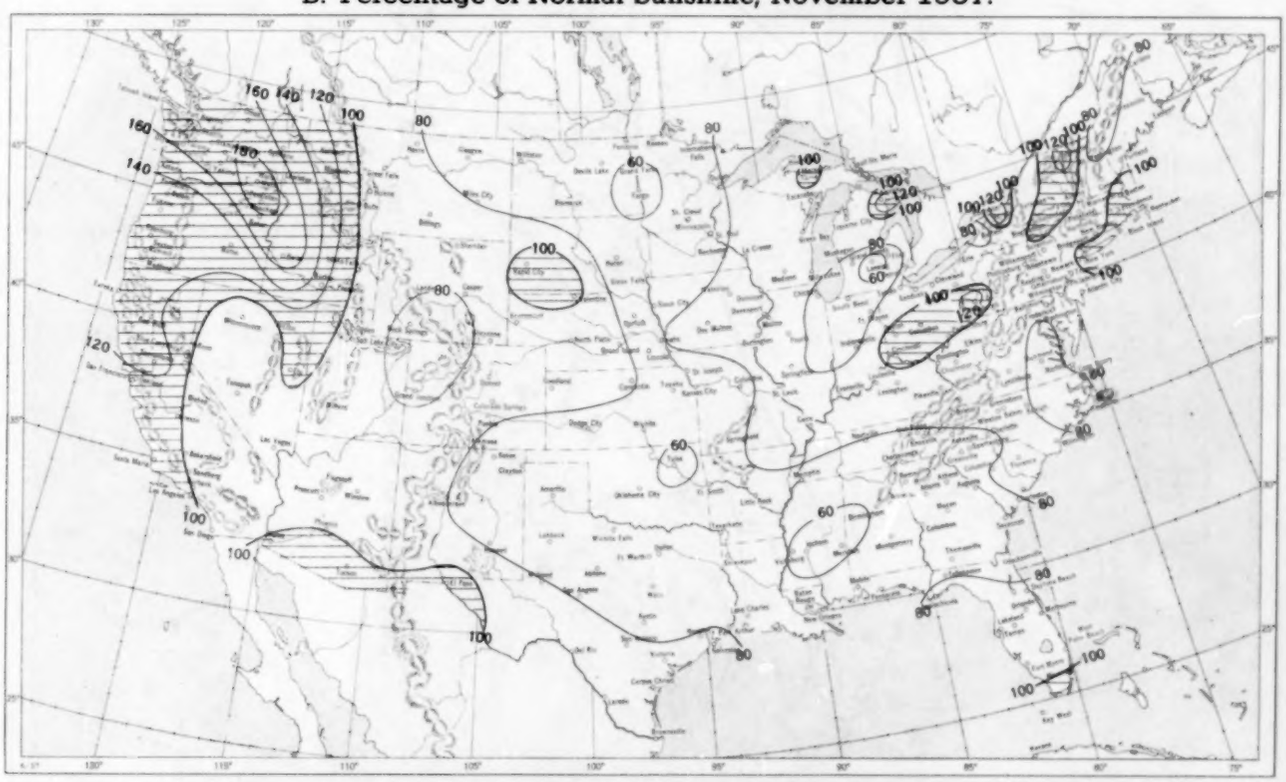

A. Computed from total number of hours of observed sunshine in relation to total number of possible hours of sunshine during month. B. Normals are computed for stations having at least 10 years of record.

Chart VIII. Average Daily Values of Solar Radiation, Direct + Diffuse, November 1957. Inset: Percentage of Mean Daily Solar Radiation, November 1957. (Mean based on period 1951-55.)

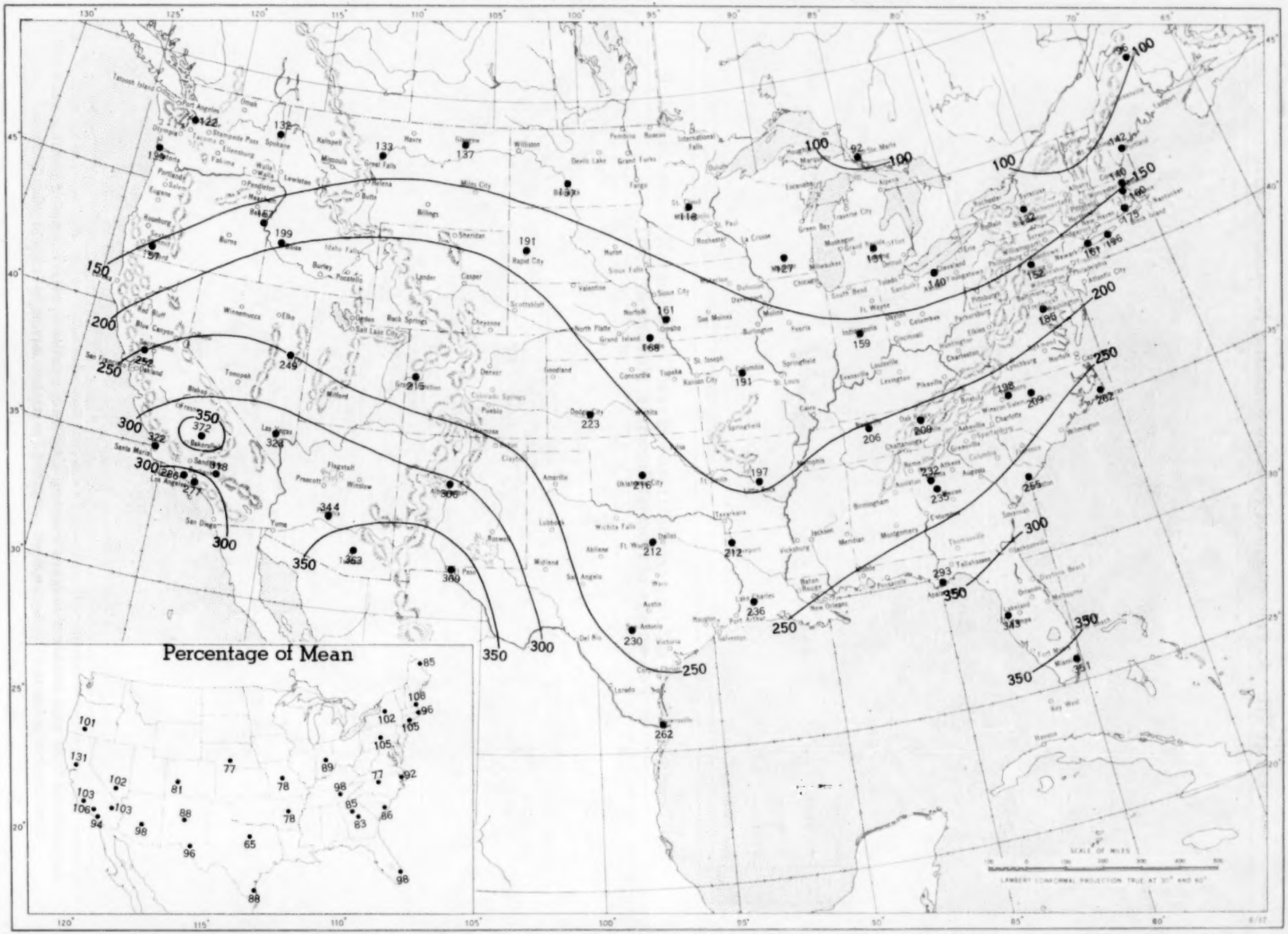

Chart shows mean daily solar radiation, direct + diffuse, received on a horizontal surface in langleys (1 langley = 1 gm. cal. cm. $^{-2}$). Basic data for isolines are shown on chart. Further estimates are obtained from supplementary data for which limits of accuracy are wider than for those data shown. The inset shows the percentage of the mean based on the period 1951-55.

Chart IX. Tracks of Centers of Anticyclones at Sea Level, November 1957.

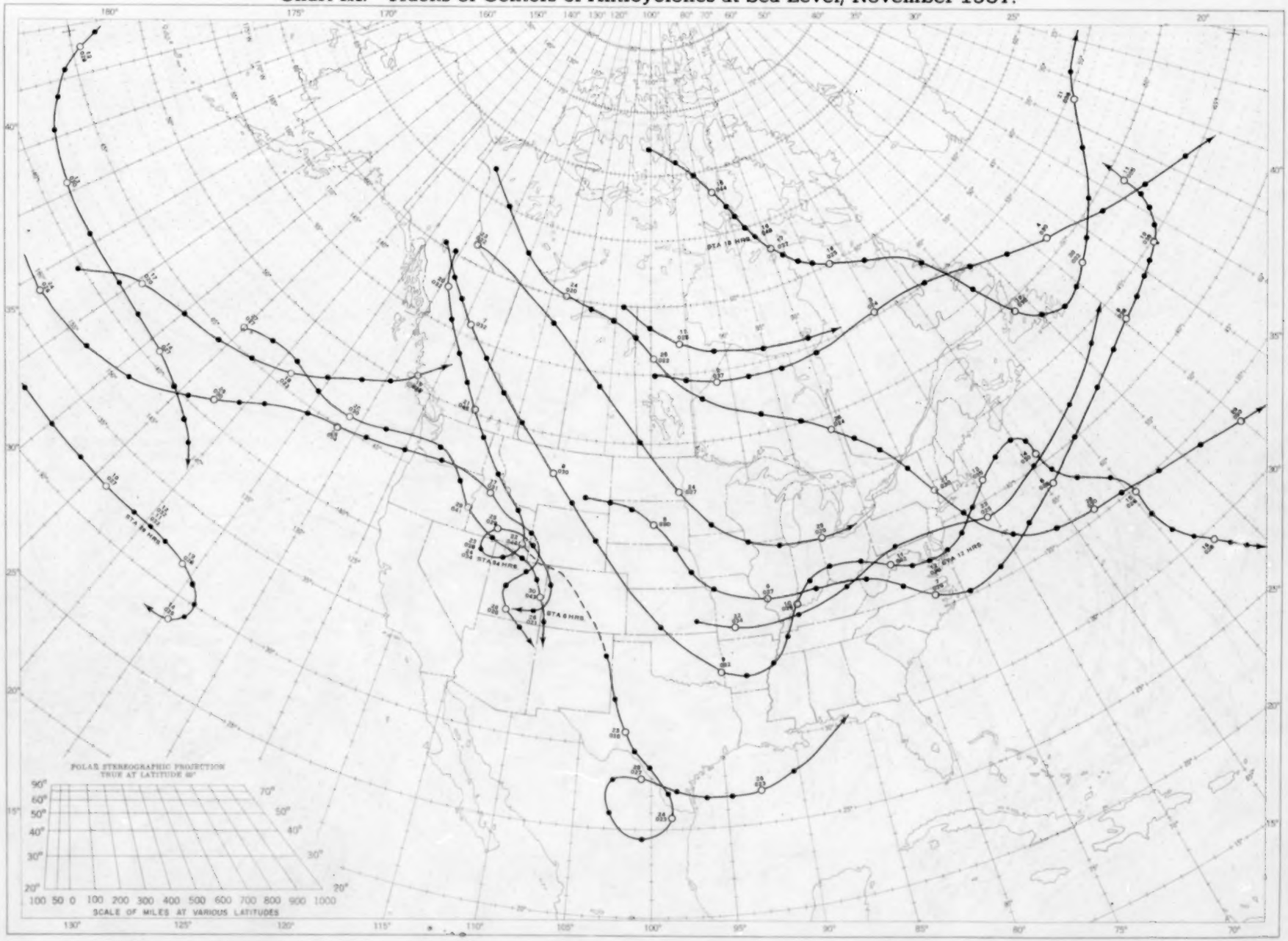

Circle indicates position of center at 7:00 a. m. E. S. T. Figure above circle indicates date, figure below, pressure to nearest millibar. Dots indicate intervening 6-hourly positions. Squares indicate position of stationary center for period shown. Dashed line in track indicates reformation at new position. Only those centers which could be identified for 24 hours or more are included.

Chart X. Tracks of Centers of Cyclones at Sea Level, November 1957.

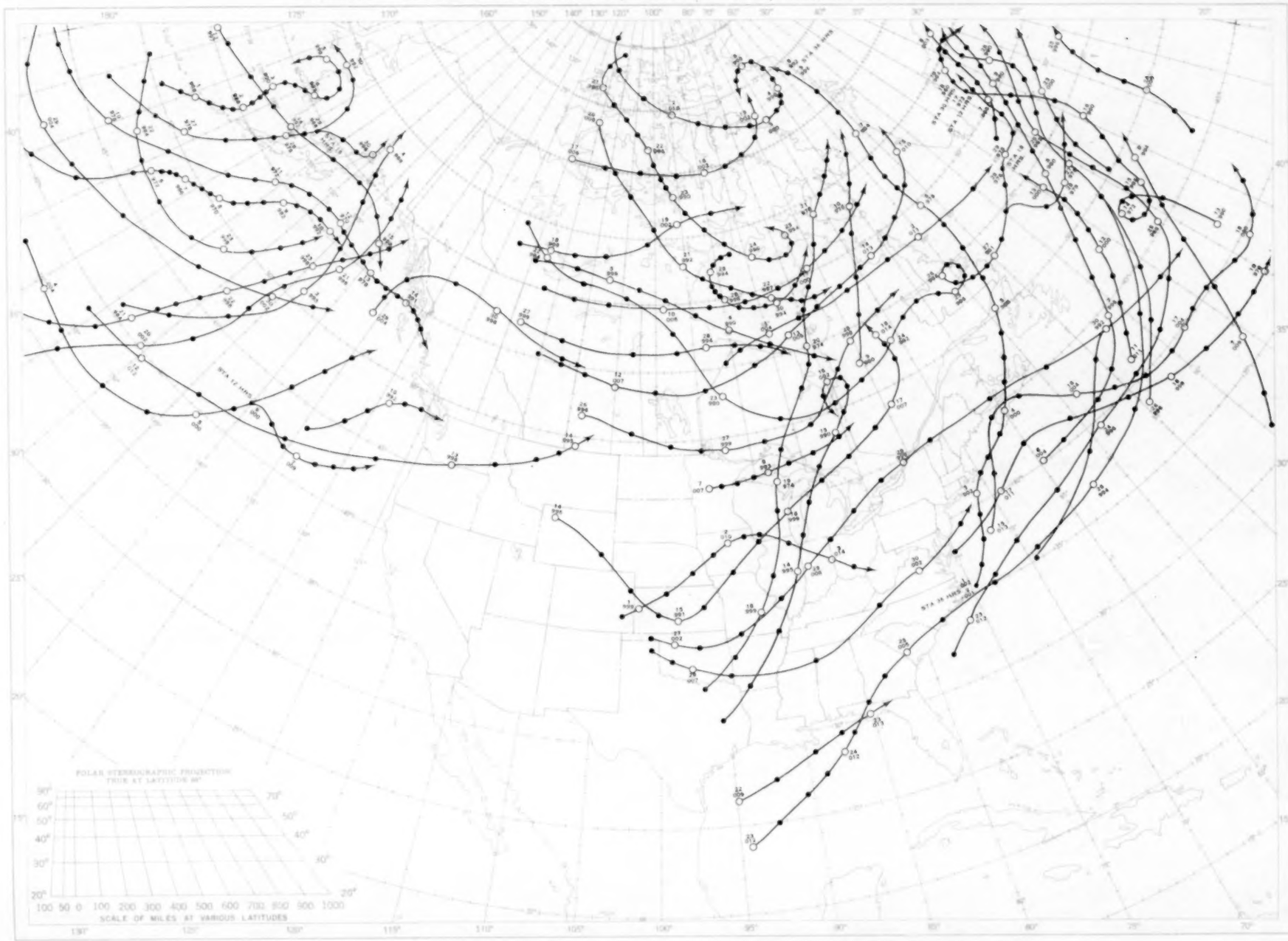

Circle indicates position of center at 7:00 a. m. E. S. T. See Chart IX for explanation of symbols.

Chart XI. Average Sea Level Pressure (mb.) and Surface Windroses, November 1957. Inset: Departure of Average Pressure (mb.) from Normal, November 1957.

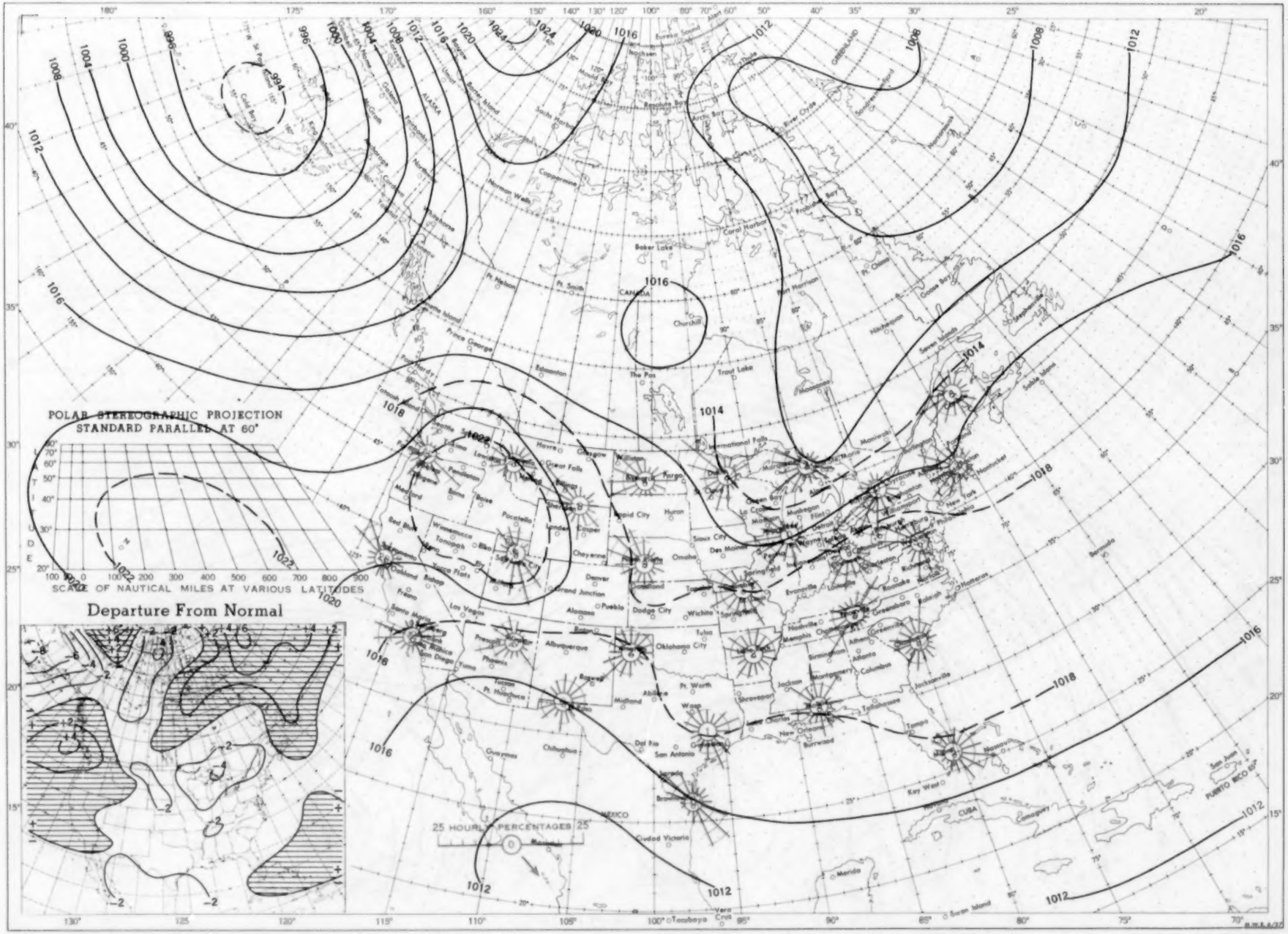

Average sea level pressures are obtained from the averages of the 7:00 a. m. and 7:00 p. m. E. S. T. readings. Windroses show percentage of time wind blew from 16 compass points or was calm during the month. Pressure normals are computed for stations having at least 10 years of record and for 10° intersections in a diamond grid based on readings from the Historical Weather Maps (1899-1939) for the 20 years of most complete data coverage prior to 1940.

Chart XII. 850-mb. Surface, 1200 GMT, November 1957. Average Height and Temperature, and Resultant Winds.

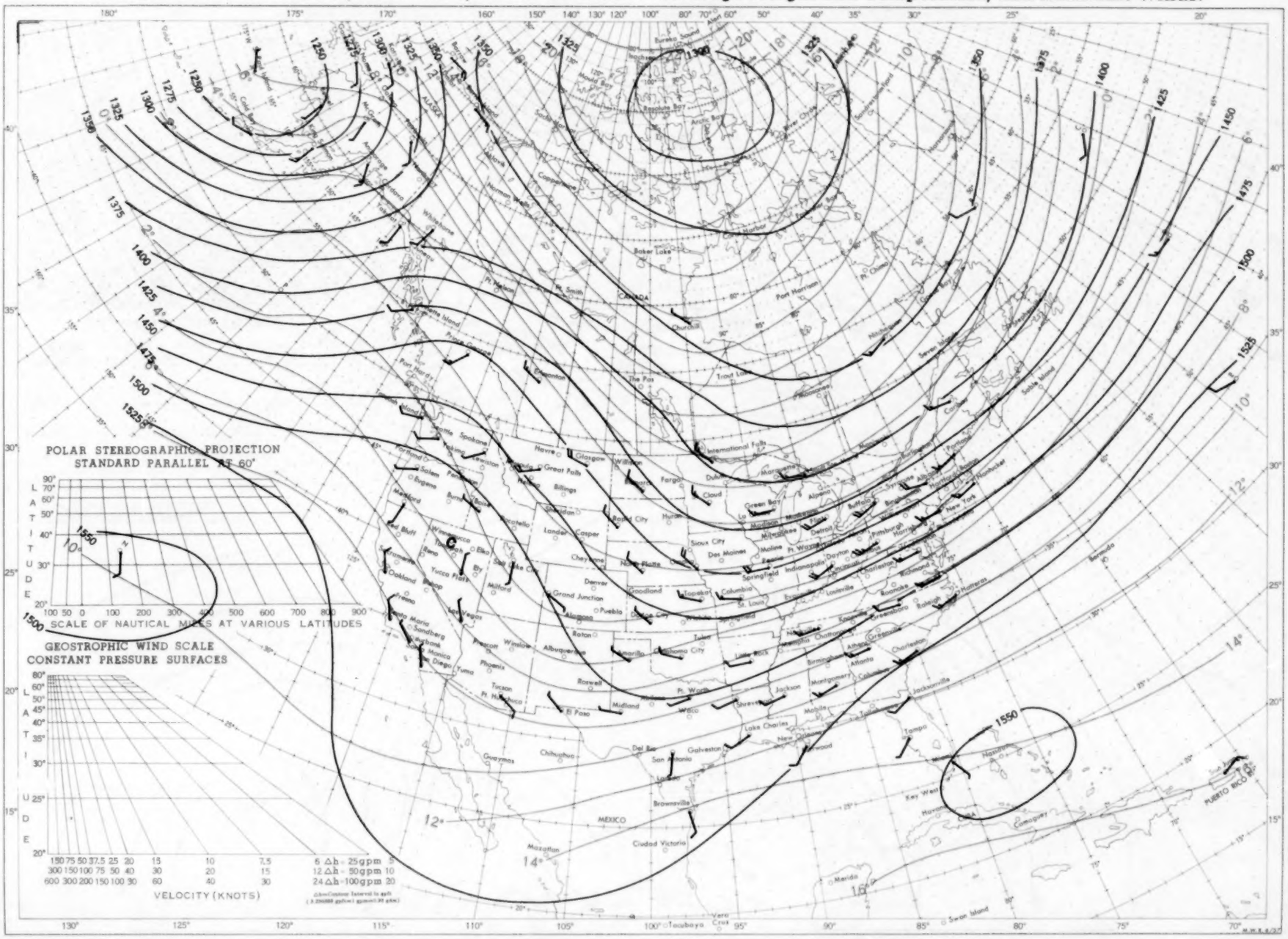

Height in geopotential meters (1 g.p.m. = 0.98 dynamic meters). Temperature in °C. Wind speed in knots; flag represents 50 knots, full feather 10 knots, and half feather 5 knots. All wind data are based on rawin observations.

Chart XIII. 700-mb. Surface, 1200 GMT, November 1957. Average Height and Temperature, and Resultant Winds.

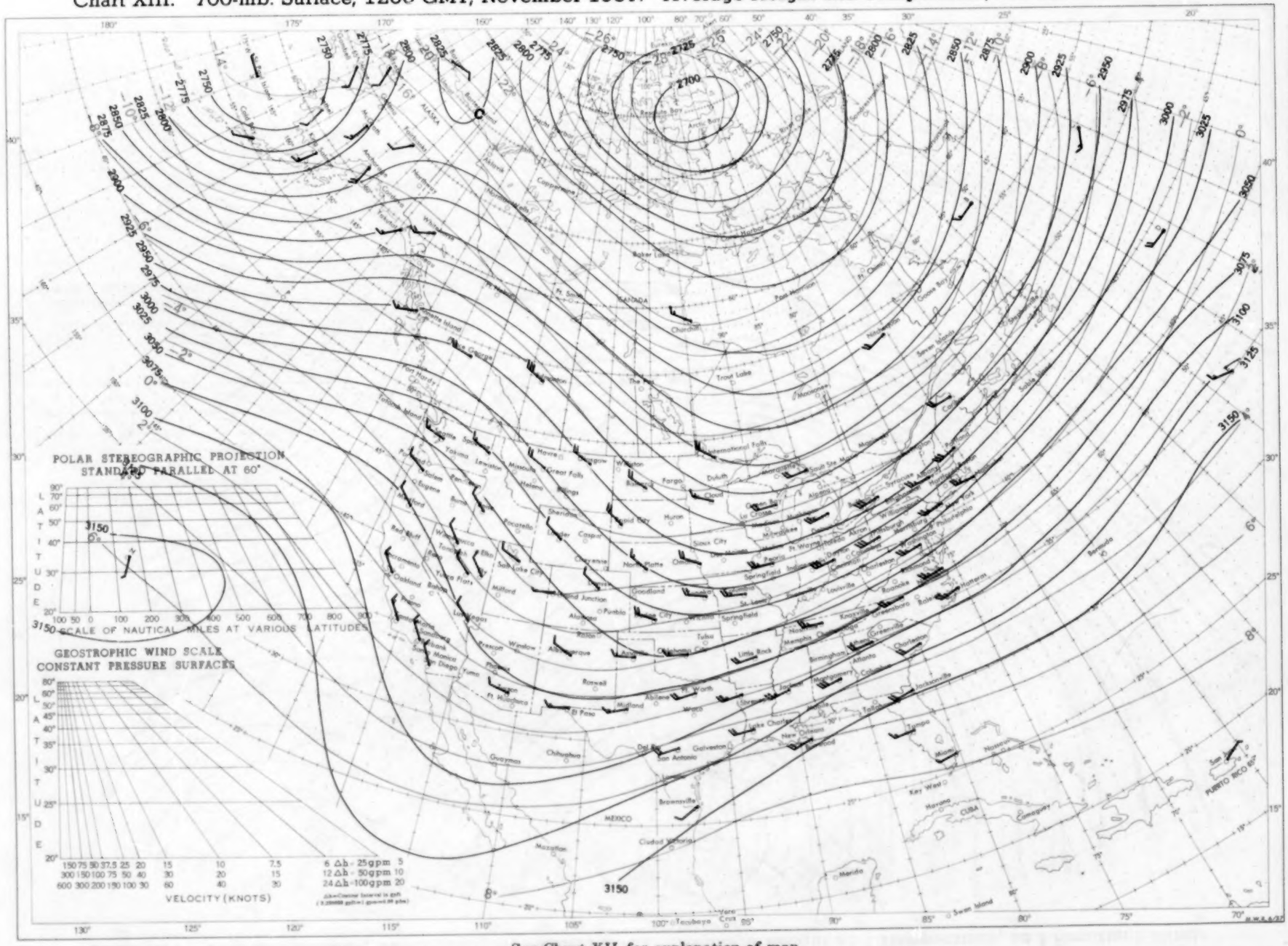

See Chart XII for explanation of map.

Chart XIV. 500-mb. Surface, 1200 GMT, November 1957. Average Height and Temperature, and Resultant Winds.

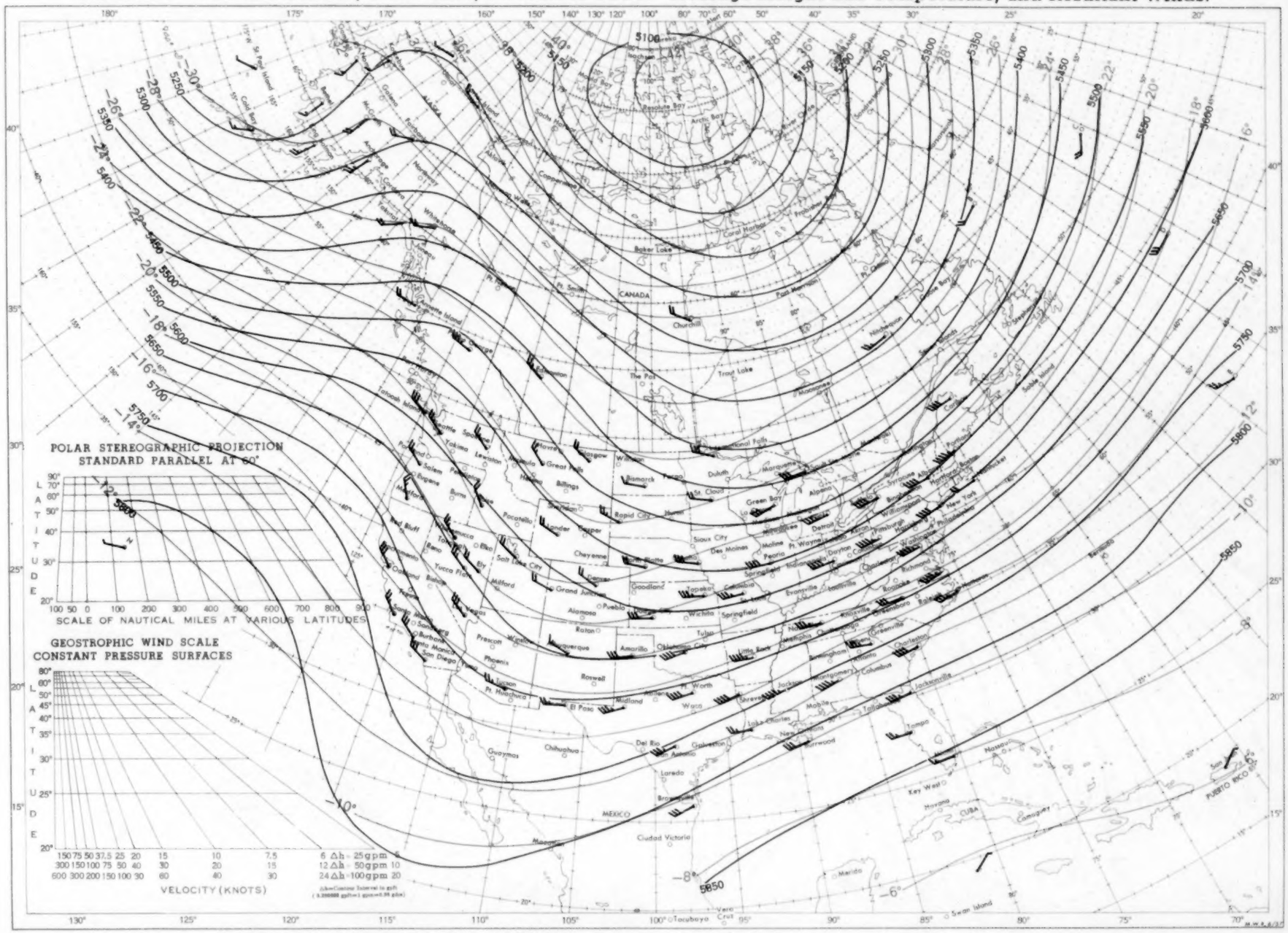

See Chart XII for explanation of map.

Chart XV. 300-mb. Surface, 1200 GMT, November 1957. Average Height and Temperature, and Resultant Winds.

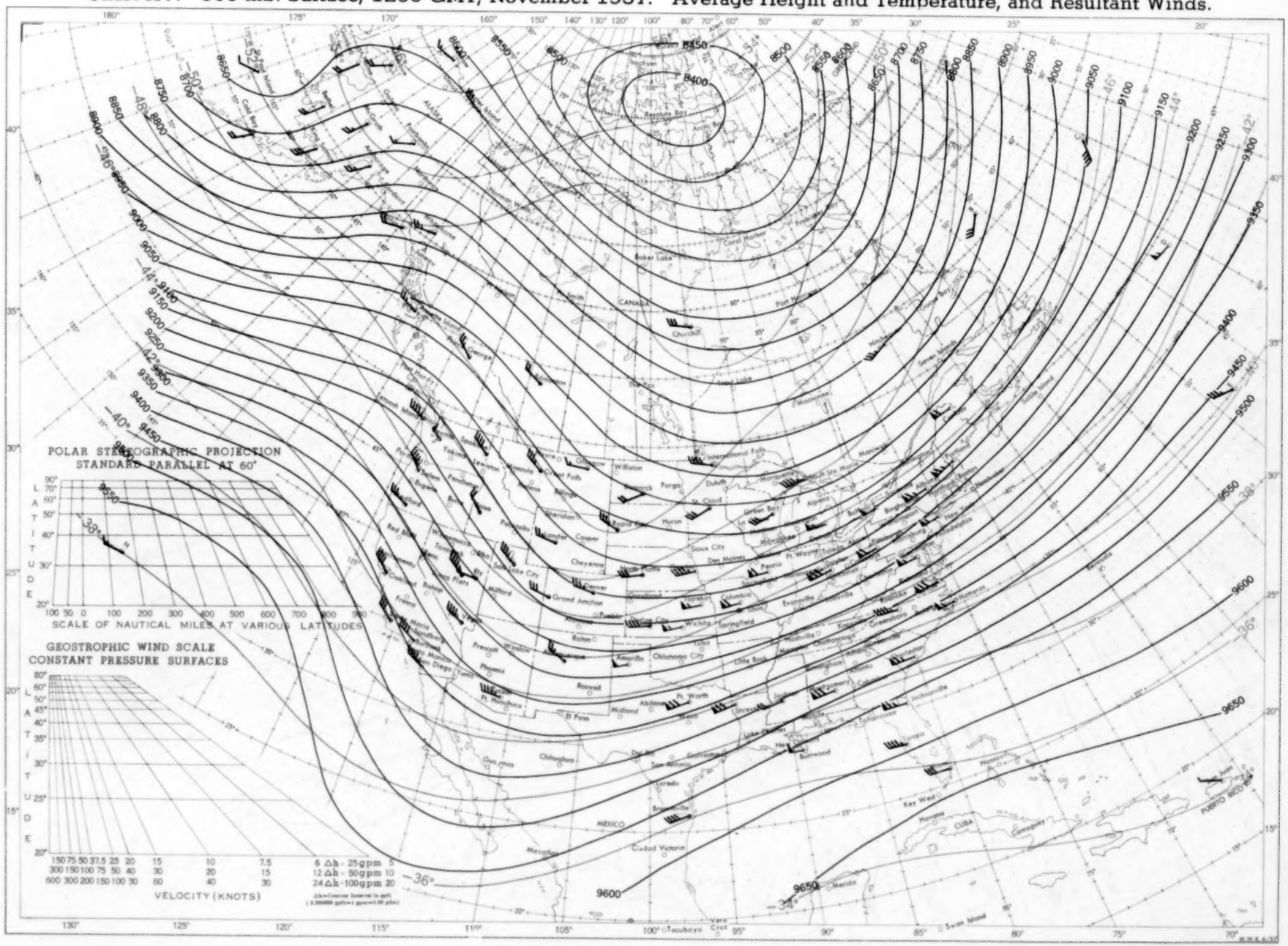

See Chart XII for explanation of map.

Chart XVI. 200-mb. Surface, 1200 GMT, November 1957. Average Height and Temperature, and Resultant Winds.

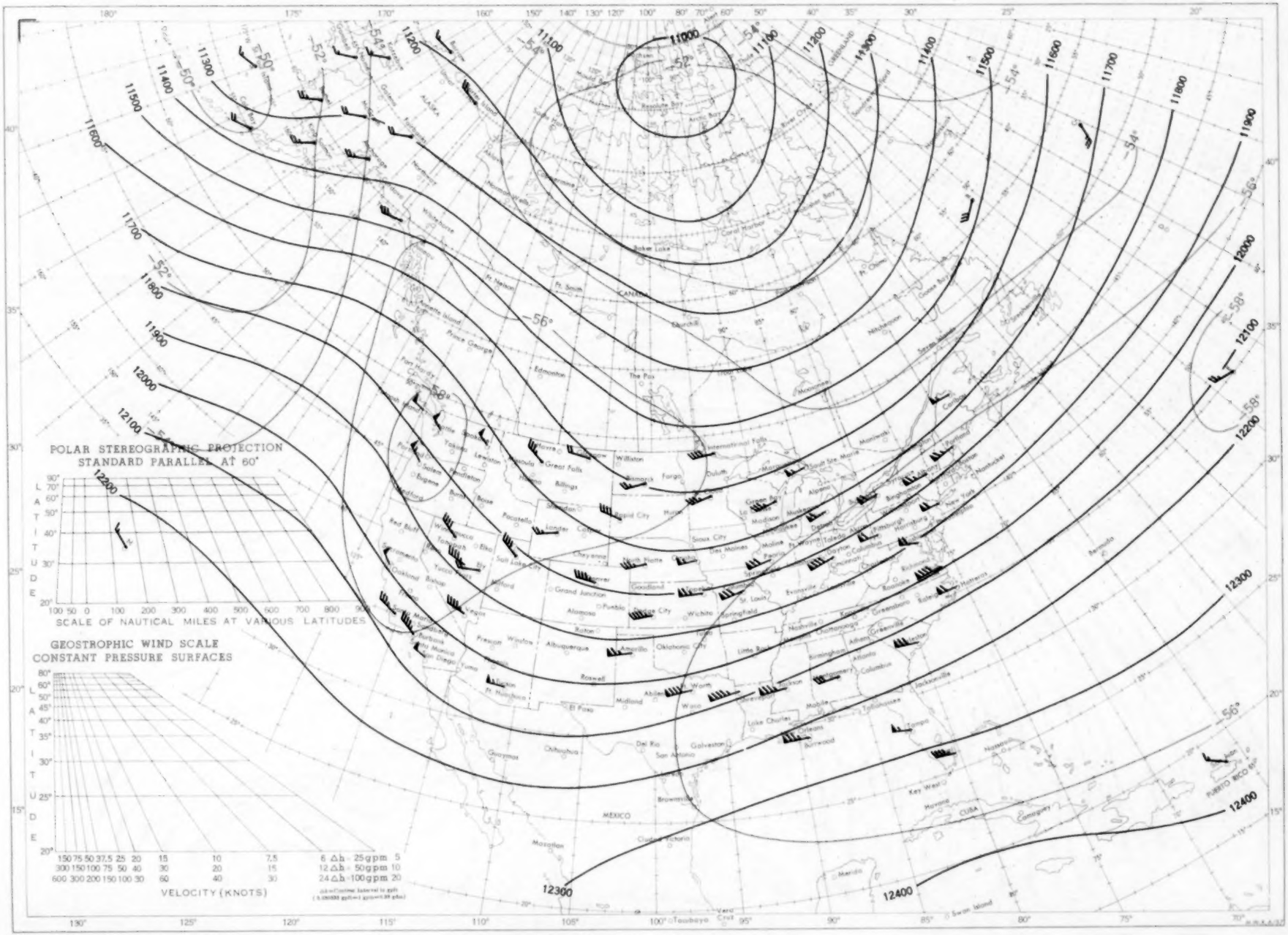

See Chart XII for explanation of map.

Chart XVII. 100-mb. Surface, 1200 GMT, November 1957. Average Height and Temperature, and Resultant Winds.

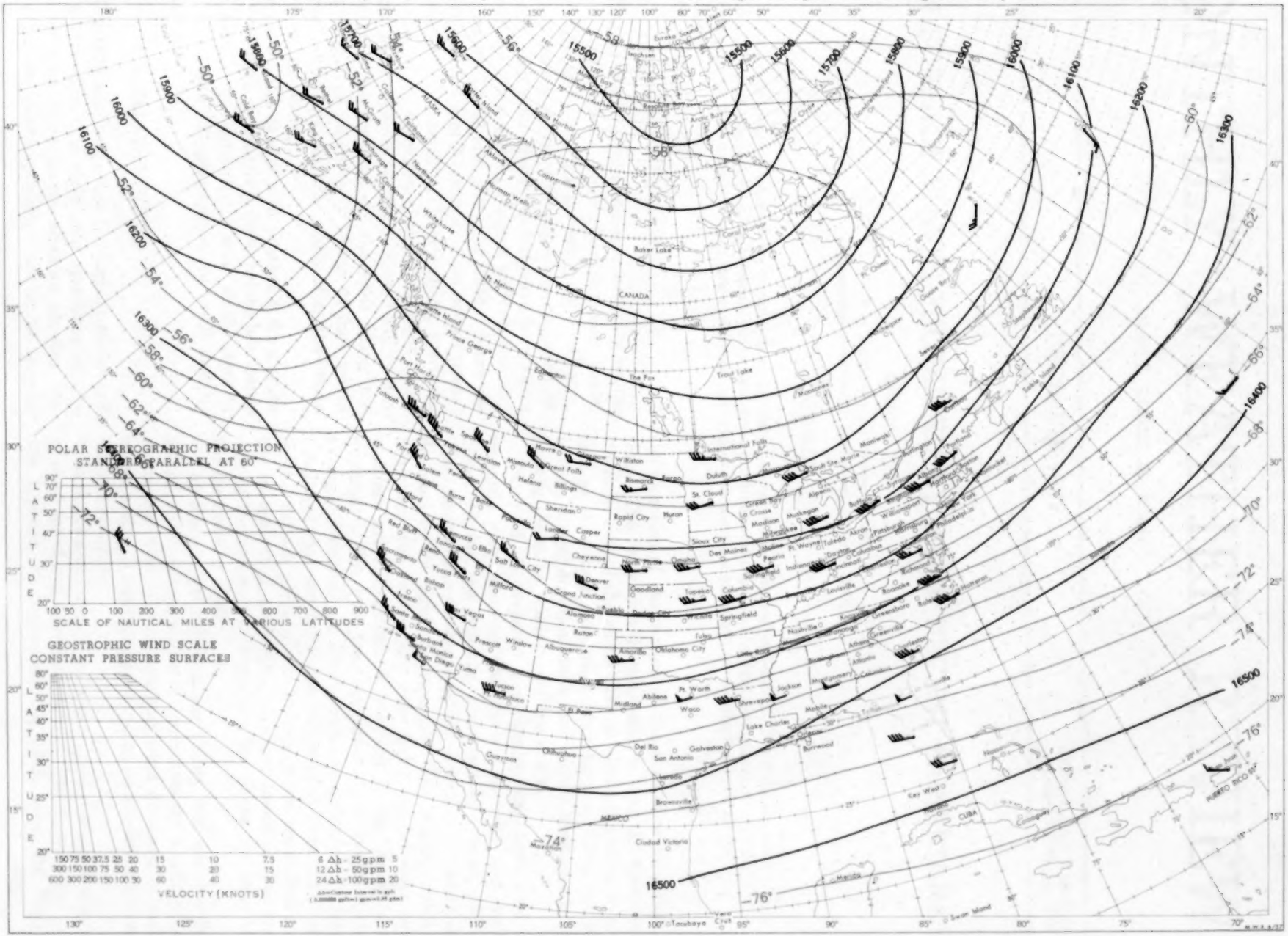

See Chart XII for explanation of map.